

~~CONFIDENTIAL~~

REVIEW OF NASA RESEARCH PROGRAMS ON THE LIFTING BODY CLASS  
OF ENTRY VEHICLES [U]

Fred J. De Meritte

Headquarters  
National Aeronautics and Space Administration  
Washington, D.C.

INTRODUCTION

The NASA Office of Advanced Research and Technology, mainly through its Ames, Langley, and Flight Research Centers, has worked for several years on the technology of advanced manned reentry vehicles. This continuing work emphasizes configurations having sufficient hypersonic lift-drag ratio to obtain (1) greater lateral and longitudinal ranging than semi-ballistic spacecraft during reentry, (2) correspondingly greater precision of return from orbit and increased operational flexibility, (3) widened allowable reentry corridors, and (4) reduced "g" loads during reentry. Emphasis has also been given to development of capability for landing at prepared land sites.

The total scope of the present research covers a wide variety of configurations and operational concepts, ranging from advanced parachutes and other landing techniques applied to current semi-ballistic spacecraft types on the one hand, to concepts having high hypersonic L/D and either horizontal or near-vertical landing capability. The present paper is confined to research being carried out on a particular class of reentry vehicles commonly known as lifting bodies. Special emphasis has been

~~CONFIDENTIAL~~

NOTICE - THIS DOCUMENT CONTAINS INFORMATION AFFECTING THE NATIONAL DEFENSE OF THE UNITED STATES WITHIN THE MEANING OF THE ESPIONAGE LAWS, TITLE 18, U.S.C. SECTIONS 793 AND 794. ITS TRANSMISSION OR REVELATION OF ITS CONTENTS IN ANY MANNER TO AN UNAUTHORIZED PERSON IS PROHIBITED BY LAW

Available to NASA Offices and  
NASA Centers Only.

given to lifting bodies with moderate lift-to-drag ratios ( $L/D \approx 1$ ). Such configurations (references 1, 2, and 3) appear to meet a number of foreseeable needs of future manned spacecraft and a substantial research effort has been generated to investigate and solve the critical problems associated with their use.

#### BACKGROUND

Historically, man's first powered heavier-than-air flight took place in December, 1903. The first airplane was a flying wing (Figure 1). Later, aircraft evolved with a fuselage body and wings. Sixty-two years later, the wings have been eliminated completely in vehicles known as lifting bodies (Figure 2).

NASA's first real interest in the lifting bodies occurred in early 1957, when the Ames Research Center developed the Ames M-1, a blunt half-cone configuration. In late 1957, the M-2 was conceived and it also is a 13-degree blunted half-cone configuration. In order to provide a horizontal landing capability, a boattailed configuration evolved. To provide adequate control of the vehicle, two elevons were added which protruded into the airstream outboard of the vertical tail. It was at this point in the evolution of the M-2 that the decision was made to flight test the vehicle to determine if a man could land a lifting body. The configuration at that time was designated the M2-F1 (Figure 3) and a lightweight version was built and flown at the Flight Research Center. By 1962, Langley Research Center research on lifting bodies, using a somewhat different design approach, had evolved the HL-10 configuration (Figure 4).

~~CONFIDENTIAL~~

~~CONFIDENTIAL~~

- 3 -

Both the HL-10 and the M-2 designs attempted to include the design objectives shown below.

- 1) a trimmed hypersonic lift-drag ratio of about 1  
(without elevon deflection for the HL-10)
- 2) a high trimmed lift capability at hypersonic speeds
- 3) subsonic trimmed lift-drag ratio of at least 3 to 5
- 4) a high volumetric efficiency
- 5) a body shape that would be compatible with a refurbishable ablation heat protection system
- 6) a vehicle that is statically stable and controllable over the operational ranges of altitudes and Mach numbers.

The Ames M-2 and the Langley HL-10 have served as focal points for the lifting body research in their respective centers. The NASA program on lifting entry covers many areas. Some of these areas are:

- 1) aerodynamic heating
- 2) thermal protection systems
- 3) static stability and control
- 4) hinge moments
- 5) pressure distribution
- 6) dynamic stability and control
- 7) flight simulators
- 8) launch vehicle/lifting entry vehicle compatibility
- 9) trajectory and entry environment
- 10) effects of upstream ablation on control effectiveness
- 11) optimum canopy arrangements from visibility and heating standpoints

~~CONFIDENTIAL~~

~~CONFIDENTIAL~~

- 12) refinement of cross ranging analyses
- 13) internal arrangements
- 14) structure
- 15) industry studies
- 16) landing
- 17) abort, and
- 18) alternate configurations.

A few examples of some of the research on lifting bodies will be presented.

#### AERODYNAMIC HEATING

Extensive aerodynamic tests have been completed at Ames on the M-2 and at Langley on the HL-10. The Langley measurements were made at Mach numbers of 8 and 20. Measurements have been made at Ames in the 12-inch shock tunnel and in the 3.5-foot hypersonic wind tunnel at Mach numbers 10, 12, and 14. Wind-tunnel measurements were made at various Reynolds numbers and angles of attack with and without roughness bands on the nose of the body.

Wind-tunnel data made at a Mach number of 8 on the HL-10 were converted into equivalent flight conditions for a portion of a 3-g entry from near earth orbit where maximum convective heating occurs. Representative results (reference 4) are shown in Figure 5. A longitudinal heating distribution is shown in the left plot of the figure and a spanwise distribution at  $x/l = 0.5$  in the right plot. Theoretical estimates of the laminar heating distribution is shown as a dashed curve and of

~~CONFIDENTIAL~~

the turbulent heating distribution as a solid line. A photograph of the HL-10 undergoing heat transfer tests is shown in Figure 6.

One of the NASA contracted studies (reference 5) has provided an estimate of the maximum equilibrium temperatures for the M-2 (Figure 7). These calculations were made both for the normal entry and the most severe abort conditions. The temperatures were calculated assuming the structure was radiatively cooled. (The calculations do not take into account the effects of the ablation process on equilibrium temperature.) The data are for an abort at 18,000 ft/sec and show dramatically that the temperatures associated with abort conditions set the requirements for the heat shield design.

#### HEAT SHIELD SYSTEMS

NASA has an extensive program on ablation heat protection systems. These programs include the characterization and evaluation of a number of materials which are suitable for lifting body heat shields. Three possible candidate materials that are currently being examined are: phenolic nylon, silicone elastomeric materials (such as the Langley Research Center's "purple blend"), and a new material that is showing considerable promise as a material of the future, polybenzimidazol. The phenolic nylon will be flight tested on NASA Scout Reentry "E" now scheduled for January launch. Elastomeric materials such as purple blend have been evaluated in the X-15 program and show considerable promise as heat shield materials for the lifting reentry-type configurations. The work on polybenzimidazol is more recent, but the material can be produced over a large density range and preliminary tests of the material show

~~CONFIDENTIAL~~

it to be an excellent candidate heat shield material. This material has been developed as part of the Ames Research Center's study that has been concerned with the aromatic heterocyclic polymers (reference 6). The Ames Research Center has been able to produce polybenzimidazol that forms very stable composites which react thermally to produce 92 percent by weight of char. An extremely hard char with excellent physical integrity is obtained. Very tough char bricks can be formed by heating the material at 1400°F for several hours. These "black bricks" can be impregnated with selected gas-forming materials which are stable enough for space application. The material is still in the development stage and considerable research is still required before this material is thoroughly characterized and evaluated.

NASA has several contracted studies in the materials area. Two of the studies are aimed directly at lifting entry. These studies are "Parametric Study of Thermal Protection Systems" and "Thermal Protection Systems." In the first study, the contractor is examining all-ablative, all-radiative, and combined radiative-ablative heat shields. Two ablation materials, two radiative materials, and two insulative materials are being examined on various size and weight vehicles. In the latter study, the contractor is examining refurbishment techniques such as replaceable panels. The contractor is looking basically at the HL-10 but has been instructed to determine what differences would occur if the vehicle was the M-2 or the SV-5.

## HANDLING AND LANDING CHARACTERISTICS

We view the low speed handling and landing characteristics as the most critical part of the flight program. It is for this reason that the Flight Research Center undertook to build the M2-F1 configuration. A three-view drawing is shown in Figure 8. This vehicle weighed approximately 1180 pounds and had a planform loading of about  $8 \text{ lb/ft}^2$ . A tubular frame was built by Flight Research Center and a contract was awarded to a sailplane manufacturer to build a light sailplane body to fit around the tubular frame. Before the vehicle was actually flown, the flight vehicle was tested in the 40 x 80-foot wind tunnel (Figure 9) at the Ames Research Center. The tests were made with and without a large center fin. In flight, the M-2 did not use the middle fin. Flight tests were performed first using a specially modified automobile as a tow vehicle to obtain some handling characteristics and for pilot familiarization with the vehicle. Nearly 400 auto tow flights were made. The vehicle, when towed by an auto, reached altitudes of about 20 feet. After the series of auto-tow tests proved that the vehicle could be handled safely, the vehicle was towed to an altitude of about 13,000 feet using a C-47 as the tow vehicle. After reaching this altitude, the M-2 was cut loose from the tow aircraft and proceeded to glide to a landing at the Flight Research Center. The first air-tow flight of the M2-F1 took place April 17, 1963 and nearly 100 flights have been made using the aircraft-tow method. This vehicle was designated M2-F1 since it was the first flight machine. The flight results were later compared with the wind-tunnel results obtained in the 40 x 80-foot wind tunnel (reference 7). Figure 10 shows a comparison of trimmed wind-tunnel and flight data. Lift coefficients are plotted versus angle of attack, drag

coefficient, and L/D in this figure. The first wind-tunnel tests were made using the stick fixed. A later wind-tunnel test was made locking the controls. The control-fixed (locked) data are the more reliable since the stick-fixed data reflects some stretch in the control cables and the controls were rigged in a different manner for the wind-tunnel tests than the way the vehicle was actually rigged for flight.

Concurrent with flight tests of the M2-F1, steps were being taken at Ames to make improvements in the M2-F1 vehicle. The outboard elevons could not readily take the aerodynamic heat to which the vehicle would be subjected by an orbital entry, and so they were removed. To recover the loss in subsonic L/D caused by this change, the vehicle boattail was extended. The control system was changed to include a split flap (top and bottom) to improve the subsonic performance, split rudders were incorporated to serve as speed brakes so they can be flared for improved directional stability at hypersonic speeds. In addition, the canopy was moved forward to improve visibility. Figure 11 is a three-view drawing of the M2-F2 (as the modified version was designated).

A comparison of the low-speed wind-tunnel performance of the M2-F1 and M2-F2 is shown in the Figure 12 (reference 7). Lift coefficients are plotted against L/D for the two configurations and the data reveal a fairly close agreement of the L/D for the two vehicles.

The M2-F1 flight program revealed that the lifting body could be landed safely and that the next step would be to test a vehicle at a more realistic planform weight. A program was generated with the following flight objectives:



- A) Specifically, to investigate
1. landing
  2. low speed handling
  3. transonic behavior
  4. adequacy of predictions
- B) In general, to evaluate the flight characteristics and piloting requirements for terminal phase of reentry ( $M < 2$ ).

Rather than build two test craft of one configuration (one being a back-up), we elected to build two vehicles incorporating different design approaches, namely the M2-F2 and the HL-10. A contract was awarded to Northrop Aircraft Corporation, Norair Division, in June 1964 to have the M2-F2 and the HL-10 built with planform loadings which approached realistic planform loadings of proposed spacecraft configurations. Provisions have been made whereby loadings can be varied from about 30 to over 55 pounds per square foot. The vehicles were built using conventional aircraft construction. They are designed to be carried aloft by the X-15's B-52 and released. Zero-zero ejection seats are incorporated and the vehicles are carried on the B-52 in such a way that the pilot can eject over the B-52 wing in an emergency. Although the vehicles are unpowered in the normal sense, they do carry small landing-assist rockets designated "instant L/D." However, the vehicles have been designed to carry the XLR-11 rocket engine which can be retro-fitted.

After conducting a glide program and gaining information and experience on the approach and landing phase, it is planned to install the

rocket engines for extension of the flight test program to Mach number of around 1.6. Figure 12 is a cut-away photograph of the M-2 showing how it will look with the XLR-11 engine installed. These two configurations were thoroughly tested in ground-based facilities to insure that designs were made that would lead to safe and flyable configurations. The wind-tunnel tests covered stability, control, airload, and hinge moments over the proposed flight range.

As part of the wind-tunnel program to verify the M2-F2 design, low speed wind-tunnel tests were made on the M2-F2 in the Ames 40 x 80-foot wind tunnel and the 12-foot pressure wind tunnel. The results show a difference in the lift coefficient and the pitching moment, Figure 14 (reference 7). The 40 x 80-foot tests were made at a Reynolds number of 25 million and the 12-foot tests were taken at 5 million Reynolds number. The 12-foot data were taken with two different transition strip configurations:  $T_1$  transition strip was placed on the nose and tail, while  $T_2$  transition was placed along the length of the body along the side and on the vertical tail to be effective at angle of attack. Data taken using transition strip  $T_2$  shows a pitch-up tendency. At the higher transonic speeds (and lower Reynolds numbers), the pitch-up is evident again in the wind-tunnel data, Figure 15 (reference 7).

Ames Research Center made tests of strakes along the bottom near the rear to study ways of controlling the pitch-up. From Figure 15, it is evident that the strakes can prevent the pitch-up over the useful flight

range. This figure shows a sketch of the strake arrangement and plots of  $C_L$  vs.  $C_m$  for no strakes, one-half, and full strakes. However, strakes have not been installed on the vehicle because of a belief that the pitch-up is possibly a Reynolds number effect based on results of Figure 14, and would not be present in the actual flight vehicle. This apparent pitch-up will be carefully studied in flight. The pitch-up area, if real, can be avoided in flight; however, to avoid the pitch-up region would mean that, in a powered version, the angle of attack (after release from the B-52) would be restricted, thereby limiting the performance of the vehicle.

The M2-F2 exhibits adverse yaw characteristics or cross coupling when the upper flaps are deflected differentially as ailerons due to the differences in pressure developed on the inside of the vertical tails. Tests were made of a small splitter plate or center fin to prevent this cross coupling. The results of these tests, as well as the configuration, are shown in Figure 16 (reference 7). The center fin configuration, though effective, was not adopted. Instead, an automatic interconnect was included in the control system. This interconnect connects the ailerons and rudders to respond together to counter-balance the coupling effect.

Wind-tunnel data show that the evolution of the M2-F1 into the M2-F2 configuration did not have any great effect on the basic aerodynamic characteristics at hypersonic speeds though there are variations in the aerodynamic heating. It is interesting to note that the M2-F1 lower flap is only about one-half the size of the lower flap of the M2-F2, but has nearly an order of magnitude greater aerodynamic heating due to different location of the flaps. The M2-F1 lower flap is just aft of the maximum

[REDACTED]

thickness point on the bottom, while the M2-F2 lower flap has been moved back well on the boattail. The results of the heating tests are shown in Figure 17 (reference 8).

Turning to the HL-10 evolution (reference 4), the HL-10 was designed to take advantage of the research guidelines previously given in the introduction. In early 1962, a screening process was initiated to develop a configuration that would have the desired characteristics. In the beginning, two configurations were selected. Both had the same planform, being highly swept bodies with blunt noses, both had gradual boattailing to reduce subsonic base drag, and both had hypersonic  $L/D \approx 1$ . One body was symmetrical, while the other body had negative camber. A comparison was made of the characteristics of the two bodies and the results are shown in Table I (reference 4). It was apparent that the negative camber vehicle met more of the design objectives shown in Table I, and therefore, it was selected as the basic configuration. The next step in the evolution process was to select a fin arrangement. Some of the fin arrangements studied are shown in Figure 18 (reference 4). As many as eight versions of some of the individual fin arrangements shown in this figure were investigated. The configuration finally selected is the one marked "Modified" and was designated the HL-10. The modified configuration was also selected to be flight tested by FRC and detailed design of this configuration was initiated by Norair. Further wind-tunnel tests indicated that improvements in the performance of the flight vehicle could be realized by further modification. Some of the further modifications would not necessarily be included in the design of any orbital versions of the HL-10. In order

[REDACTED]

to improve the subsonic L/D, three modifications were proposed. They were: reduce trailing-edge thickness of basic elevon, add outer-surface tip-fin flaps capable of two positions, and provide full trailing edge closure of split rudder on control fin. Wind-tunnel tests indicated that these changes would improve the subsonic L/D from 3.3 to 4.6. Other modifications were proposed that would improve the transonic stability. Wind-tunnel tests had shown that the HL-10 has a slight tendency to pitch-up. As in the case of the M-2, it is not known if the pitch-up is real or a Reynolds number effect; however, Langley proposed modifications to the HL-10 to improve transonic stability and cure the pitch-up tendency. The modifications were to add a two-position upper-surface elevon flap and a two-position inner-surface tip-fin flap. The effect of the modification to improve transonic stability is shown in Figure 19 (reference 4). Pitching moment coefficients at a Mach number of 0.8 with and without the transonic fixes are shown. The pitch-up shown by the wind-tunnel data has been completely cured. Figure 20 (reference 4) shows rear view photographs of the basic HL-10 and the HL-10 with the surfaces deflected for both the subsonic fixes and the transonic fixes. The elevon serves dual functions in that it is deflected downward to reduce base drag, thereby improving the subsonic performance, and is deflected upward to improve the transonic performance. It should be emphasized that the subsonic and transonic fixes are all two-position flaps.

After consideration of the proposed modifications, it was decided to incorporate the modifications into the flight vehicle.

SPECIAL WIND-TUNNEL TESTS IN SUPPORT OF THE FLIGHT PROGRAM

A series of tests were made at the Langley Research Center to determine the separation characteristics of the M2-F2 and the HL-10 from the B-52. The separation phase of the flight is a very critical portion of the flight because the relatively lightweight vehicles are in the flow field of the B-52. It is important that the motions during the separation phase be determined as well as possible. Another test in support of the flight program is the spin characteristics of the vehicles. A cooperative program between Ames and Langley to determine the spin characteristics is underway.

In addition to the separation and spin tests, 60-inch scale models of both vehicles were flown in the Langley Research Center's full-scale wind-tunnel. The models were air-jet powered and were dynamically scaled. The general handling qualities, including stability, Dutch roll, etc., were studied. As an example of the results from this type test, the HL-10 model tests indicated that the Dutch-roll oscillation will damp over the angle-of-attack range (reference 4). The model also exhibited good stability and control characteristics to the maximum test angle-of-attack of 45 degrees, which is well in excess of the normal angle-of-attack range. Figure 21 is a photograph of the HL-10 being tested in the Langley Research Center's Full-Scale Wind-Tunnel.

The M2-F2 has been thoroughly tested in the 40 x 80-foot wind tunnel at the Ames Research Center. Before the HL-10 is flown, it also will be tested in the 40 x 80-foot wind tunnel. Figure 22 shows a photograph of the M2-F2 in the 40 x 80-foot wind tunnel.

### STABILITY AND CONTROL THROUGHOUT REENTRY FLIGHT SPECTRUM

Tests of the M-2 and the HL-10 have been made over a Mach number range from zero to excess of Mach 20. Configurations have been evolved that are stable over the entire Mach number range. Tests have been made using models from 28 feet in length to as small as several inches in length. Figure 23 shows a plot of  $C_m$  versus Mach number at various angles of attack for the M2-F2 configuration (reference 9). The vehicle has adequate stability over the required angle-of-attack range. There is some pitch-up instability exhibited in the wind-tunnel results at transonic speeds. These angles are above the normal angle-of-attack range for gliding flight. Figure 24 is a plot of the L/D trimmed and direction stability versus Mach number for the M-2 and the HL-10 (references 9 and 4). The directional stability of the M-2 is controlled by flaring the rudder angle (both right and left rudders extended). From reentry down to supersonic speeds, the rudders are flared about 25 degrees; for transonic speeds, the rudders are flared about 5 degrees; and for low subsonic speeds, the rudders have no flare.

### LANDING STUDIES

NASA studies have been looking at conventional landing modes using wheels and skids, and also emergency landing in water. Figure 25 is a photograph of the HL-10 landing gear arrangement (reference 4). Landing tests have been made on simulated runways with and without the small landing parachutes of the type carried by some military aircraft for added deceleration. Tests of the lifting body ditching in water have been made which show favorable ditching characteristics. When used with a parachute, the HL-10, for example, could enter the water equally well nose- or tail-first.

Figure 26 (reference 4) is a photograph of the HL-10 entering the water, simulating a parachute entry. The "g" load imposed on the crew is considerably less than the "g" load imposed on the crew by a ballistic-type manned spacecraft, being in the order of three "g's" compared to eight "g's" for the Mercury water landing. Preliminary tests of the HL-10 landing horizontally in water have not been too promising as yet, but tests are still underway.

The landing capability of lifting reentry-type vehicles would be considerably improved by the use of some type of small engine to give the vehicle a go-around capability at the landing site. Studies in this area to date have been very limited, but some trade-off studies have been made comparing a vehicle with a small jet engine having the capability of a conventional airplane-type go-around with a vehicle using short duration rockets with capability to give the vehicle enough powered flight to conduct a loop-type go-around. The power could also be used to improve L/D at landing. Such a capability would, of course, be obtained at the cost of additional weight.

#### FLIGHT SIMULATORS

Simulator studies play an important role in NASA's assessment of handling qualities of various aircraft. In the case of lifting body spacecraft, this is no exception. The performance of the M-2 and the HL-10 has been thoroughly analyzed using various simulators. Reference 10 shows some simulator results of an early version of the HL-10. Figure 27 (reference 11) is a plot of simulator data for the M2-F2 showing roll



control characteristics for a  $q = 100$  psf with rudder interconnects but with dampers off. The rudder interconnect ties the rudder to the ailerons to balance out adverse yaw. The vehicle has a stability augmentation system (dampers) which is available to the pilot if he wishes. The data in Figure 27 are plotted as angle-of-attack versus Mach number and show the boundaries of controllable flight. The lines shown are actually lines of equal pilot rating using a modified Cooper scale. The Cooper ratings are listed at the end of each line. The Cooper scale goes from zero to ten, with the lower the number the better the flying qualities. For the FRC analysis, since the vehicle is not intended for use in precise maneuvers, a criterion of a pilot rating of 6-1/2 or lower has been arbitrarily selected as acceptable. The adverse yaw region is that where the sideslip induced by the ailerons produces a moment (dihedral effect) that retards the initial roll acceleration. The extreme case is roll reversal. As the condition progresses further into the adverse region, the control becomes sluggish. The favorable yaw region is where the sideslip induced by ailerons aids the rolling moment. The extreme of this is pilot-induced oscillation (P.I.O.). Preliminary investigations have shown that the stability augmentation system with washout will improve the condition in the favorable region. The stability augmentation system also can handle any excursions the vehicle might make into the pitch-up region if the pitch-up should be real.

#### STUDIES

Over the past few years, NASA has conducted in-house and has sponsored a number of industry studies on mission analysis and other aspects of lifting entry.

The principal study contracts in force at the present time, or planned, are summarized in Table II. These studies include the mission-analysis type studies which are the minimum manned M-2/GLV study and the study of the effects of vehicle size on costs and research potential of manned HL-10. Both of these studies deal with orbital lifting reentry and the problems involved in making an orbital flight with a lifting body. In addition, two studies deal with thermal protection. These latter studies are (1) refurbishment techniques of thermal protection systems and (2) a parametric study of thermal protection systems for lifting bodies. One of the two remaining studies is associated with the analytical prediction of the aerodynamic behavior of lifting bodies, while the other study is associated with the concept of a new class of lifting reentry vehicles which incorporates VTOL technology for landing.

#### VARIABLE GEOMETRY REENTRY VEHICLES

Work has been underway at Langley Research Center (reference 12) for some time to examine a reusable lifting body reentry vehicle which possesses greater subsonic L/D. The greater subsonic L/D provides improved aerodynamic performance in the low speed horizontal landing condition. In particular, vehicles using this concept would make the landing problem easier through the improved L/D and also the high lift coefficients at low angles of attack. The concept shown in Figure 28 utilizes a basic body of elliptic cross section conforming to a minimum hypersonic wave drag shape as defined by Suddath's modification to Eggers' minimum wave drag work (references 13 and 14). The basic body was modified by the addition of a canopy and protective storage for two highly cambered deployable wing panels and the addition of aft control surfaces.

~~CONFIDENTIAL~~

From an operational standpoint, the vehicle would be placed in earth orbit in the wings-folded condition by any one of several possible lower stage booster types. The wing panels would remain folded during reentry and glide, and deployed after the vehicle reaches subsonic speeds.

Experimental studies have been made over the speed range from  $M = 0.3$  to 10.0. Various types of controls have been examined, including chin flaps, upper and lower trailing flaps, ventral fins, aft body trim flaps, and wing trailing-edge flaps.

While the basic body shape appears favorable from an aerodynamic heating standpoint, the ventral fins and fin-body juncture appear as potential problem areas. Tests are currently in progress to determine the temperature distribution characteristics of the configuration at a Mach number of 7.

Shown in Figures 29 and 30 is a summary of results for the trimmed configuration. Figure 29 shows the subsonic trim characteristics with the wings deployed.  $C_{L_{TRIM}}$  and  $L/D$  are plotted against angle of attack. A value of  $L/D = 8$  and  $C_L = 0.65$  is obtained at an angle of attack near  $0^\circ$ . These results indicate excellent landing performance, and since the body will be at relatively low angle of attack, the pilot will have good visibility as well. The use of  $30^\circ$  wing flaps (Fowler-type tested), indicated by the dashed curves in Figure 28, provides high trimmable lift coefficients at angles of attack below  $20^\circ$  which may be used for emergency or abort conditions and improved water-ditching characteristics. Here it should be noted that, while no vertical tail is shown and results indicate no

~~CONFIDENTIAL~~

requirement under normal conditions, the imposition of cross wind landing capability would require the addition of such.

Figure 30 indicates the supersonic-hypersonic characteristics with the wing panels fully retracted. At  $M = 10$ , the trimmed  $(L/D)_{\max}$  is in excess of 2.5, with a corresponding  $C_L = 0.1$ . Use of the aft controls (ventral fins and body trim flaps) provides stable longitudinal trim from angles of attack near  $0^\circ$  to values in excess of  $50^\circ$ . As a matter of interest, the basic elliptic body on which the configuration was based has been tested at  $M = 10$  and an  $L/D$  of 3.5 was obtained, indicating further potential gains for the configuration.

#### LIFTING BODIES WITH VERTICAL LANDING CONCEPTS

NASA has been studying an entirely different concept of spacecraft that would utilize the vertical landing concept in conjunction with both moderate and high  $L/D$  spacecraft.

Vertical landings with near zero-zero (zero forward speed - zero vertical speed) touchdown are desirable. Zero-zero touchdown would help the problem of emergency landings on unprepared land or water, day/night cycle, and possibly the adverse weather problem.

A class of vehicles is being examined that is different from the horizontal landers that could incorporate one of several means for providing vertical descent. These vehicles have moderate-to-high  $L/D$  and have been designed from hypersonic considerations only. At low supersonic speeds (around  $M = 2.0$ ), possibly a drogue parachute could be

~~CONFIDENTIAL~~

deployed. A series of subsonic terminal landing devices are being examined. These include the parachute, limp paraglider (which is similar in principle to the higher L/D gliding parachute), rotor, and various turbo fans, lift fans, or lift engines. One concept that is undergoing feasibility study at LRC (reference 15) has been designated propulsive lifting landing with aerodynamic maneuvering entry. The transition from aerodynamic flight to the propulsive lift mode might be accomplished directly or indirectly. The indirect method includes deployment of a parachute at subsonic speeds. At about 40,000 feet altitude, lift fans are rotated out of the body into the airstream. These are started up and checked out, shortly afterward the parachute is jettisoned, and landing is made at near zero-zero speeds. The spacecraft does carry fuel for a short hover time and can, in principle, maneuver precisely to any point within a given zone as the situation demands. This concept is illustrated in the next figure (Figure 31). The sketch shows a possible arrangement for both the moderate and high L/D configurations.

#### REFERENCES

References to the bulk of the pertinent NASA research on lifting re-entry are given in references 4, 10, 16 through 56. The published reports on the M-2 are given in references 16 through 29. The HL-10 reports are given in references 4, 10, 30 through 47, while the reports relating to the variable geometry research are given in references 48 through 56.

~~CONFIDENTIAL~~

SUMMARY

In this paper, I have attempted to outline very briefly the scope of work NASA is doing on the lifting entry class of vehicles. The research will continue, with possibly more emphasis on alternate configurations, so that at such time as a new spacecraft development program may be undertaken, there will be adequate data available on the various types of configurations and operational concepts that an intelligent choice can be made.

~~CONFIDENTIAL~~

## NOMENCLATURE



$b$	wing span, ft.
$C_D$	drag coefficient
$C_L$	lift coefficient
$C_m$	pitching moment coefficient
$C_{m\alpha}$	slope of pitching moment coefficient
$C_{n\beta}$	directional stability parameter
$L/D$	lift-drag ratio
$l$	model length, ft.
$q$	dynamic pressure, lb/ft <sup>2</sup>
$\dot{q}$	heating rate, Btu/ft <sup>2</sup> - sec.
$\bar{q}$	heat transfer parameter, average control heating/body nose heating
$Re_\theta$	Reynolds number based on momentum thickness
$V_I$	entry velocity at 400,000 foot altitude
$x, y$	model coordinates
$\alpha$	angle of attack, deg.
$\delta_e$	elevon deflection, deg.
$\delta_i$	initial entry angle, deg.
$\delta_{fu}$	upper flap deflection, deg.
$\delta_{fl}$	lower flap deflection, deg.

## REFERENCES

1. Love, E.S.; and Pritchard, E.B.: A Look at Manned Entry at Circular to Hyperbolic Velocities. 2nd Manned Space Flight Meeting (Dallas, Texas), Am. Inst. Aeron. Astronaut., Apr. 1963, pp. 167-180
2. Love, E.S.: Factors Influencing Configuration and Performance of Multipurpose Manned Entry Vehicles. J. Spacecraft Rockets, vol. 1, no. 1, Jan.-Feb. 1964, pp. 3-12.
3. Syvertson, C.A.; Swenson, B. L.; Anderson, J. L.; and Kenyon, G.C.; Some Considerations of the Performance of a Maneuverable, Lifting-Body, Entry Vehicle. Vol. 16, pt. one of Advances in the Astronautical Sciences, Norman V. Petersen, ed., Western Periodicals Company, (North Hollywood, Calif), c.1963, pp. 898-918.
4. Rainey, Robert W.: Summary of an Advanced Manned Lifting Entry Vehicle Study. NASA TMX 1159
5. Anon.: Minimum Manned Lifting Body Entry Vehicle Study (Contract No. NAS 4-839 - Monthly Progress Letter No. 4, McDonnell Aircraft Corporation.
6. Parker, John, private communication, Ames Research Center, NASA.
7. Jones, Lloyd, private communication, Ames Research Center, NASA.
8. Seegmiller, Henry L., private communication, Ames Research Center, NASA.
9. Keener, E. R., private communication, Ames Research Center, NASA.
10. Moul, Martin.T.; and Brown, Lawrence W.: Some Effects of Directional Instability on Lateral Handling Qualities of an Early Version of a Manned Lifting Entry Vehicle. NASA TMX 1162.
11. Iliff, Kenneth; Informal report, Flight Research Center, NASA.
12. Henry, B. Z., Jr.; and Spencer, Bernard, Jr.; informal report, Langley Research Center, NASA.
13. Eggers, A. J., Jr.; Resnikoff, M. M.; and Dennis, David H.: Bodies of Revolution Having Minimum Drag at High Supersonic Airspeeds, NACA report -1306, 1958.
14. Suddath, Jerrold H.; and Oehman, Waldo I.: Minimum Drag Bodies with Cross-Sectional Ellipticity. NASA TN 2432.
15. Love, E. S.: informal report, Langley Research Center, NASA.
16. Kenyon, George C., and Edwards, George G.: A Preliminary Investigation of Modified Blunt  $13^{\circ}$  Half-Cone Re-Entry Configuration



- [REDACTED]
17. Rakich, John V.: Supersonic Aerodynamic Performance and Static-Stability Characteristics of Two Blunt-Nosed Modified  $13^\circ$  Half-Cone Configurations. NASA TM X-375, 1960.
  18. Dennis, David H., and Edwards, George G.: The Aerodynamic Characteristics of Some Lifting Bodies. NASA TM X-376, 1960.
  19. Kenyon, George C., and Sutton, Fred B.: The Longitudinal Aerodynamic Characteristics of a Re-Entry Configuration Based on a Blunt  $13^\circ$  Half Cone at Mach Numbers to 0.92. NASA TM X-571, 1961.
  20. Rakich, John V.: Aerodynamic Performance and Static Stability of a Blunt-Nosed Boattailed  $13^\circ$  Half-Cone at Mach Numbers of 0.60 to 5.0. NASA TM X-570, 1961.
  21. Kenyon, George C.: The Lateral and Directional Aerodynamic Characteristics of a Re-Entry Configuration Based on a Blunt  $13^\circ$  Half Cone at Mach Numbers to 0.90. NASA TM X-583, 1961.
  22. Hassell, James L., Jr., and Ware, George M.: Investigation of the Low Subsonic Stability and Control Characteristics of a 0.34-Scale Free-Flying Model of a Modified Half-Cone Reentry Vehicle. NASA TM X-665, 1962.
  23. Spencer, Bernard, Jr., and Phillips, W. Pelham: Low-Speed Aerodynamic Characteristics of a Modified Blunt  $13^\circ$  Half-Cone Lifting-Body Configuration Having Deployable Horizontal Tails With or Without Variable-Sweep Wings. NASA TM X-847, 1963.
  24. Syvertson, C. A., Swenson, B. L., Anderson, J. L., and Kenyon, G.C.: Some Considerations of the Performance of a Maneuverable, Lifting-Body Entry Vehicle. Advances in the Astronautical Sciences, vol. 16, part one, American Astronautical Society, September 1963.
  25. Horton, Victor W., Layton, Garrison P., Jr., and Thompson, Milton O.: Exploring New Manned Spacecraft Concepts. Astronautics and Aeronautics, AIAA, May 1964.
  26. Stambler, Irwin: Manned Maneuverable Reentry. Space/Aeronautics, vol. 41, no. 5, May 1964.
  27. Axelson, J. A.: Pressure Distributions for the M-2 Lifting Entry Vehicle at Mach Numbers of 0.23, 5.2, 7.4, and 10.4. NASA TM X-997, September 1964.
  28. Horton, Victor W., Eldredge, Richard, C., and Klein, Richard E.: Flight-Determined Low-Speed Lift and Drag Characteristics of the Lightweight M2-F1 Lifting Body. NASA TN.
- [REDACTED]

- 
29. Smith, Harriet J.: Evaluation of the Lateral-Directional Stability and Control Characteristics of the Lightweight M2-F1 Lifting Body at Low Speeds. NASA TN.
  30. Rainey, Robert W., and Ladson, Charles L.: Preliminary Aerodynamic Characteristics of a Manned Lifting Entry Vehicle at a Mach Number of 6.8. NASA TM X-844.
  31. Ware, George M.: Aerodynamic Characteristics of Model of Two Thick 74° Delta Manned Lifting Entry Vehicles at Low Subsonic Speeds. NASA TM X-914.
  32. Ladson, Charles L.: Aerodynamic Characteristics of a Manned Lifting Entry Vehicle Designated HL-10 at a Mach Number of 6.8. NASA TM X-915.
  33. Dunavant, James C., and Everhart, Philip E.: Investigation of Heat Transfer to a Manned Lifting Entry Vehicle, Designated HL-10, at Mach 8. NASA TM X-998.
  34. Rainey, Robert W., and Ladson, Charles L.: Aerodynamic Characteristics of a Manned Lifting Entry Vehicle at  $M = 0.2$  to 1.2. NASA TM X-1015.
  35. McShera, J. T., Jr., and Campbell, James F.: Stability and Control Characteristics of a Manned Lifting Entry Vehicle at Mach Numbers from 2.29 to 4.63. TM X-1019.
  36. Ware, George M.: Effect of Fin Arrangement on Aerodynamic Characteristics of Thick 74° Delta Manned Lifting Entry Vehicle at Low Subsonic Speeds. NASA TM X-1020.
  37. Harris, Julius: Longitudinal Aerodynamic Characteristics of a Manned Lifting Entry Vehicle at a Mach Number of 19.7. NASA TM X-1080.
  38. Everhart, Philip E., and Hamilton, H. Harris: Investigation of Roughness Induced Turbulent Heating to the HL-10 Manned Lifting Entry Vehicle. NASA TM X-1101.
  39. Campbell, James R., and McShera, J.T., Jr.: Stability and Control Characteristics from Mach Number 1.50 to 2.86 of a Model of a Manned Lifting Entry Vehicle. NASA TM X-1117.
  40. McShera, J. T., Jr., and Campbell, James F.: Aerodynamic Characteristics from Mach Numbers 1.50 to 2.86 of a Lifting Entry Vehicle With Adaptor Section and With a Saturn Launch Vehicle. NASA TM X-1125.
  41. Harvey, William D.: Pressure Distributions on the HL-10 Manned Lifting Entry Vehicle at a Mach Number of 19.5. NASA TM X-1135.
- 

- [REDACTED]
42. Johnston, Patrick: Stability Characteristics of a Manned Lifting Entry Vehicle at Mach Number of 20.3 in Helium. NASA TM X-1156.
  43. Spencer, Bernard F.: An Investigation of Methods of Improving Subsonic Performance of a Manned Lifting Entry Vehicle. NASA TM X-1157.
  44. Ladson, Charles L: Aerodynamic Characteristics of a Manned Lifting Entry Vehicle with Modified Tip Fins at  $M = 6.8$ . NASA TM X-1158.
  45. Ware, George M.: Full-Scale Wind Tunnel Investigation of the Aerodynamic Characteristics of the HL-10 Manned Lifting Entry Vehicle. NASA TM X-1160.
  46. Silvers, H. Norman, and Campbell, James F.: Stability Characteristics of a Manned Lifting Entry Vehicle with Various Fins at Mach Numbers from 1.50 to 2.8. NASA TM X-1161.
  47. Campbell, James F.: Effects of Variation in Tip Fin Geometry on Stability Characteristics of a Manned Lifting Entry Vehicle at Mach Numbers from 1.50 to 2.86. NASA TM X-1176.
  48. Spencer, Bernard, Jr.: Longitudinal Aerodynamics Characteristics at Mach Numbers of 0.40 to 1.10 of a Blunted Right Triangular Pyramidal Reentry Configuration Employing Variable-Sweep Wing Panels. NASA TN D-1518.
  49. Spencer, Bernard, Jr.: Transonic Investigation of a Pyramidal Reentry Configuration with Cambered Variable-Sweep Wings and Various Longitudinal Controls. NASA TN D-2033.
  50. Spencer, Bernard, Jr., and Phillips, W. Pelham: Low Speed Aerodynamic Characteristics of a Modified  $13^\circ$  Half-Cone Lifting-Body Configuration Having Deployable Horizontal Tails or Variable Sweep Wings for Improving Lift and Lift-Drag Ratio. NASA TM X-847.
  51. Spencer, Bernard, Jr., Henry, Beverly Z., and Putnam, Lawrence E.: The Transonic Longitudinal and Lateral Aerodynamic Characteristics of a Low-Fineness Ratio Elliptic Hypersonic Configuration Employing Variable Sweep- Wing Panels for Improving Subsonic Lift and Performance. NASA TM X-768.
  52. Spencer, Bernard, Jr., and McShera, John T.: Longitudinal and Lateral Aerodynamic Characteristics at Mach Numbers of 3.00, 3.96, and 4.65 of a Low Fineness Ratio Elliptic Hypersonic Configuration Having Variable Sweep Wing Panels. NASA TM X-807.
  53. Putnam, Lawrence E.: Hypersonic Aerodynamic Characteristics of a Reentry Configuration with Variable Sweep Wings. NASA TM X-965.
- [REDACTED]

~~CONFIDENTIAL~~

54. Spencer, Bernard, Jr., and Trescott, Charles D., Jr.: The Effects of Reynolds Number at Low Subsonic Speeds on the Aerodynamic Characteristics of a Lifting Body Reentry Configuration Having Variable-Sweep Wing Panels. NASA TM X-1010.
55. Foster, Gerald V., Fournier, Roger H., and Spencer, Bernard, Jr.: Static Aerodynamic Characteristics at Mach Numbers from 1.50 to 4.63 of a Lifting Reentry Configuration Having Variable-Sweep Wings. NASA TM X-1064.
56. Trescott, Charles D., and Spencer, Bernard, Jr.: Hypersonic Aerodynamic Characteristics of a Lifting Reentry Vehicle Model with Four Types of Longitudinal Control. Proposed NASA TM L-4210.

~~CONFIDENTIAL~~

TABLE I - CAMBER EFFECTS

Research guidelines:	Vehicle with negative camber	Symmetrical vehicle
Hypersonic $L/D \approx 1$ , $\delta_e = 0^\circ$	x	
Hypersonic high trimmed $C_L$	x	
Subsonic trimmed $L/D \geq 4$	x	x
High volumetric efficiency	x	x
Promising body shape	x	x
Stable and controllable	x	
Additional considerations:		
Lower heating rates and loads	x	x (local)
Lower $\alpha$ for subsonic $C_L$		x
Reduced subsonic flow separation	x	

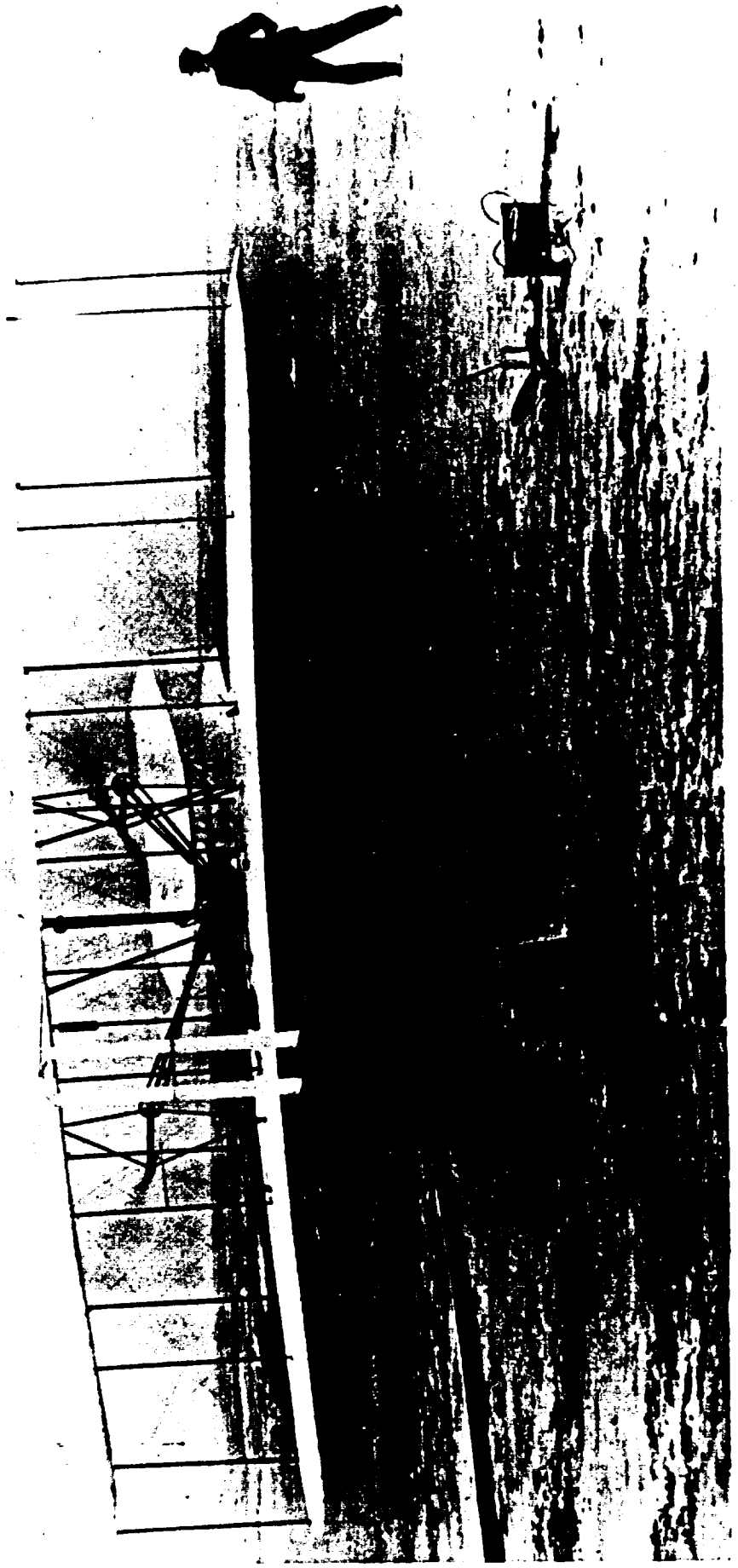
TABLE II

## CURRENT AND PLANNED LIFTING BODY STUDIES

Study	Center	Contractor	Start
Minimum manned M-LGLV (Identification of weights, cost, and technology)	FRC	Norair McDonnell	4/65
Follow-on study on Selected Problems	FRC	Norair McDonnell	3/66 (est.)
Effects of vehicle size on costs and research potential of manned HL-10	LRC	-	3/66 (est.)
Parametric study of thermal protection systems - all ablative, radiative, combined, two types ablation material and radiative cooled systems; s/c types, sizes, weights	MAD	General Electric	6/65
Thermal Protection System - refurbishment techniques	LRC	Martin	5/65
Examination of adequacy of existing analytical methods of providing aerodynamic behavior of lifting bodies	ARC	Norair	3/65
Analytical study of the use of the Propulsive lift concept for the descent and landing of manned entry vehicles	LRC	-	1/66 (est.)



# WRIGHT BROTHERS FIRST FLIGHT



NASA RV65-16273  
11-22-65



# M2-F2 LOW SPEED RESEARCH VEHICLE

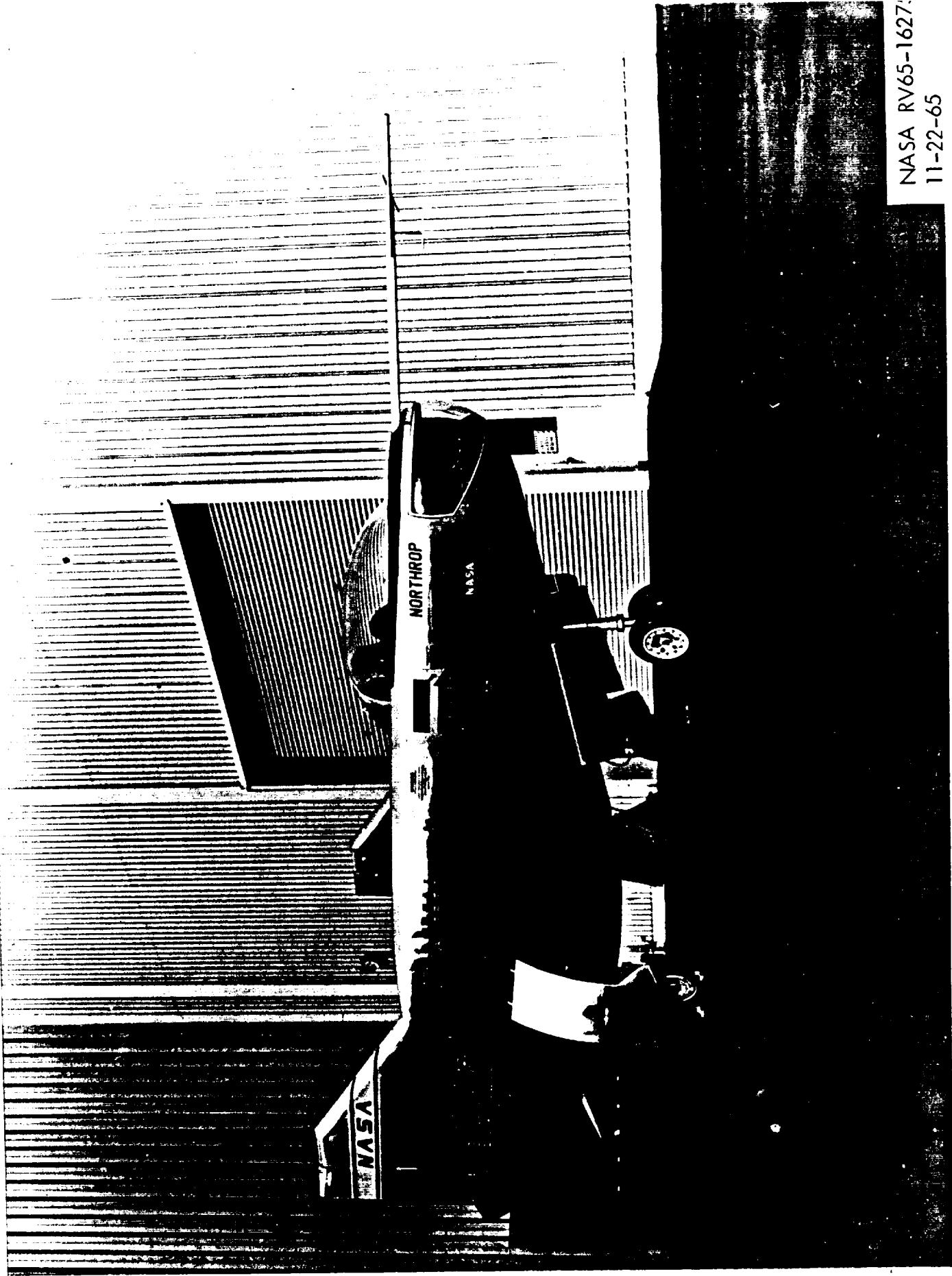


Figure 2

NASA RV65-1627:  
11-22-65

# M2-F1 LIGHT WEIGHT RESEARCH VEHICLE

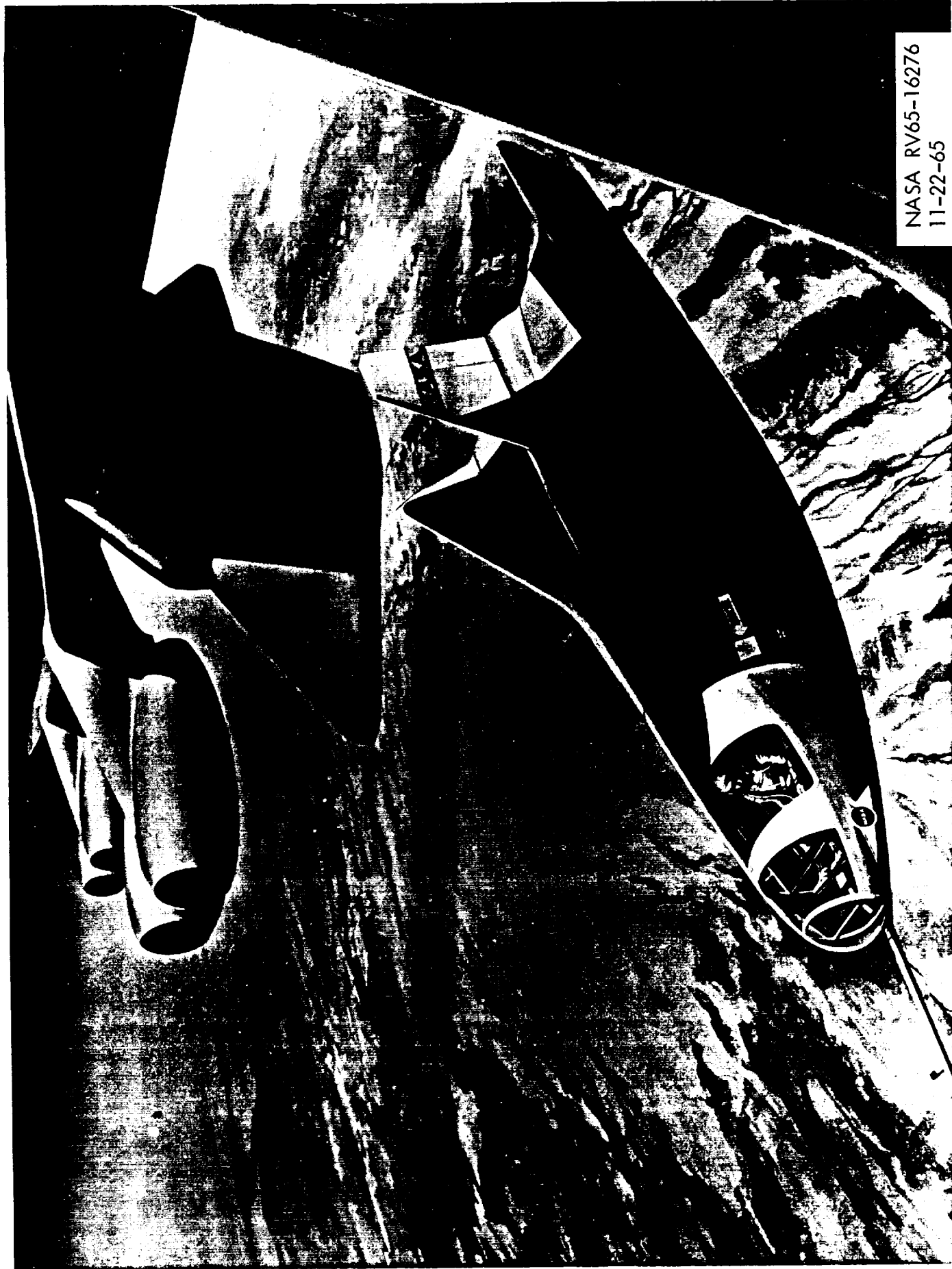


Figure 3

NASA RV65-16271

11-22-65

# HL-10 LOW SPEED RESEARCH VEHICLE



NASA RV65-16276  
11-22-65

# MAXIMUM HEATING DISTRIBUTION DURING 3g ENTRY

$$V_e = 25,500 \text{ ft/sec}; \alpha = 30^\circ; \delta_e = 0^\circ$$

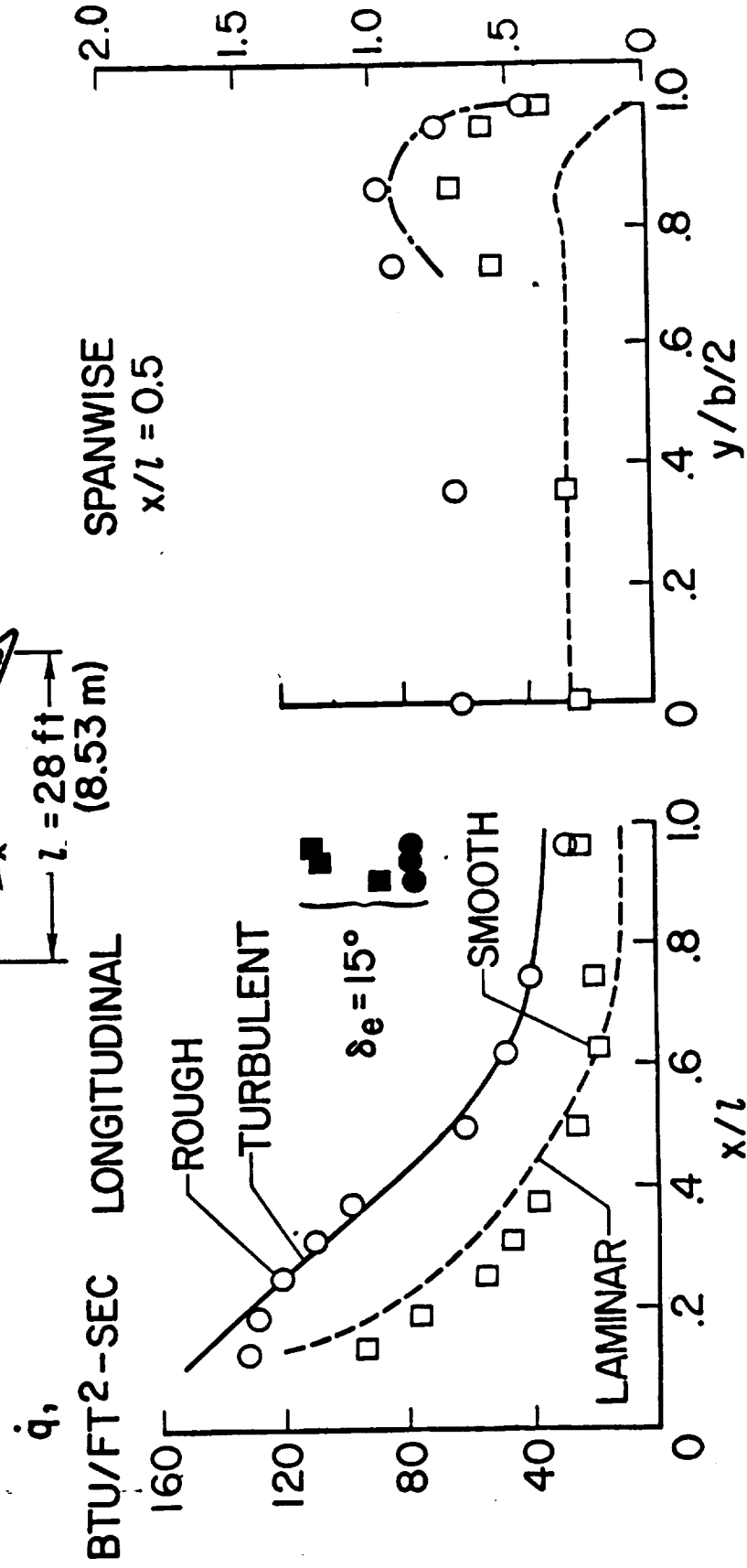
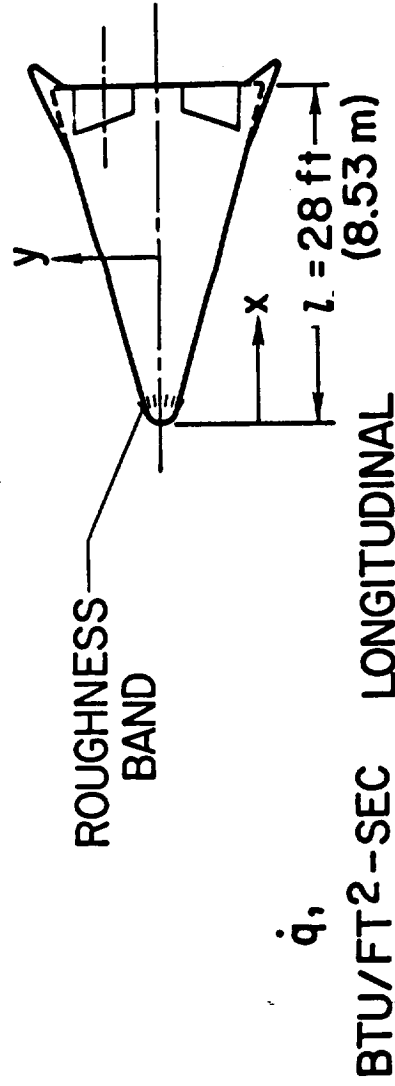
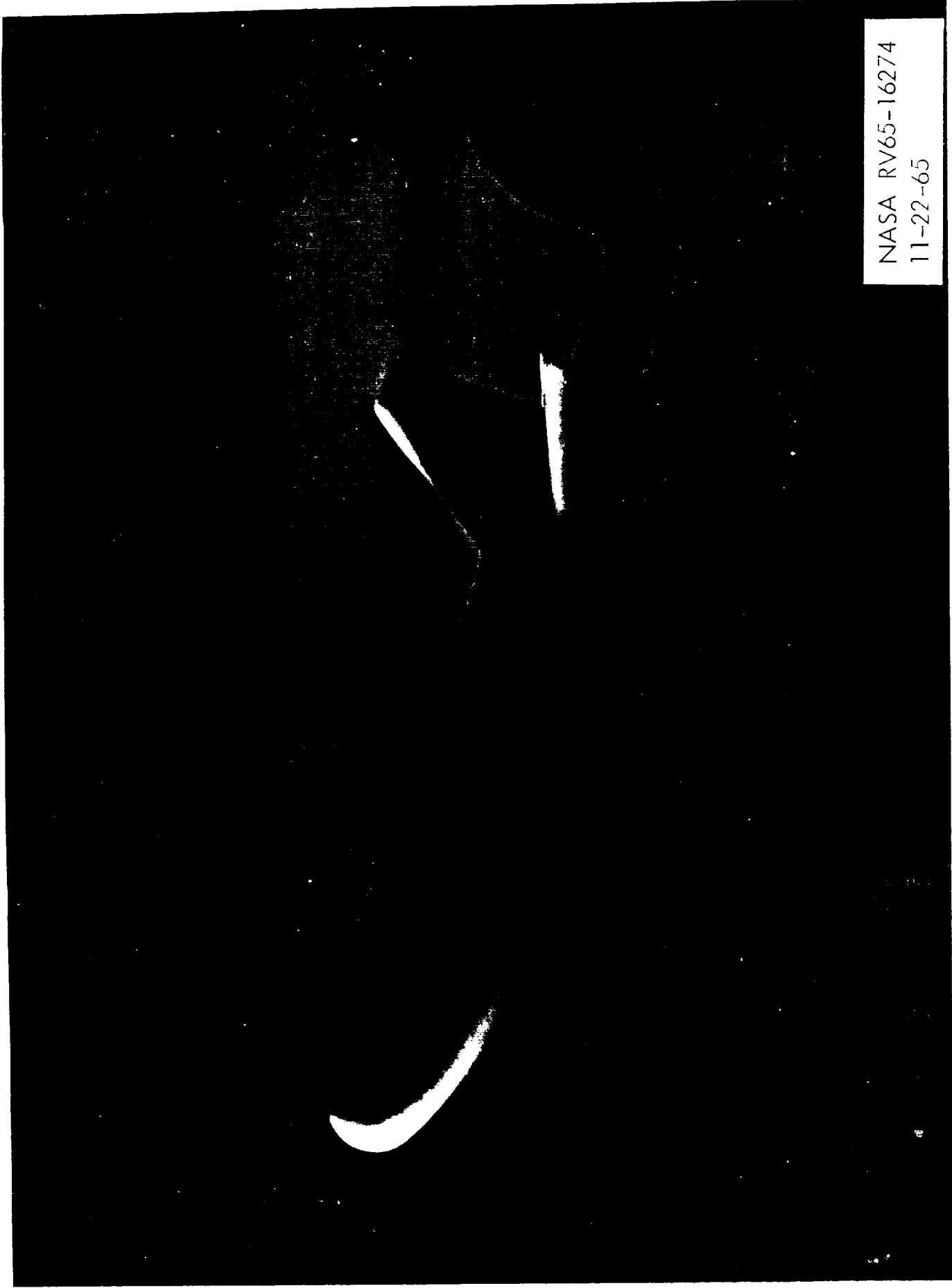


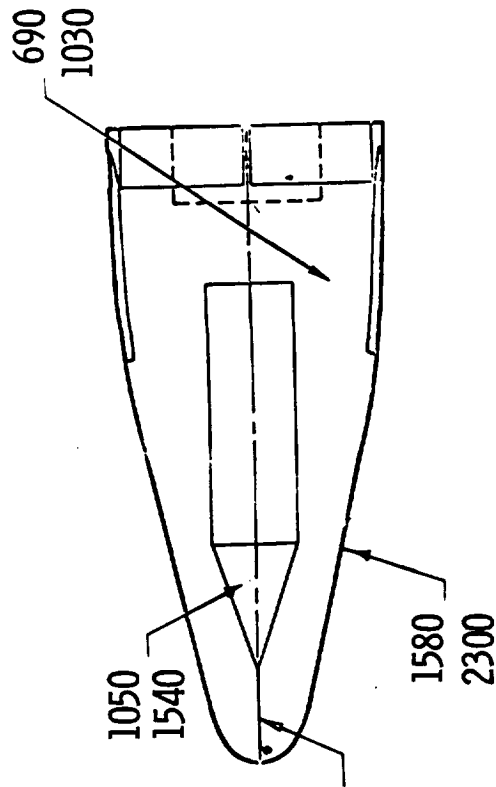
Figure 5

# AERODYNAMIC HEATING TEST OF HL-10



NASA RV65-16274  
11-22-65

# MAXIMUM RADIATION EQUILIBRIUM TEMPERATURES



ENTRY:

NOMINAL 1010 °F

ABORT 1180 °F

NOTE:

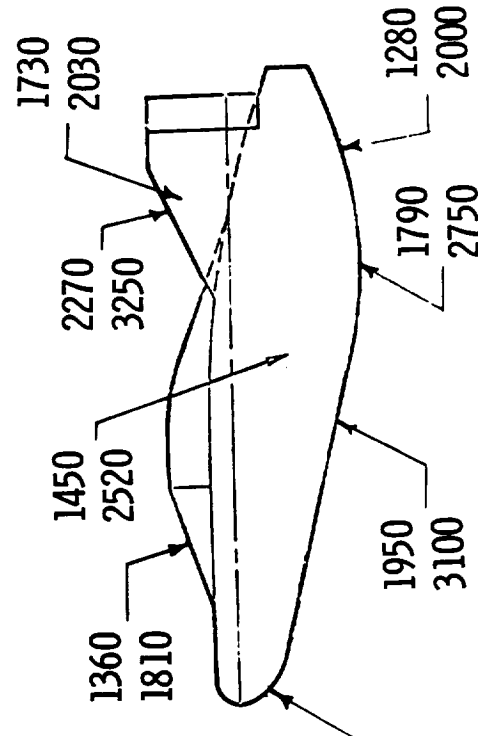
TEMPERATURES ARE BASED  
ON TRANSITION CRITERIA

( $Re_{\theta}/M_i = 200$ ).

ABORT:

$V_1 = 18,200$  FT/SEC

$\gamma_1 = 4.3^\circ$

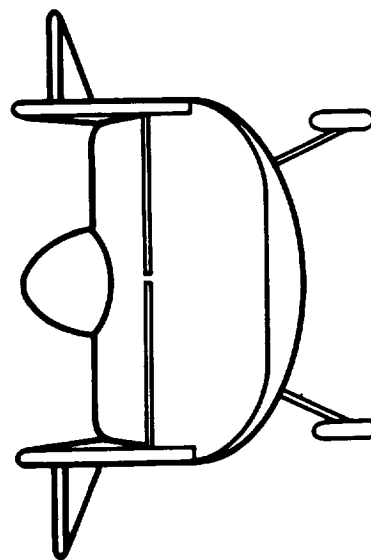
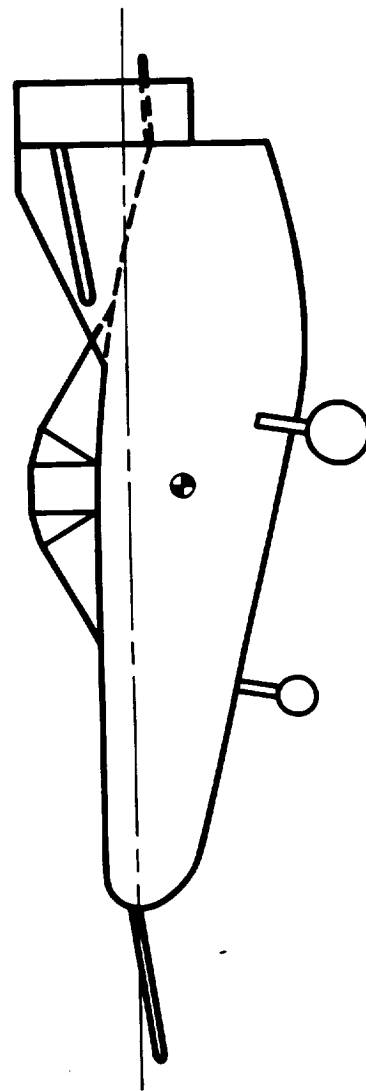
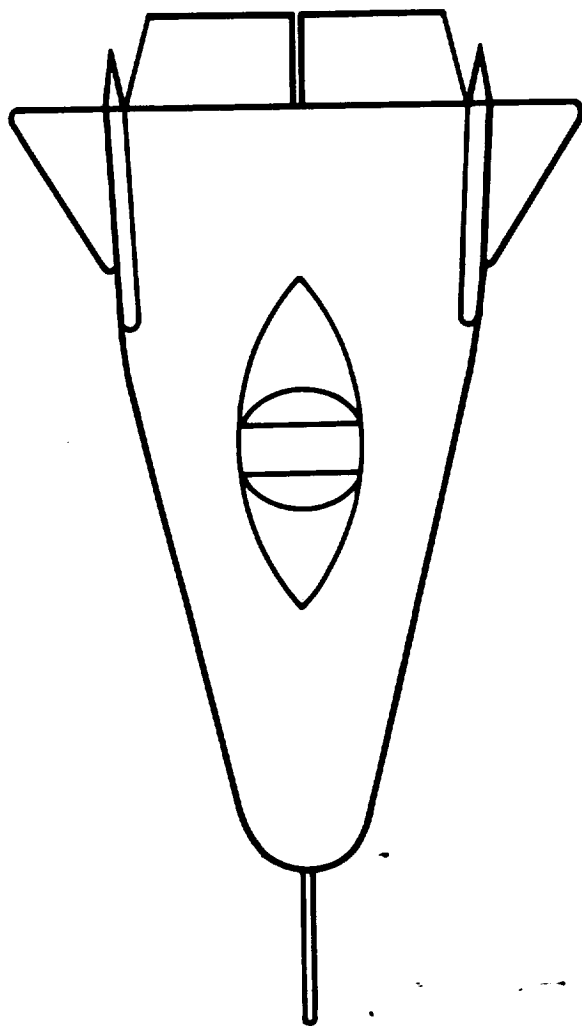


ENTRY:

NOMINAL 3200 °F

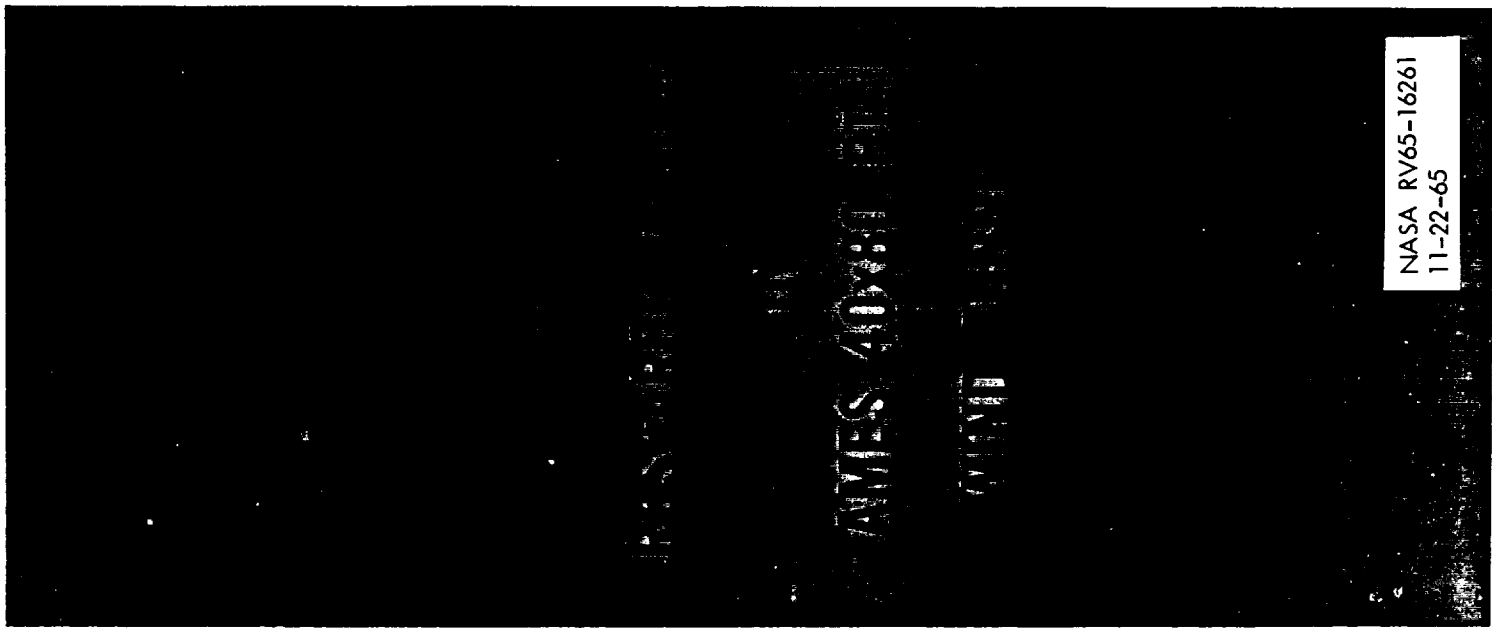
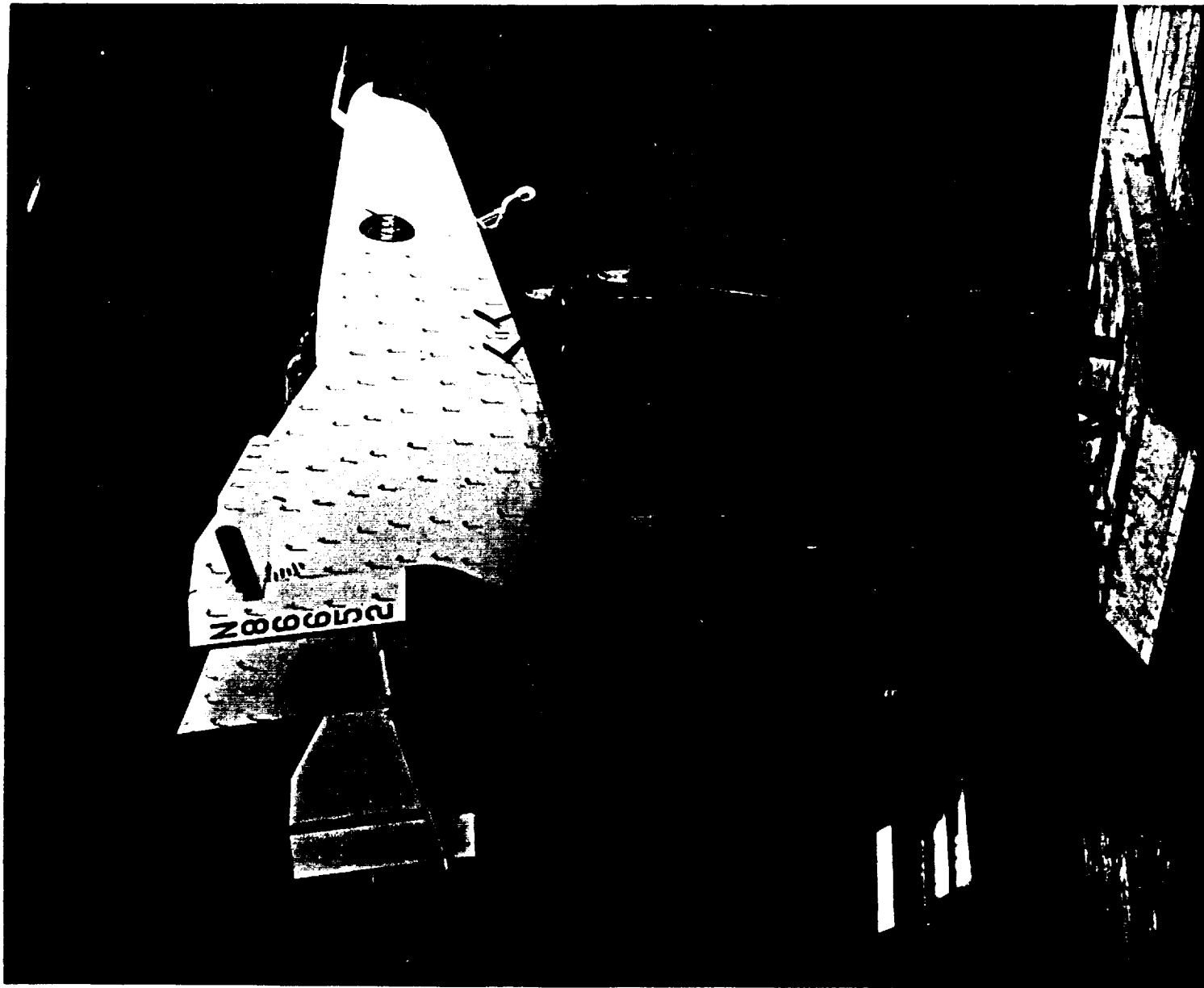
ABORT 3650 °F

# M2-F1 RESEARCH VEHICLE



NASA RV65-16279  
11-22-65

Figure 8

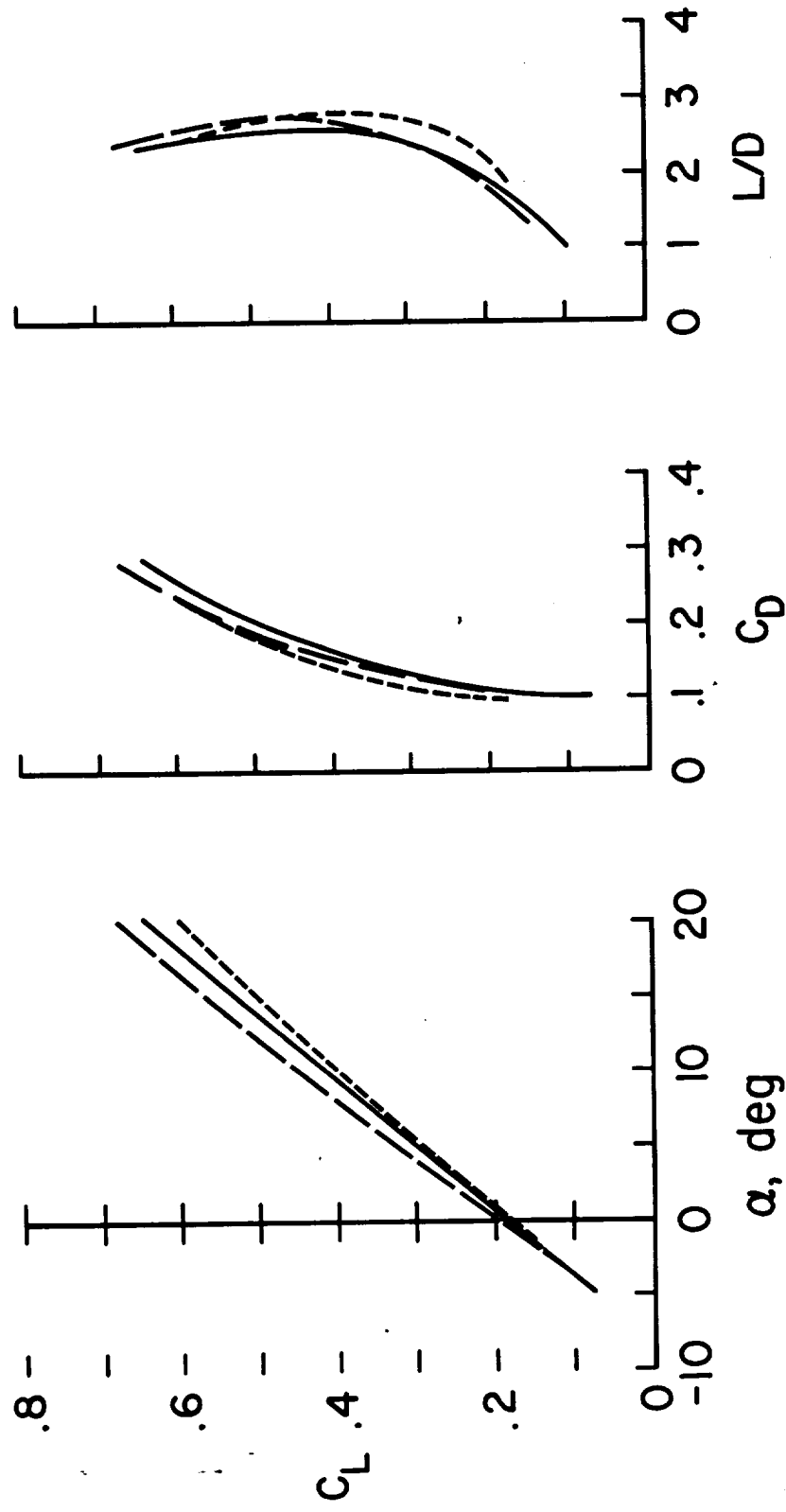


NASA RV65-16261  
11-22-65

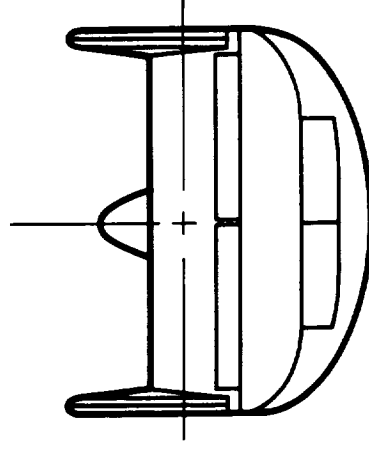
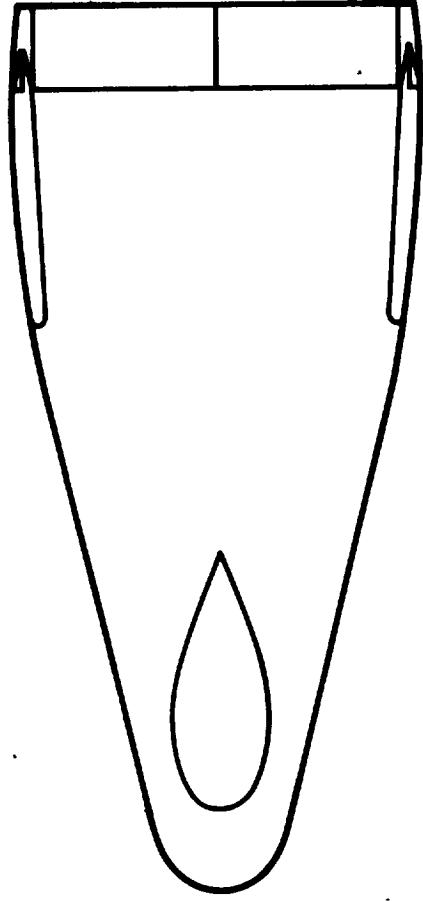


# M2-F1 LOW SPEED TRIMMED LIFT-DRAG CHARACTERISTICS

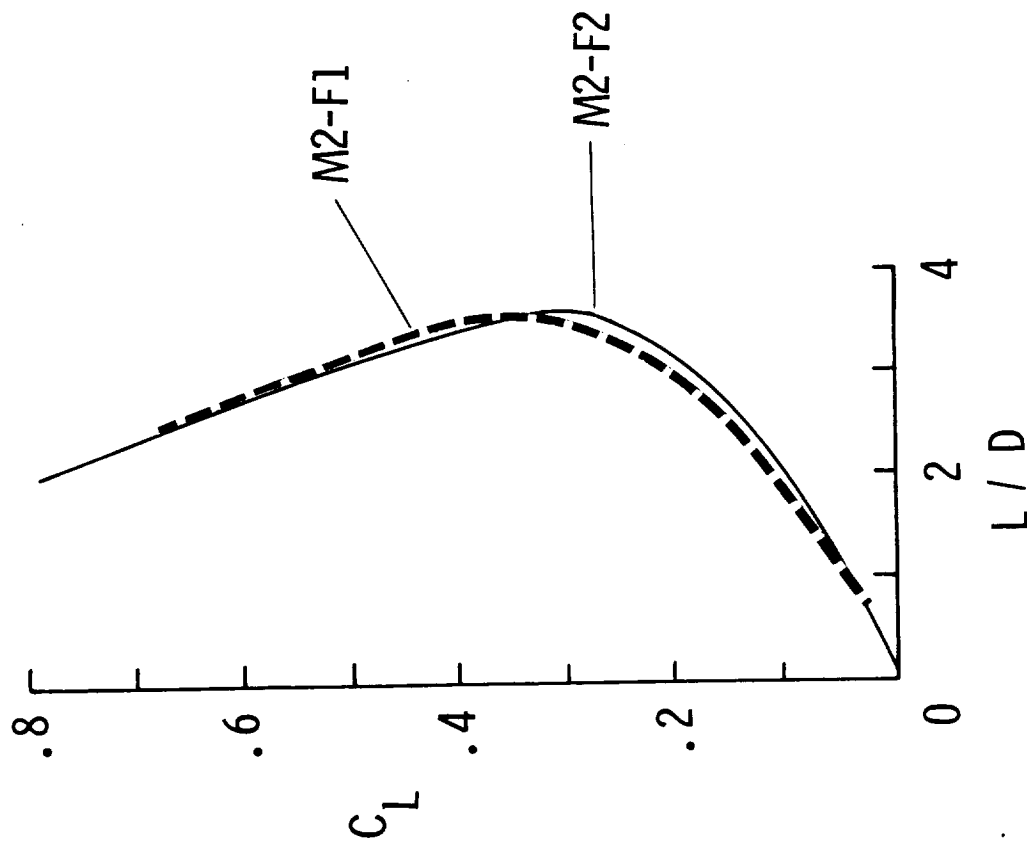
----- FLIGHT  
 ——— 40x80 FT W.T. CONTROL FIXED  
 - - - 40x80 FT W.T. STICK FIXED



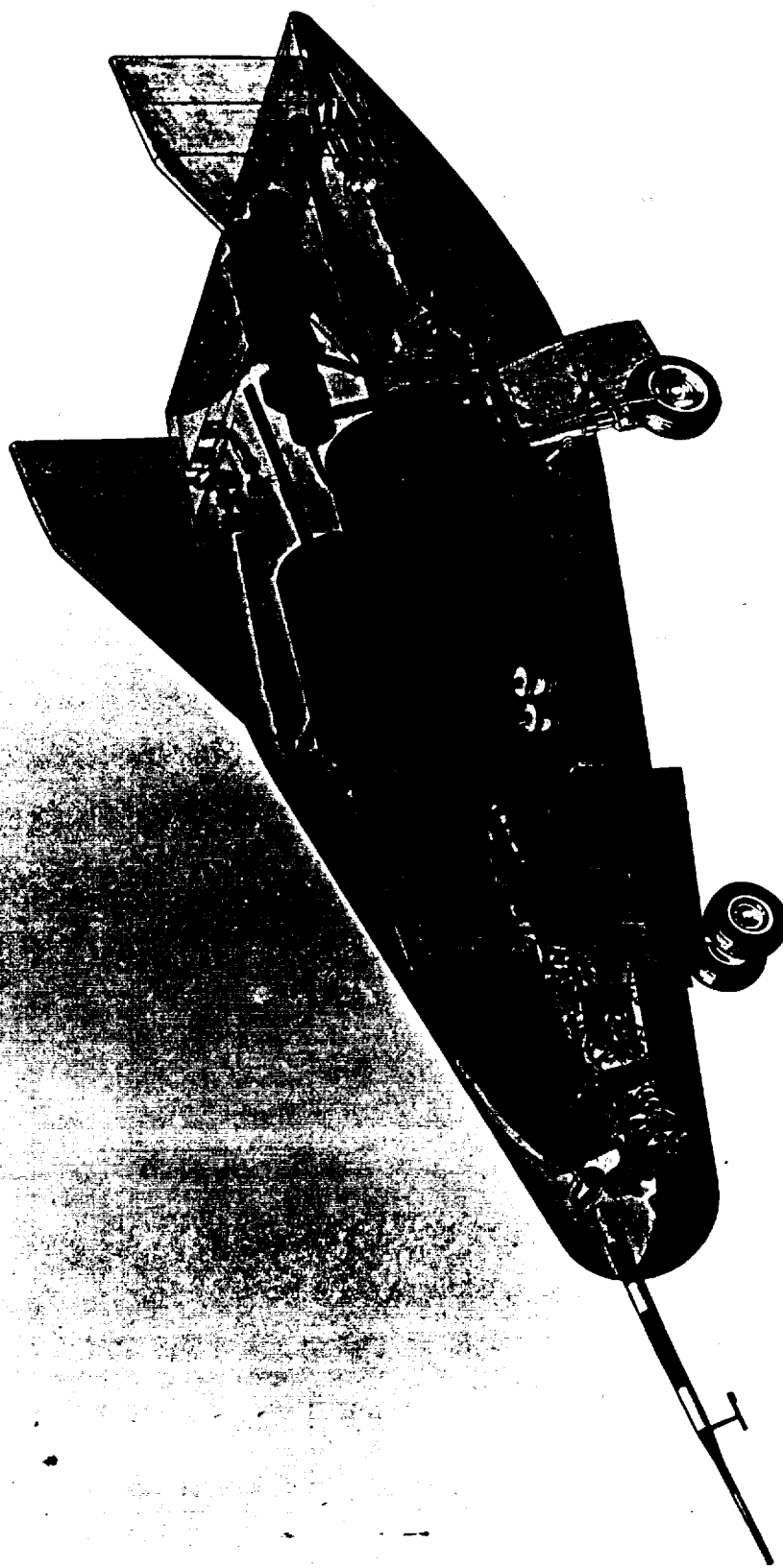
# M2-F2 CONFIGURATION



# COMPARISON OF LOW SPEED L/D FOR M2-F1 AND M2-F2



# M-2/XLR-11 VEHICLE



NASA RV65-16270  
11-22-65

NORTHROP

# LOW SPEED CHARACTERISTICS

— 40x80 FT W.T.  
 -- 12 FT P.W.T.

T<sub>1</sub> TRANSITION STRIP 1  
 T<sub>2</sub> TRANSITION STRIP 2

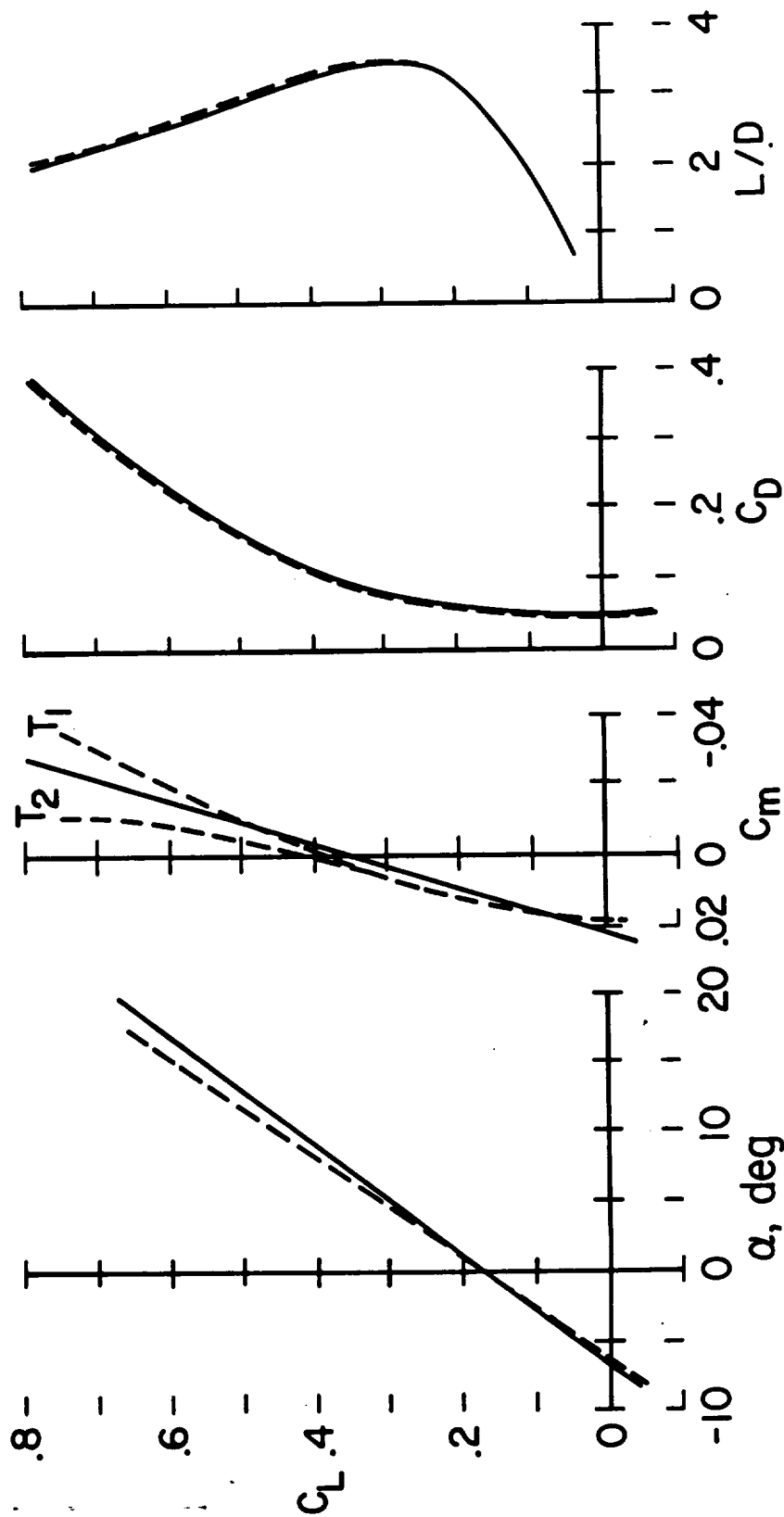


Figure 14

# M2-F2 TRANSONIC PITCH-UP?

1.0

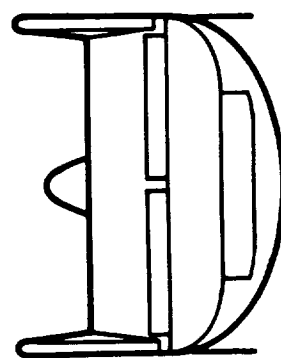
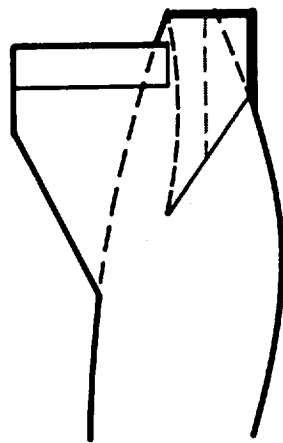
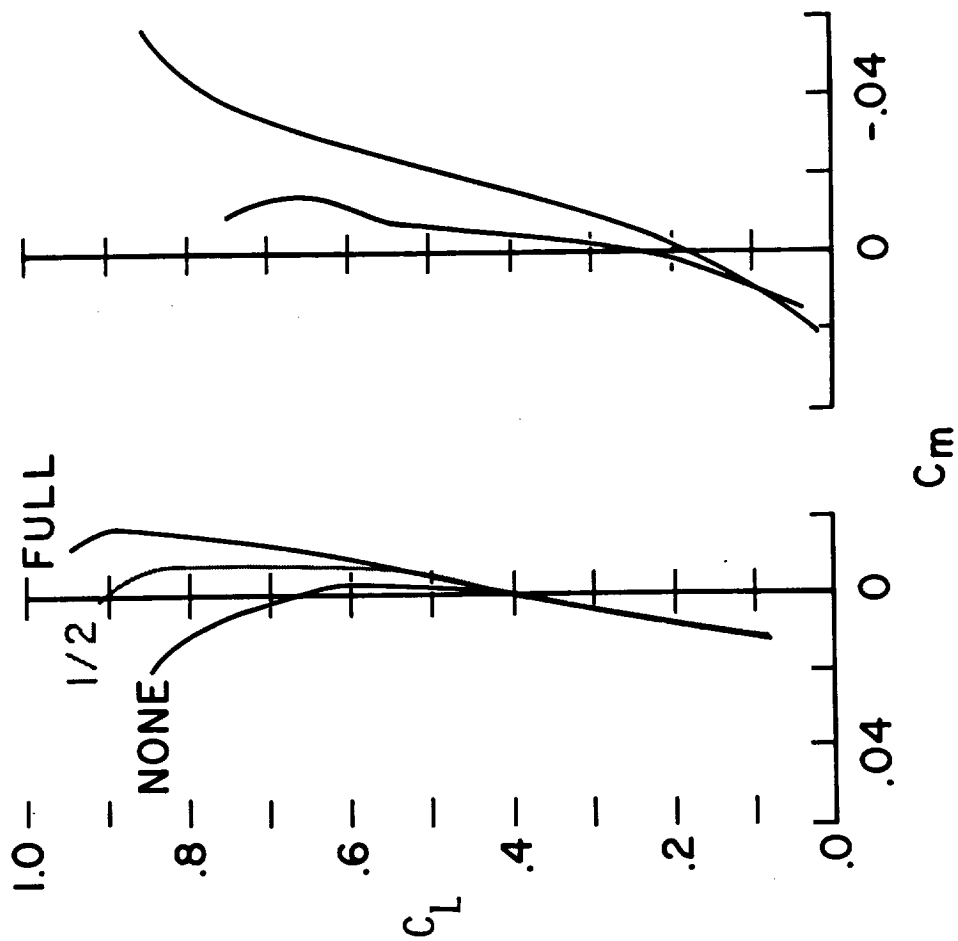
$\delta f_l = 35^\circ$

0.95

$\delta f_u = -20^\circ$

M=0.8

STRAKES



# M2-F2 CONTROL CROSS COUPLING

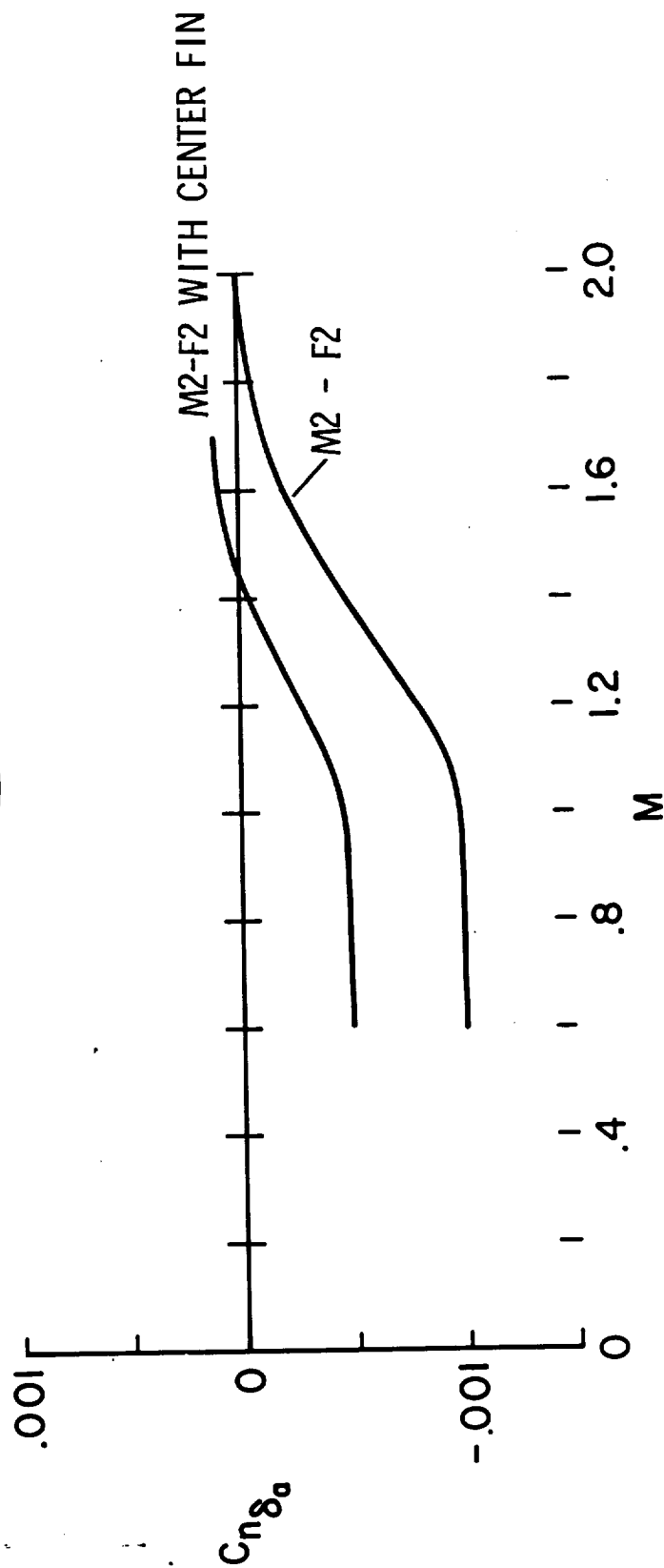
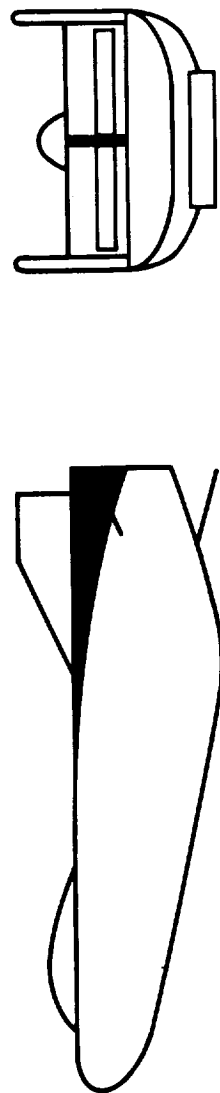
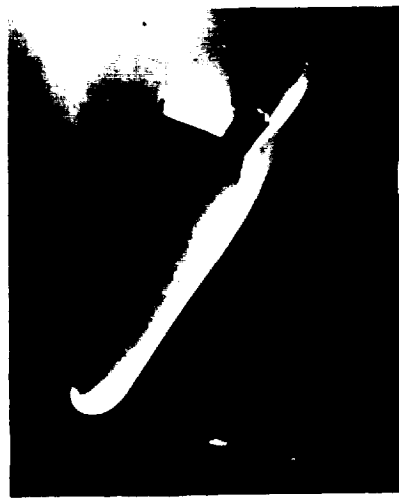


Figure 16

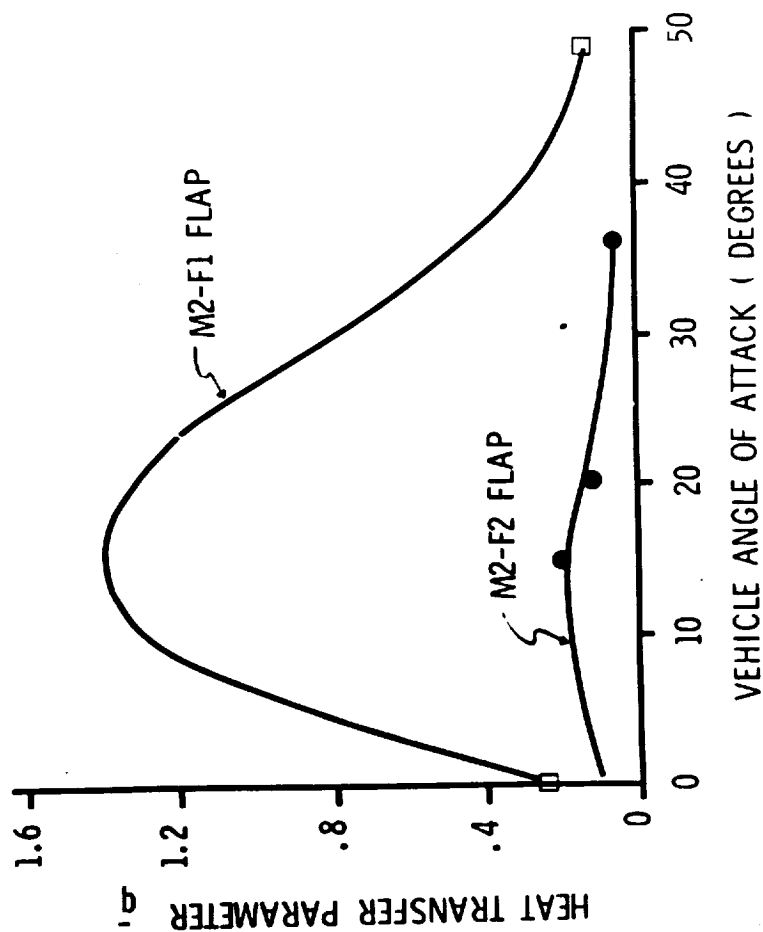
# M2-F1 AND M2-F2 PITCH CONTROL HEATING COMPARISON



M2-F1



M2-F2





# SOME OF THE HL-10 FIN ARRANGEMENTS STUDIED

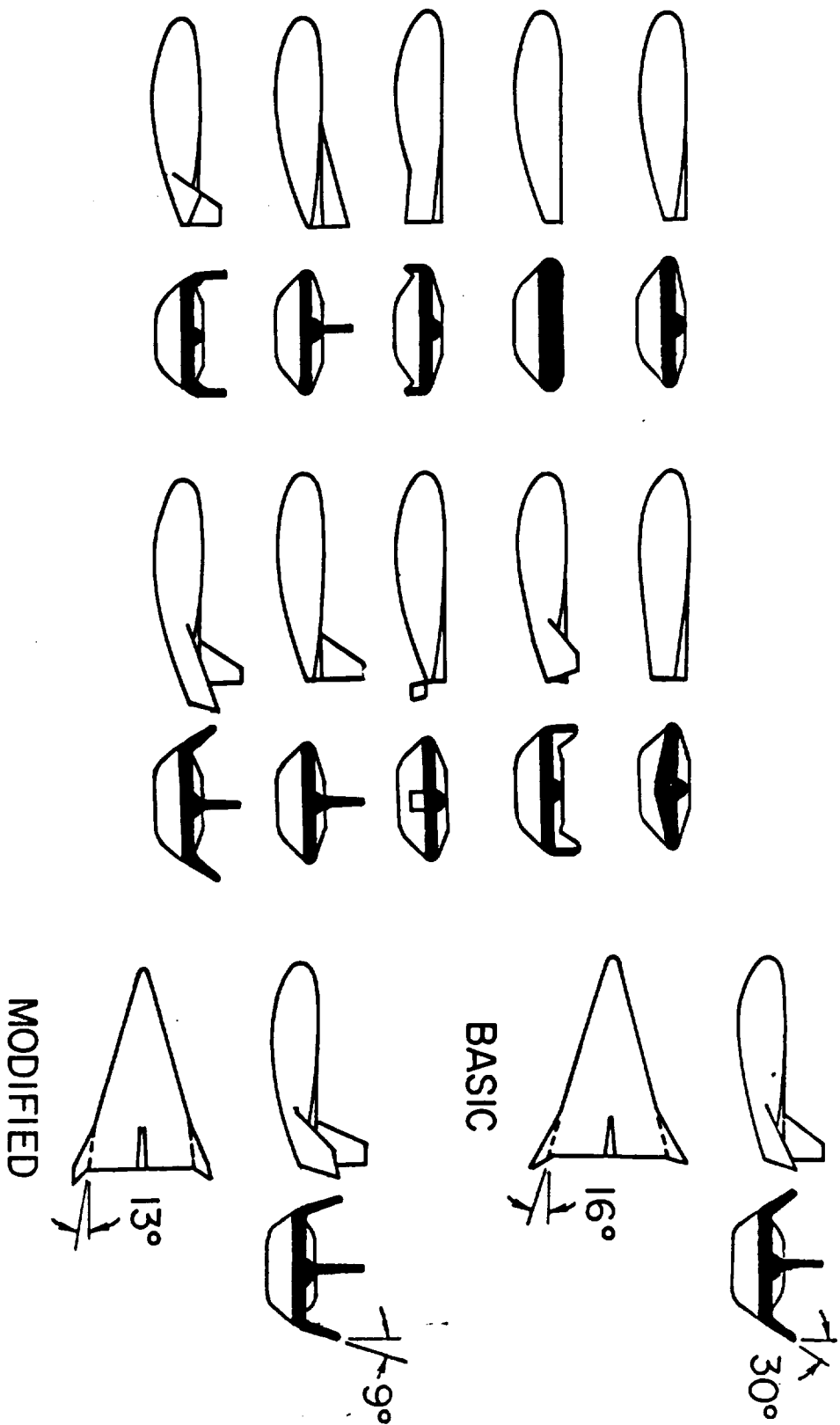


Figure 13

# HL-10 TRANSONIC LONGITUDINAL STABILITY

○ WITHOUT TRANSONIC FIXES

$M \approx 0.8; \delta \epsilon = 0^\circ$

□ WITH TRANSONIC FIXES

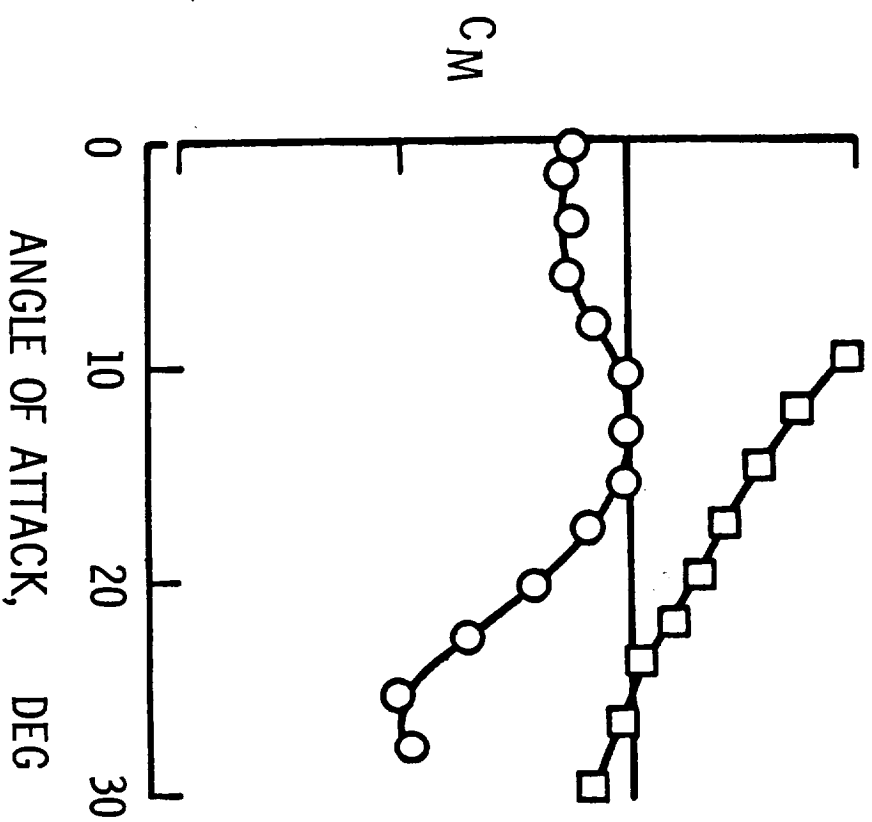
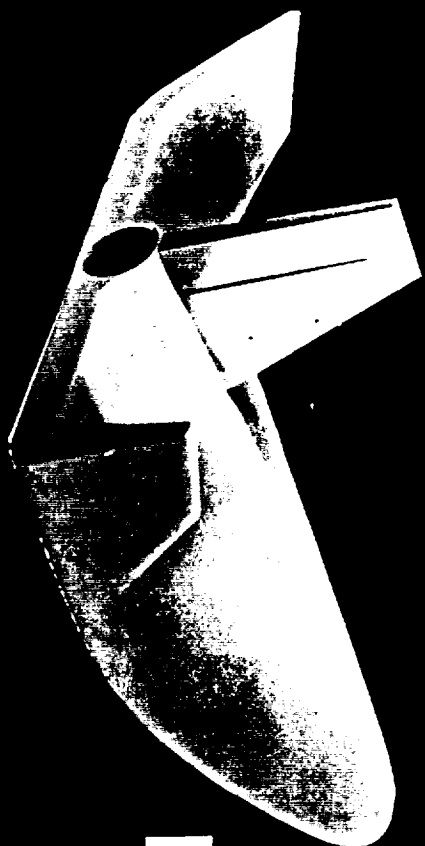


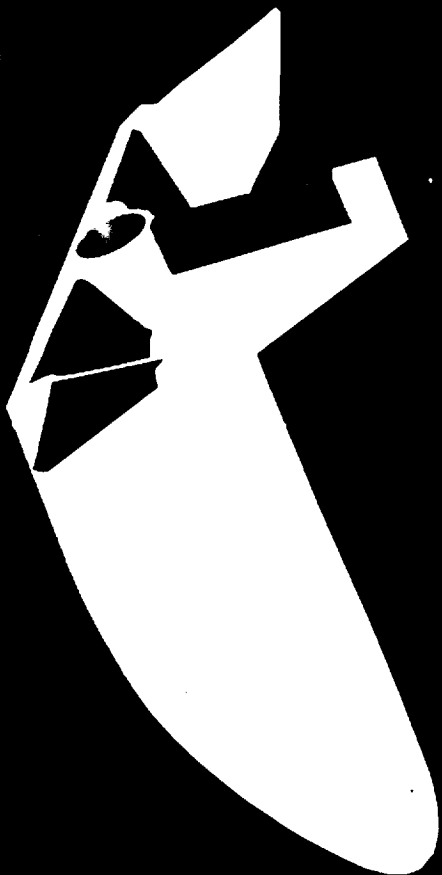
Figure 19

# HL - 10 VEHICLE WITH MODIFICATIONS

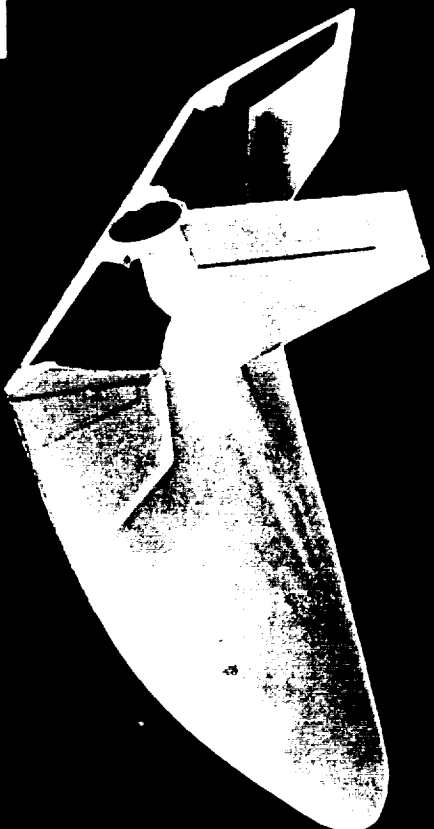


WITHOUT FIXES

WITH SUBSONIC FIXES



WITH TRANSONIC FIXES



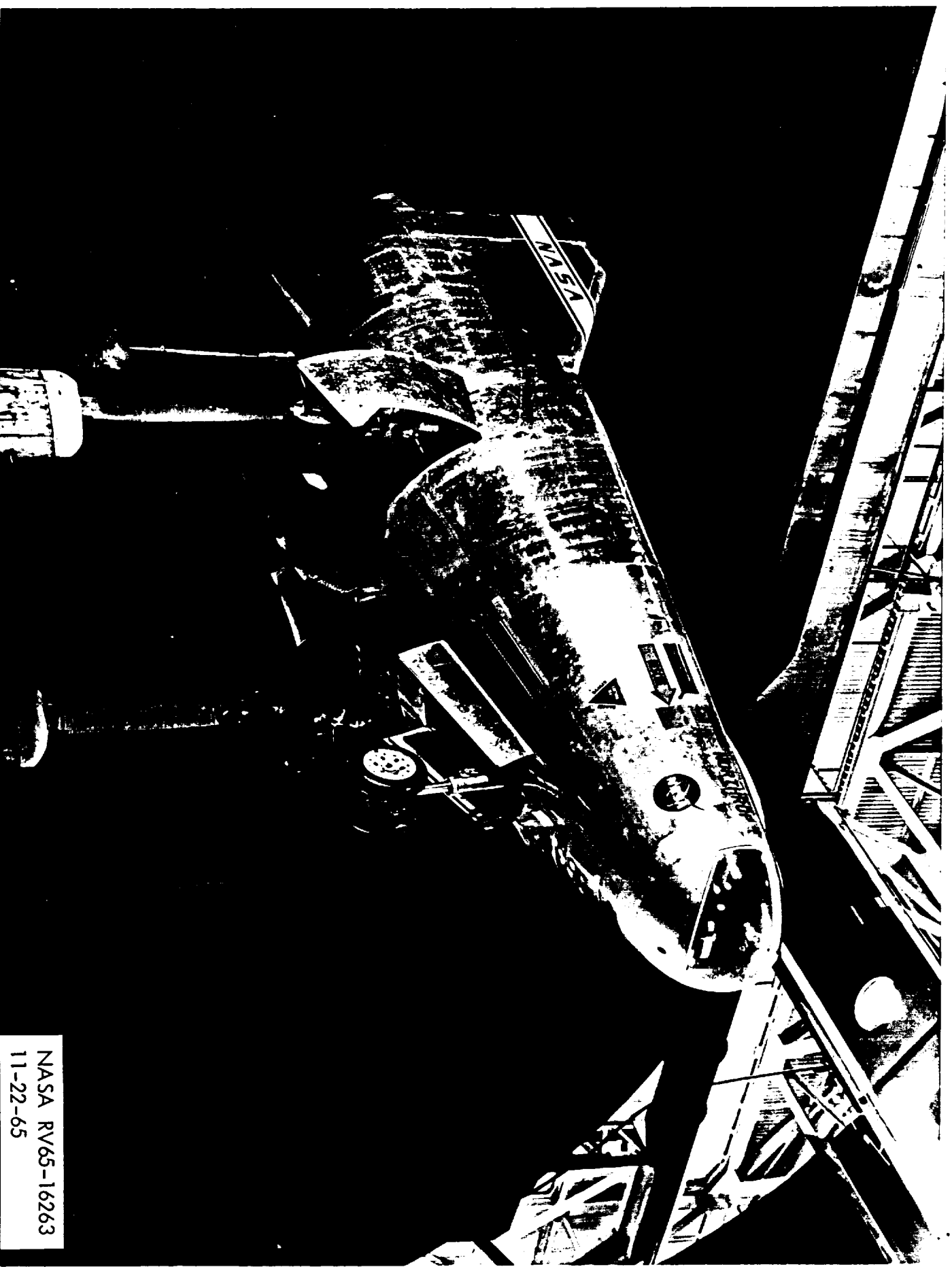
NASA R. 65-16260  
11-22-65

# HL-10 IN LRC FULL SCALE WIND TUNNEL



NASA RV65-16262  
11-22-65

# M2-F2 RESEARCH VEHICLE IN AMES 40X80 FT. WIND TUNNEL



NASA RV65-16263  
11-22-65

# M2-F2 STABILITY CHARACTERISTICS

$\alpha$ , DEG  
 0  
 6  
 12  
 37

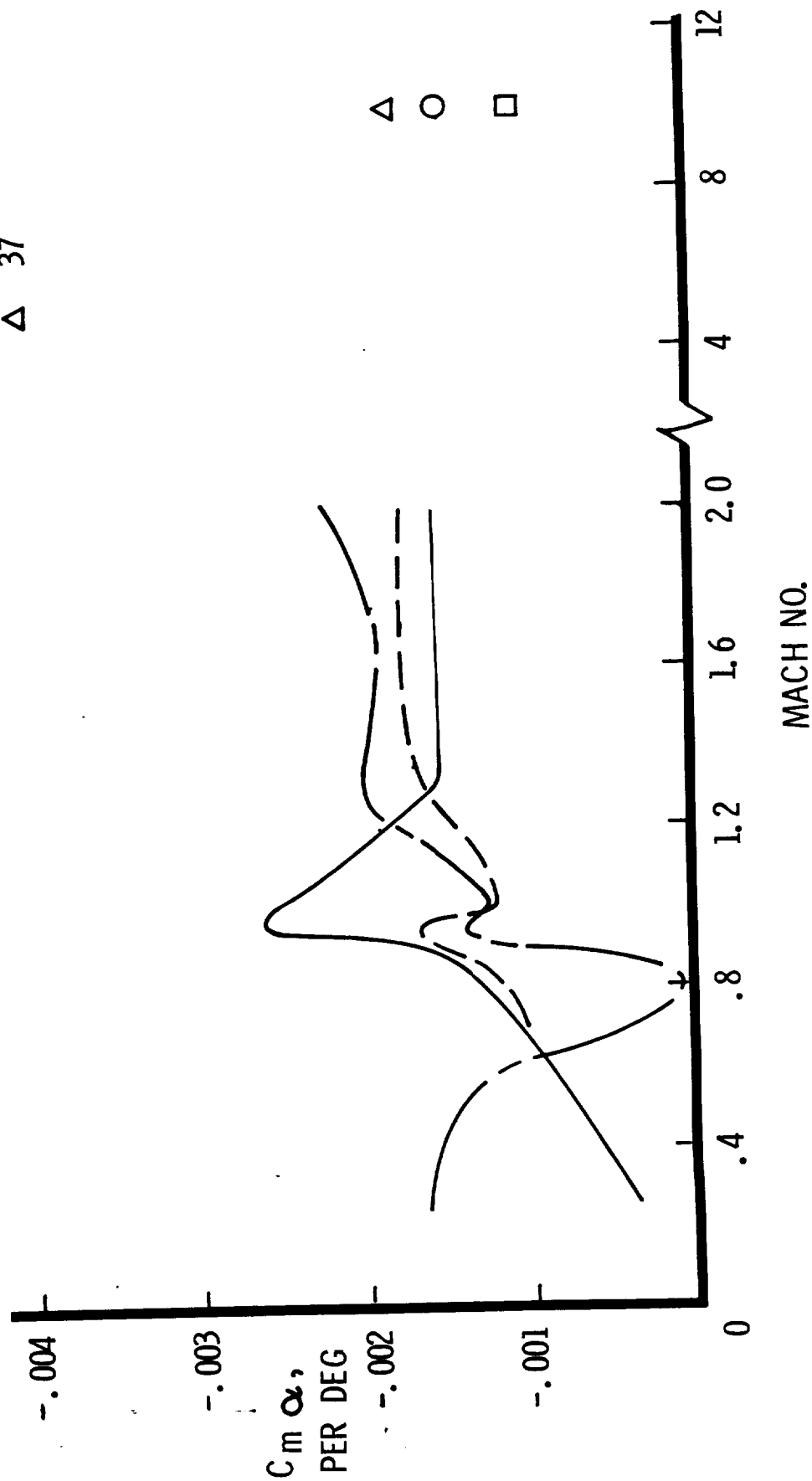
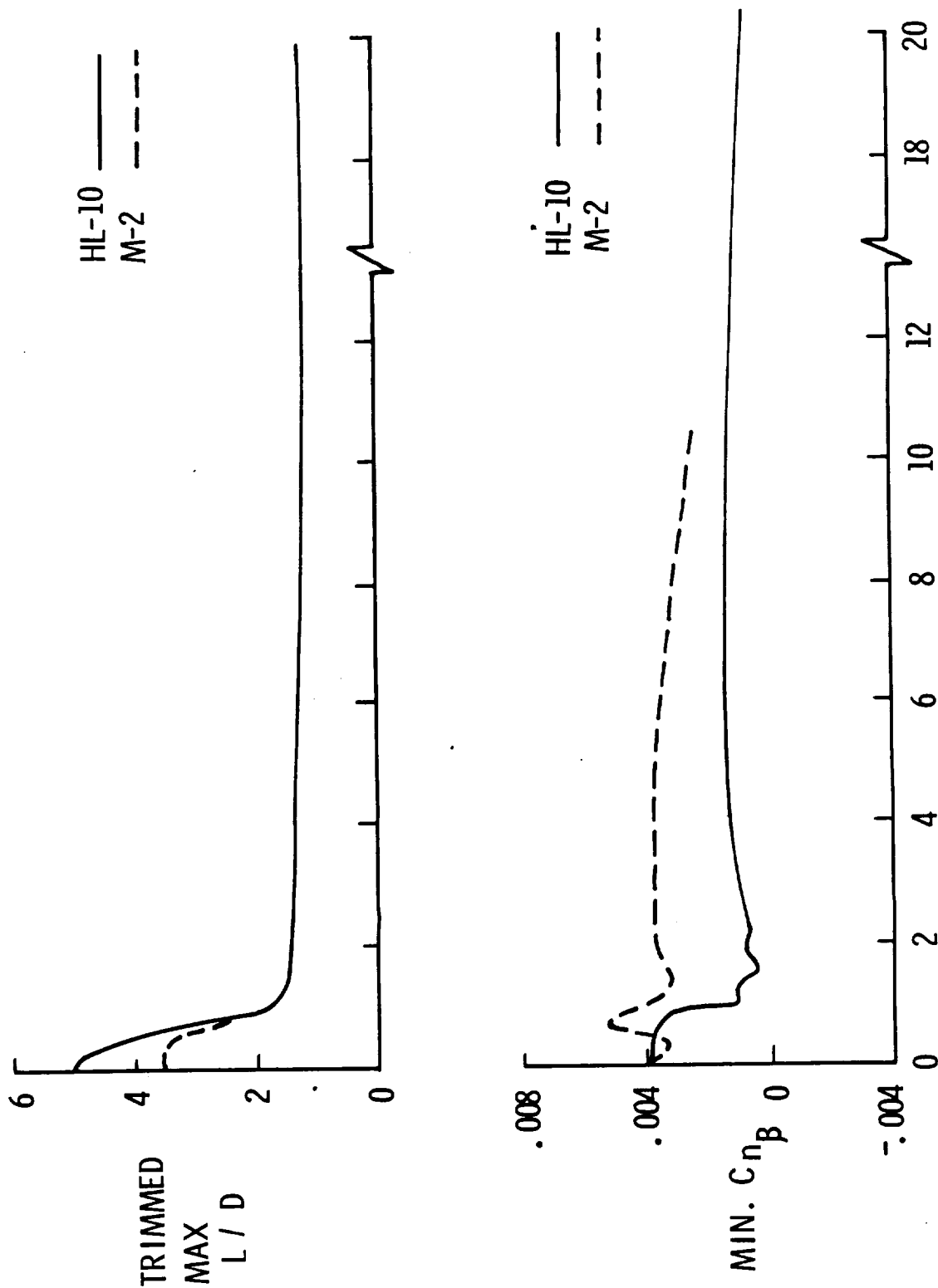


Figure 23

# M2-F2 AND HL-10 CHARACTERISTICS



# HL-10 GROUND LANDING STUDIES



Figure 25



# HL-10 NEAR VERTICAL WATER LANDINGS

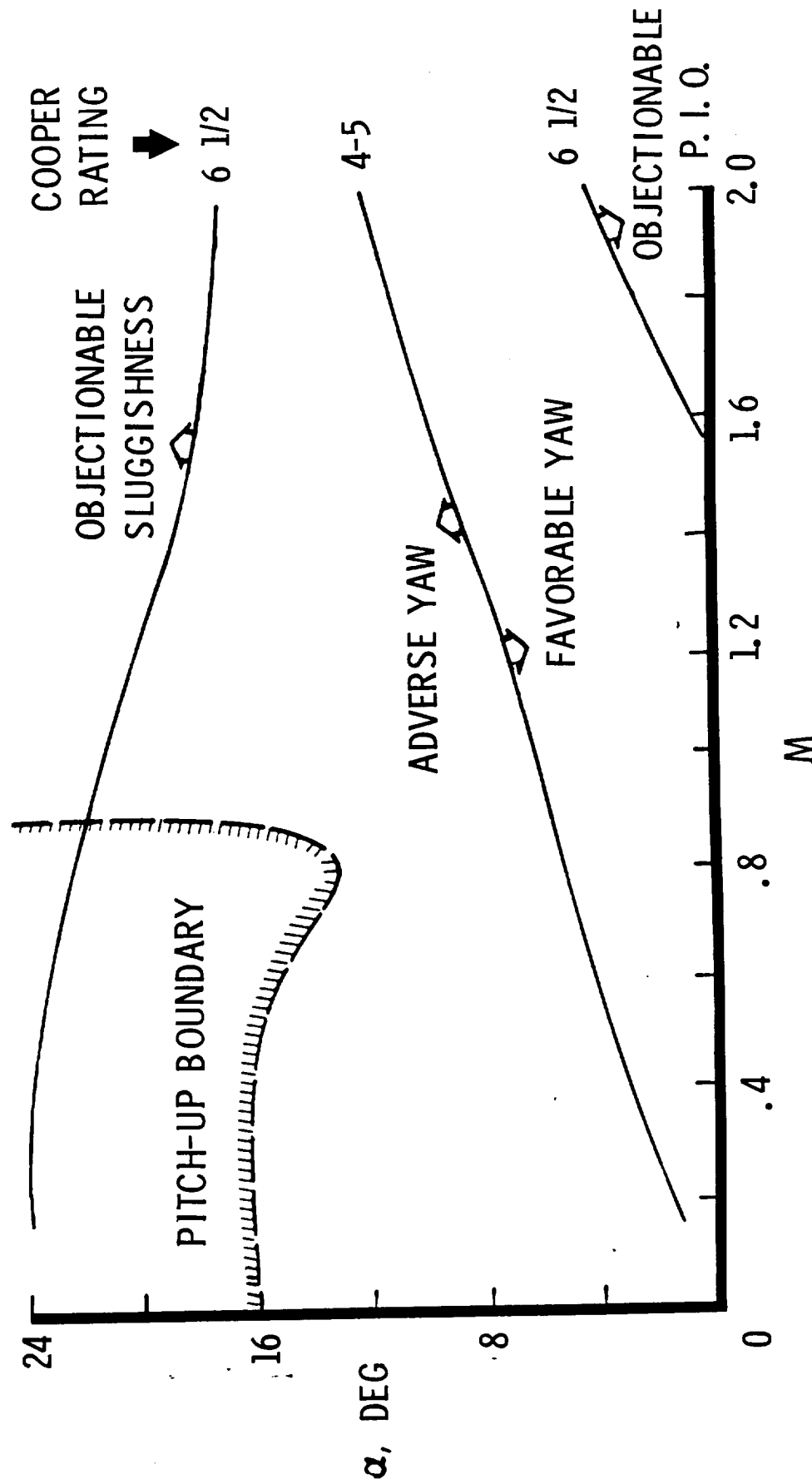


NASA RV65-10272

Figure 26

# M2-F2 ROLL CONTROL CHARACTERISTICS

WITH RUDDER INTERCONNECT  
DAMPERS OFF,  $q = 100$  PSF



# VARIABLE GEOMETRY SPACECRAFT MODEL

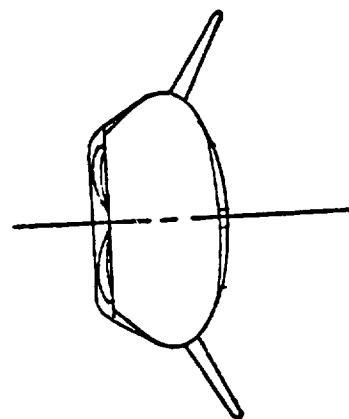
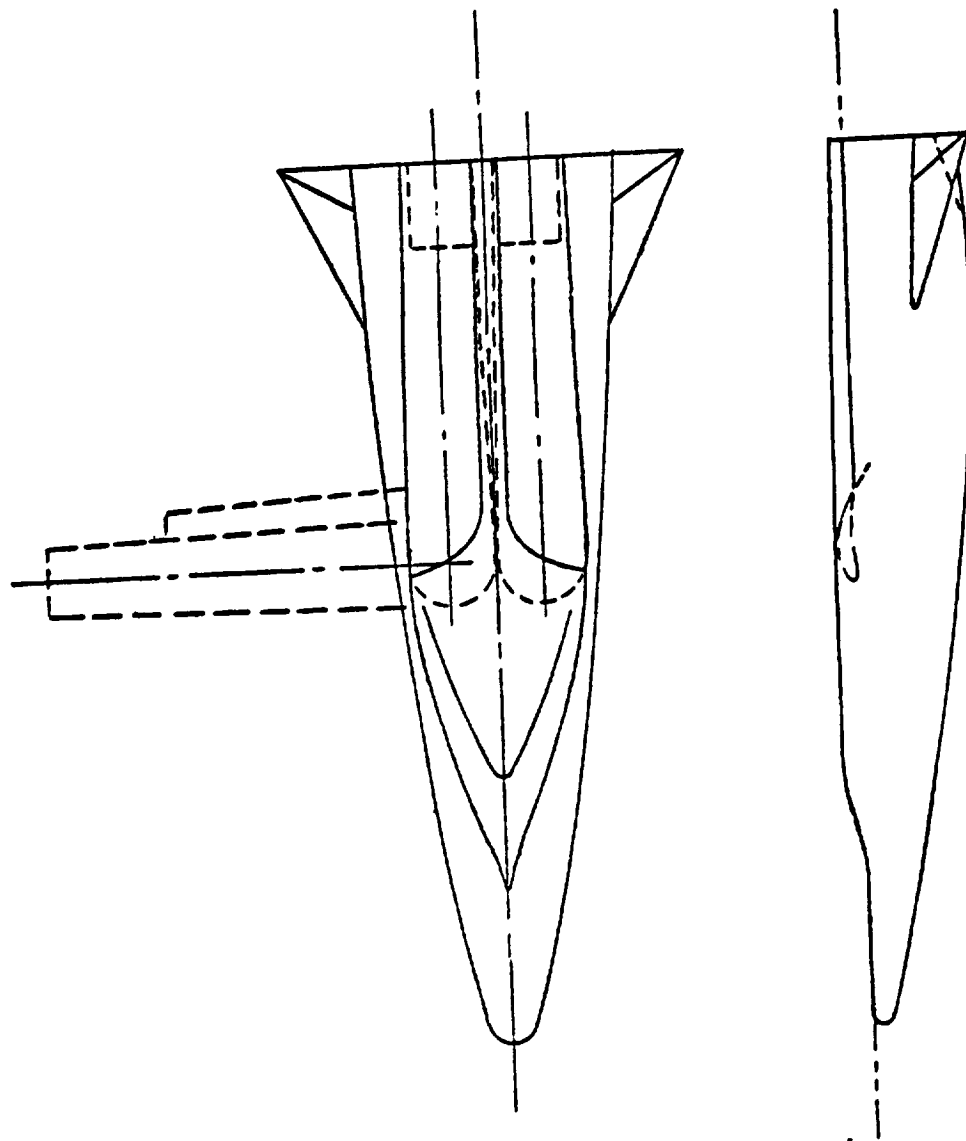
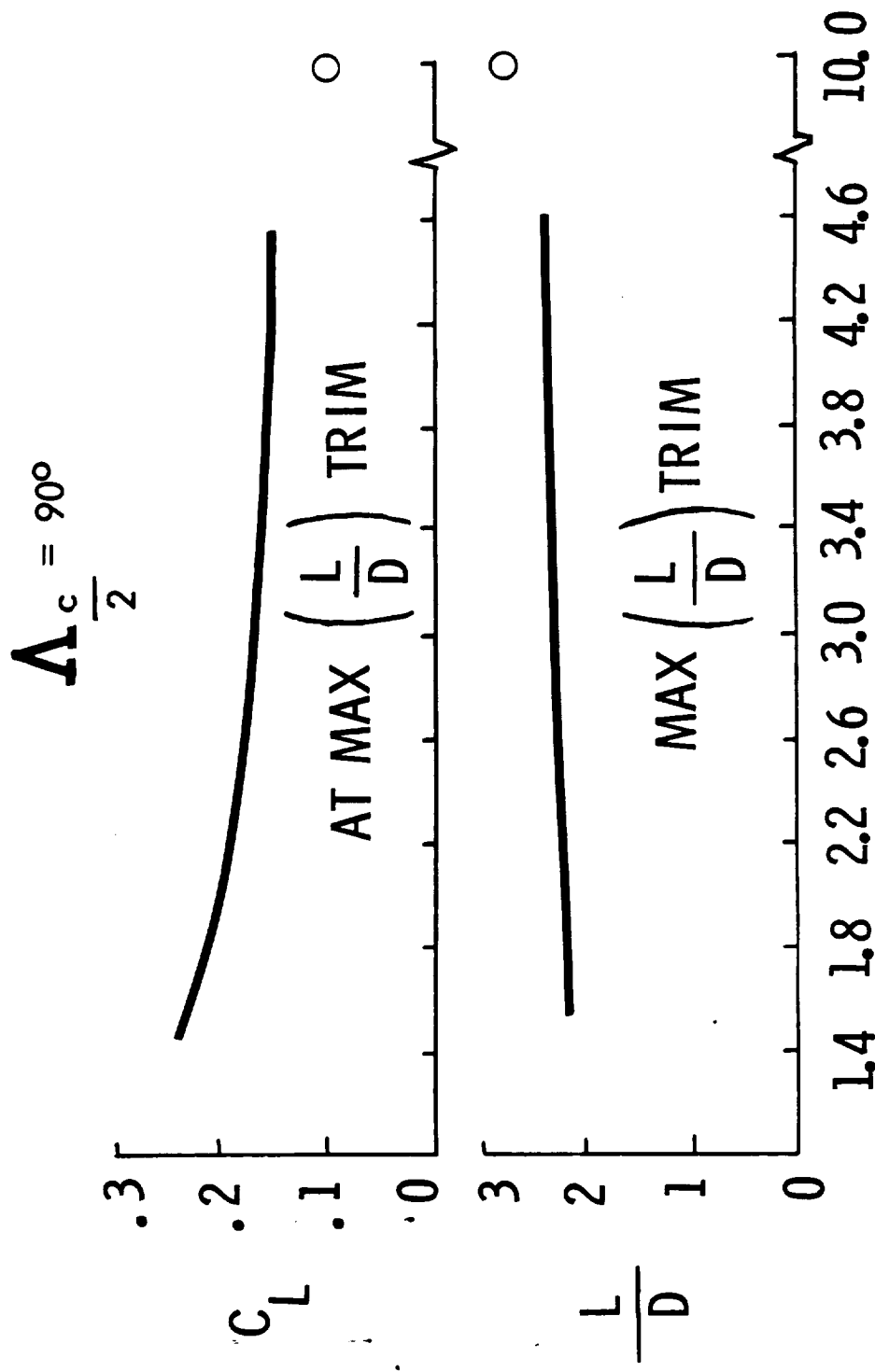


Figure 28

# VARIABLE GEOMETRY SPACECRAFT SUPersonic-HYPersonic CHARACTERISTICS



NASA RV65-16264  
11-22-65

Figure 30

# VARIABLE GEOMETRY SPACECRAFT LANDING

## CHARACTERISTICS - $M=0.3$ , $\Lambda_C=0^\circ$ , $R/FT=12 \times 10^6$

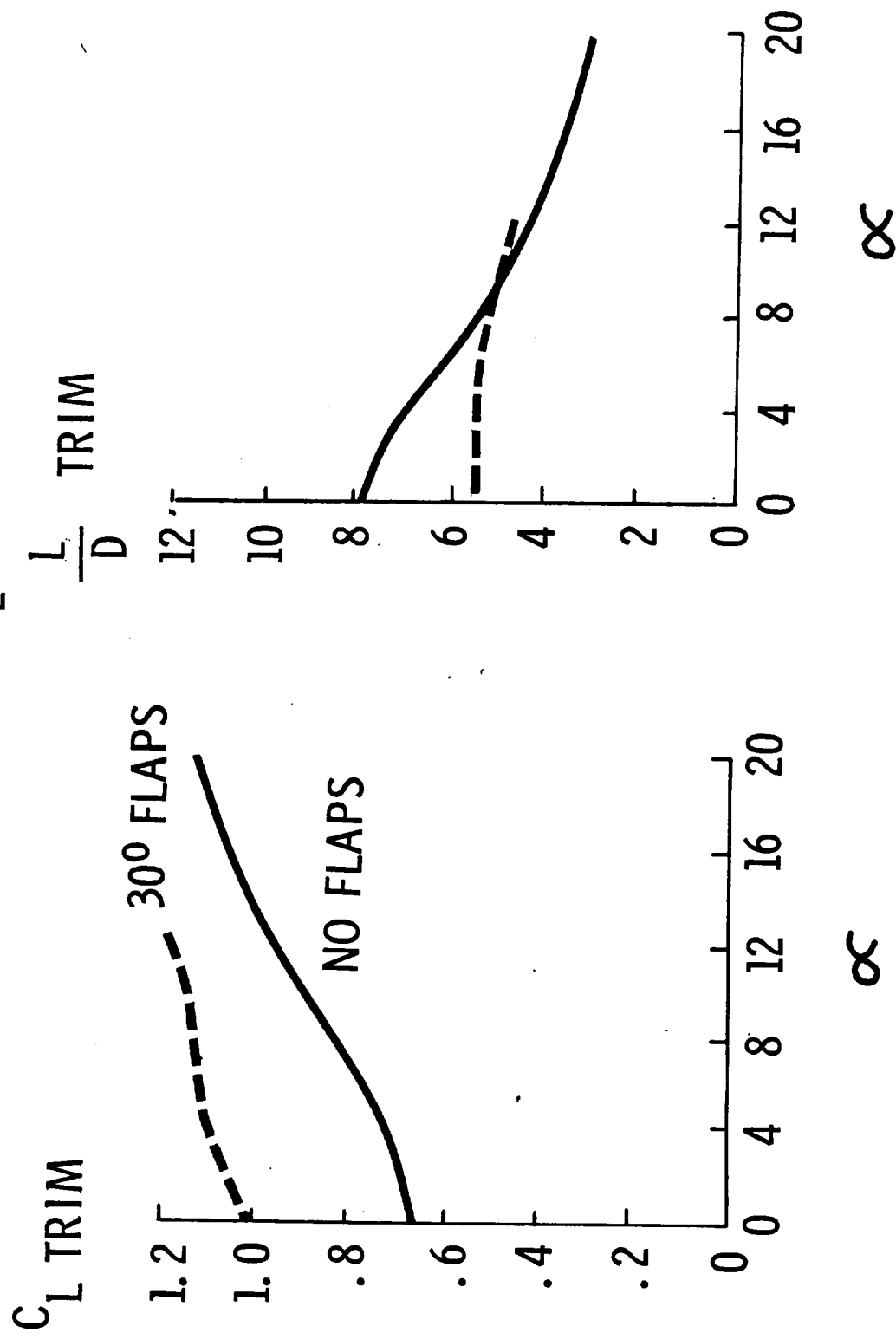
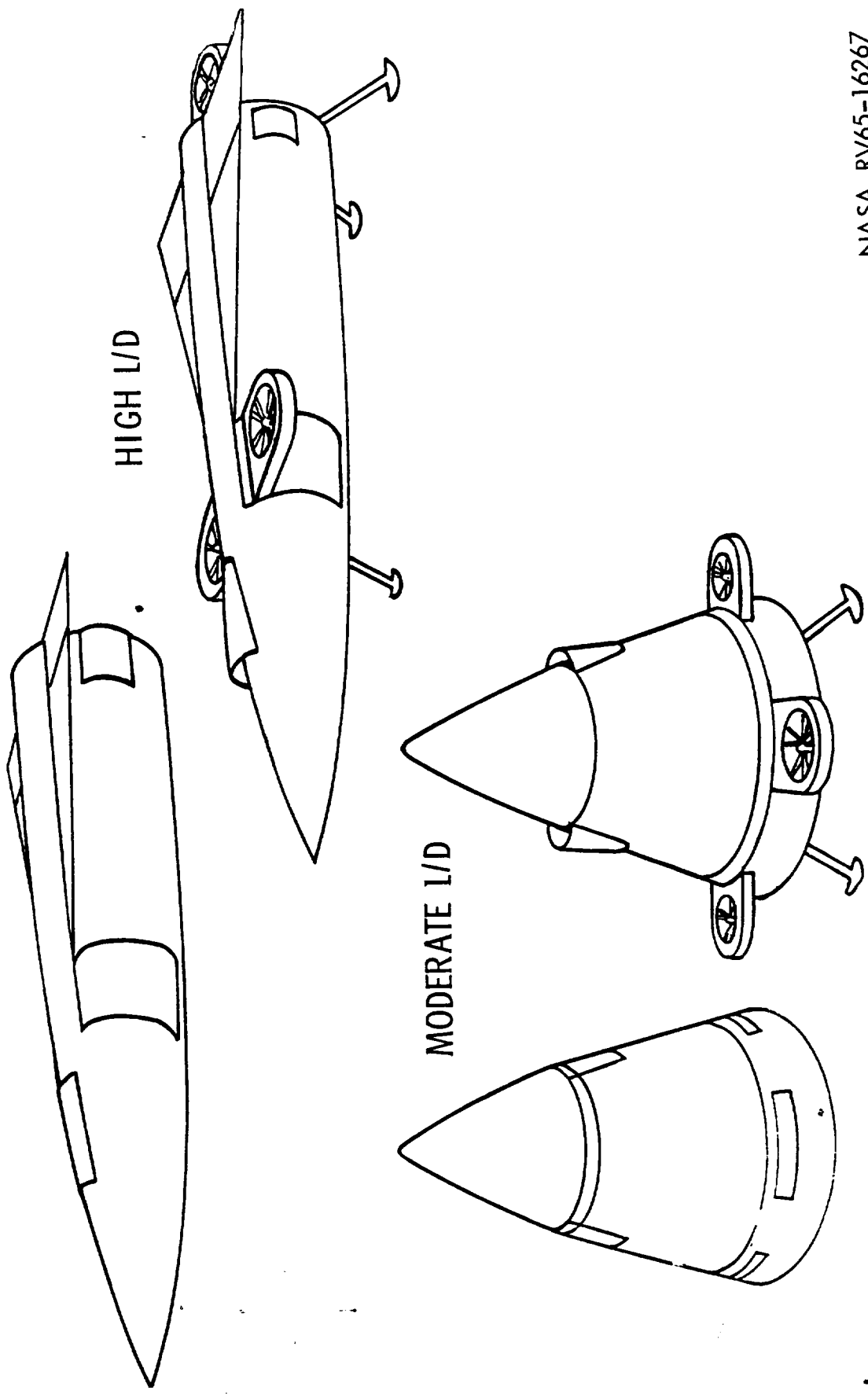


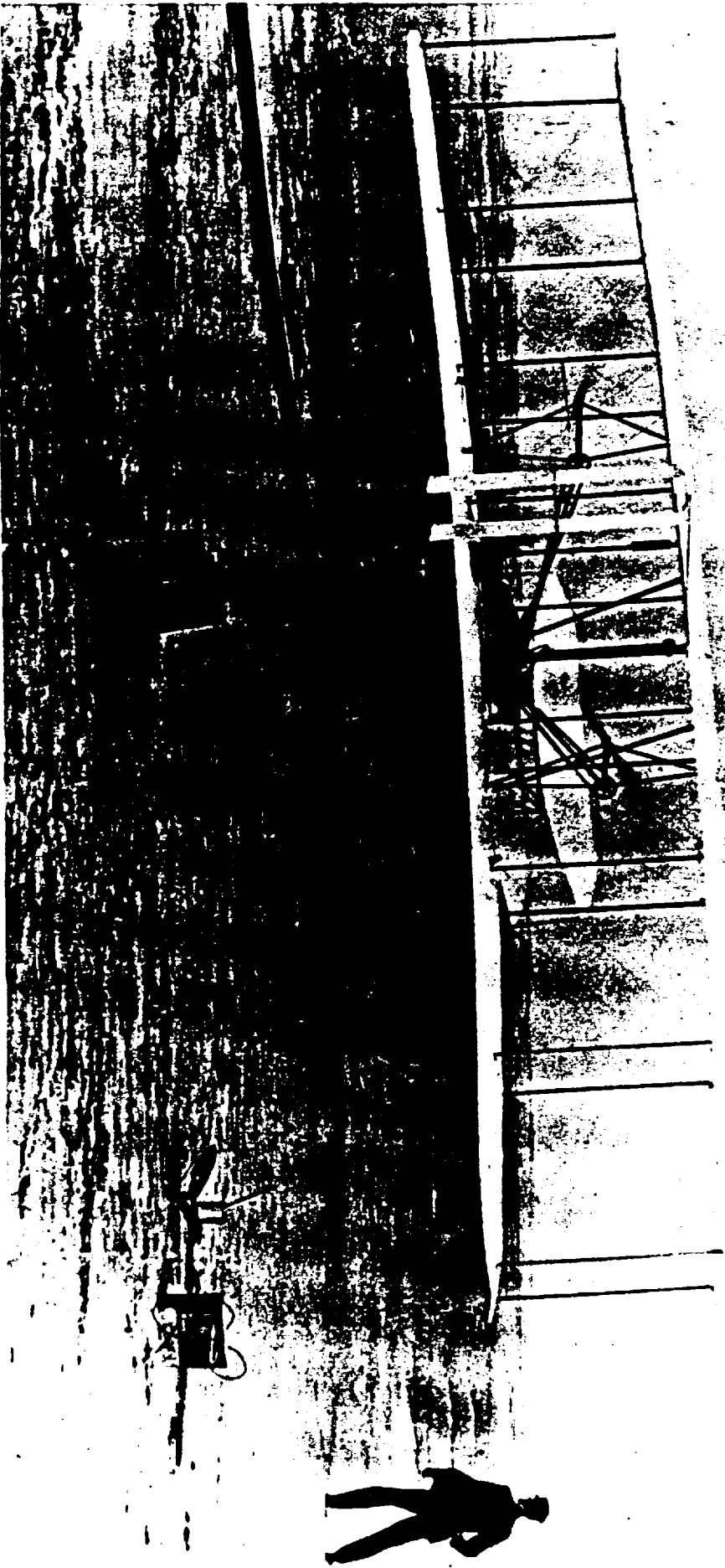
Figure 29

# VERTICAL LANDING CONCEPTS

## ILLUSTRATIVE LIFT-FAN APPLICATIONS

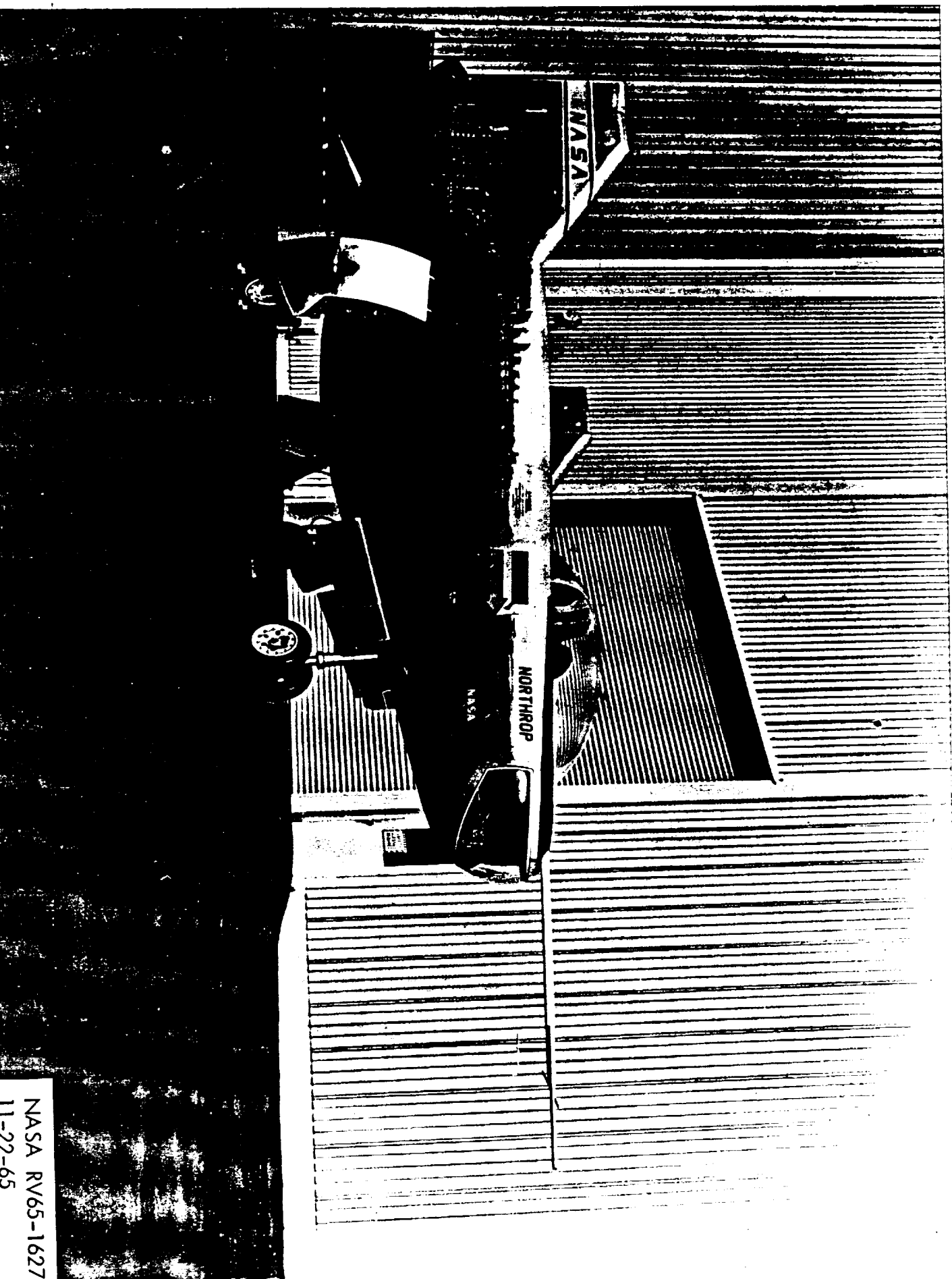


# WRIGHT BROTHERS FIRST FLIGHT



NASA RV65-16273  
11-22-65

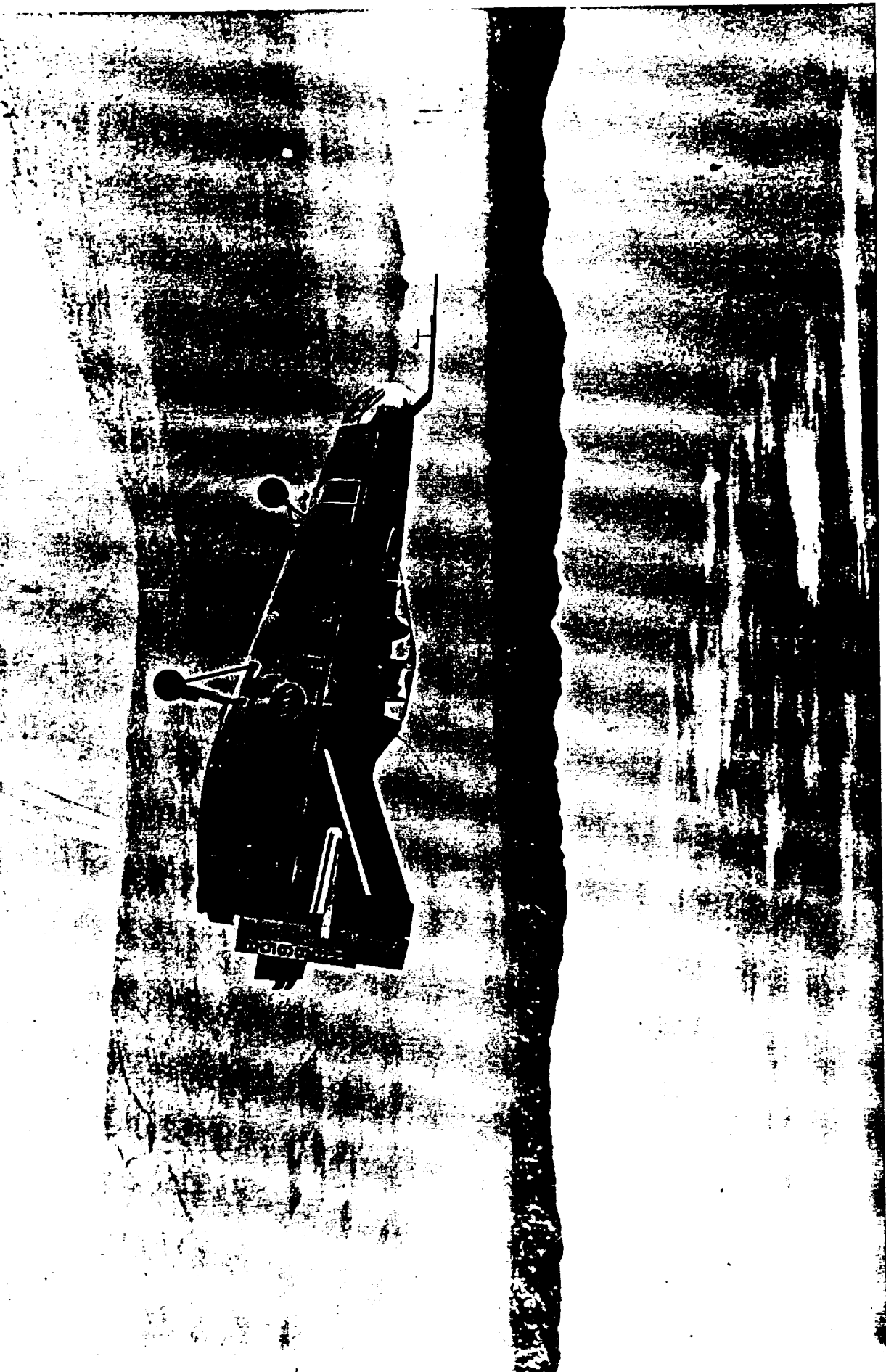
# M2-F2 LOW SPEED RESEARCH VEHICLE



NASA RV65-1627  
11-22-65



# M2-F1 LIGHT WEIGHT RESEARCH VEHICLE



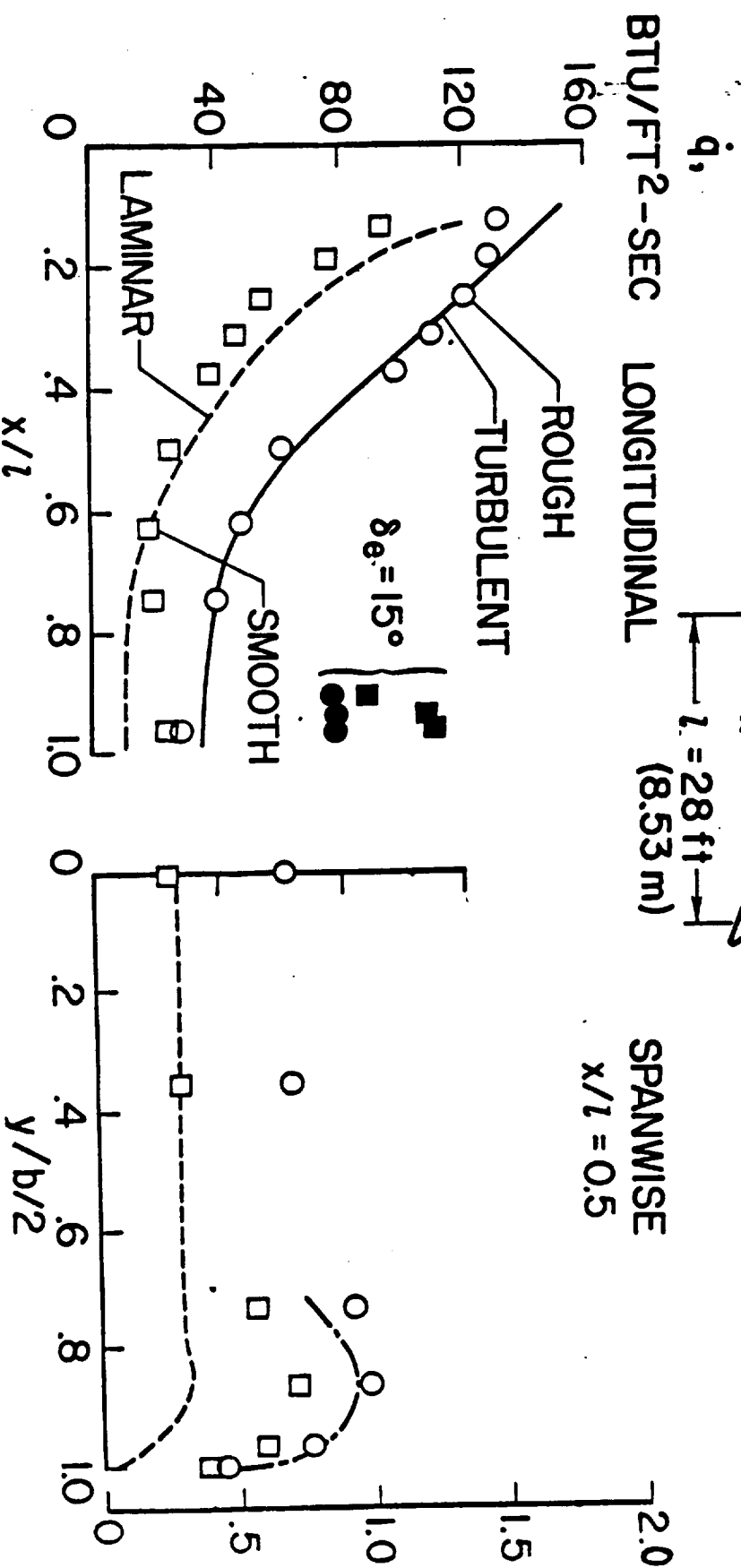
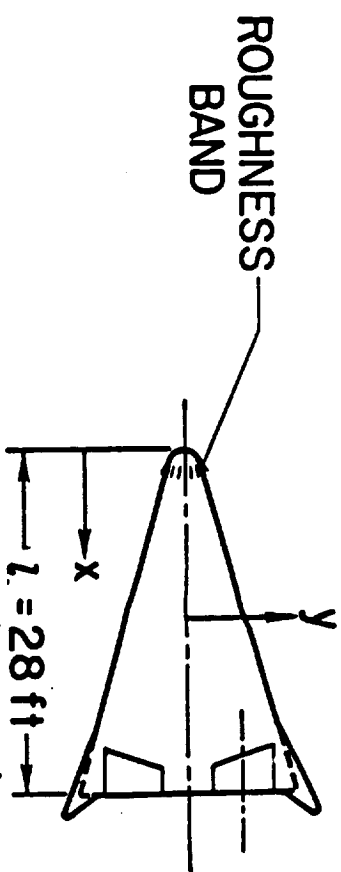
# HL-10 LOW SPEED RESEARCH VEHICLE



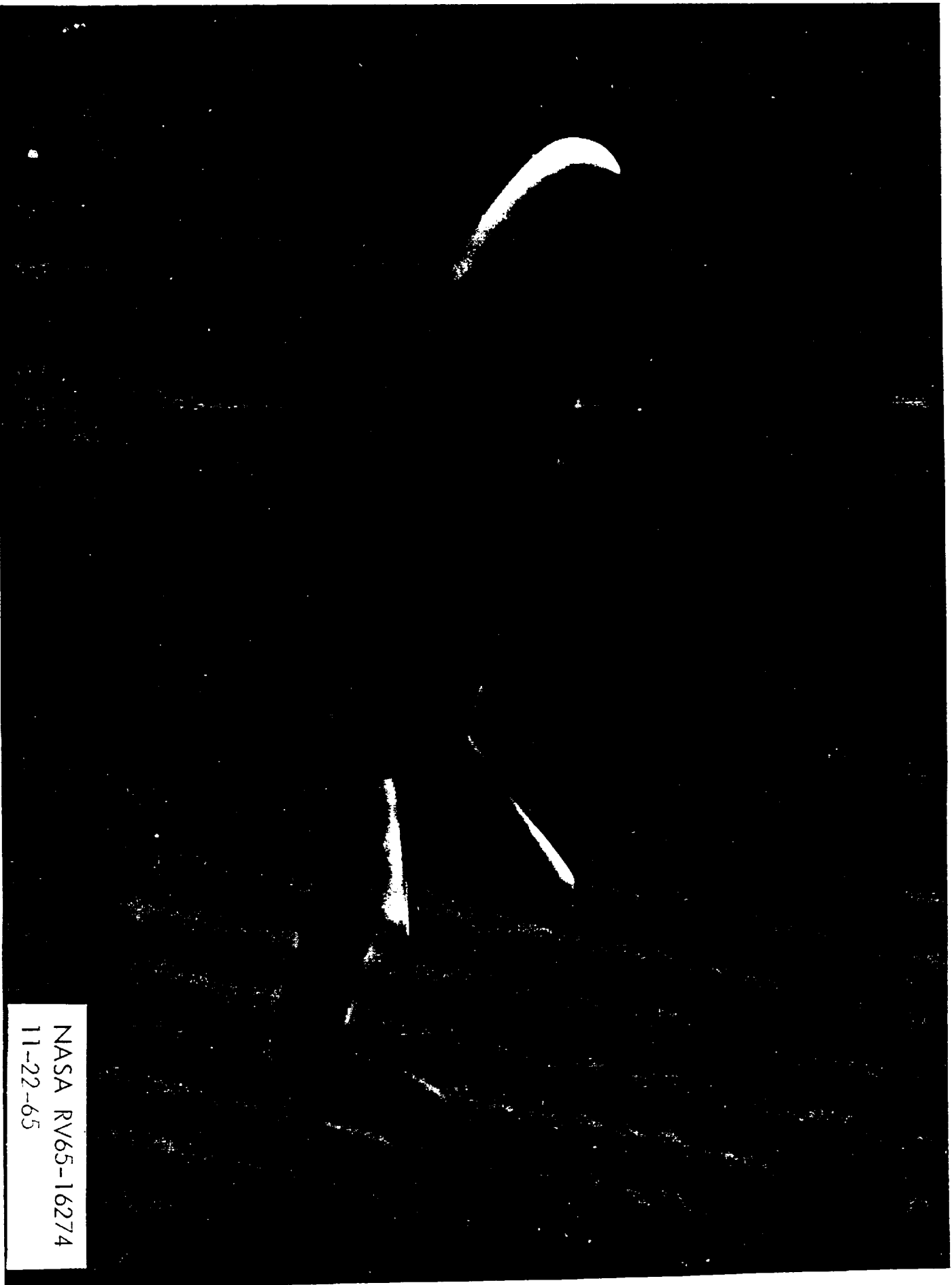
NASA RV65-16276  
11-22-65

# MAXIMUM HEATING DISTRIBUTION DURING 3g ENTRY

$$V_e = 25,500 \text{ ft/sec}; \alpha = 30^\circ; \delta e = 0^\circ$$

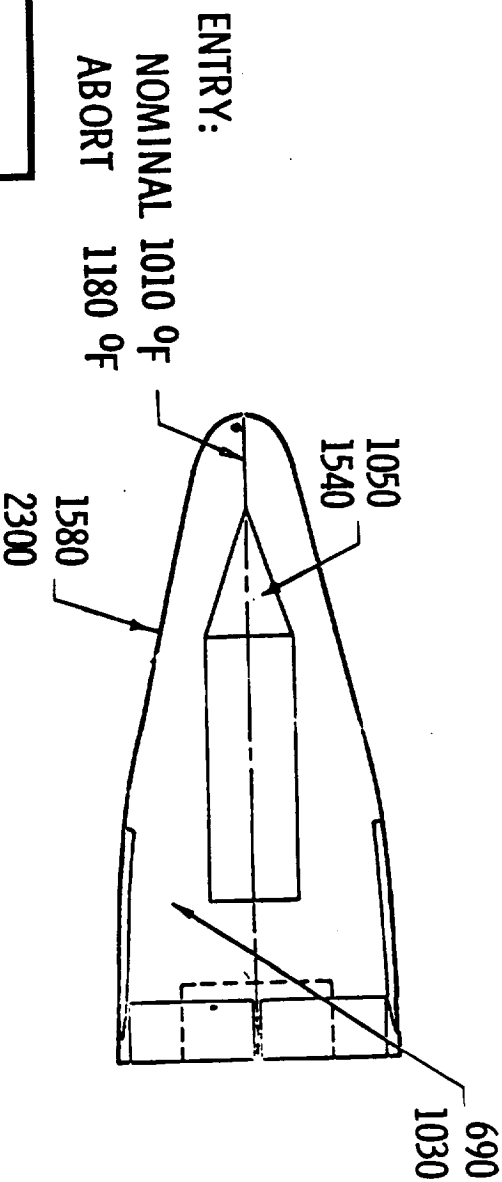


# AERODYNAMIC HEATING TEST OF HL-10



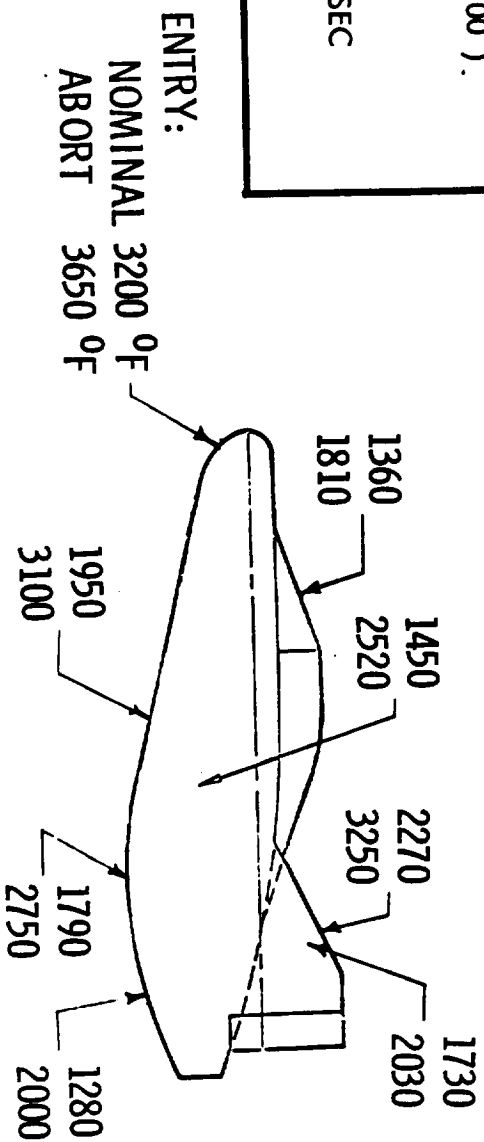
NASA RV65-16274  
11-22-65

# MAXIMUM RADIATION EQUILIBRIUM TEMPERATURES



NOTE:  
TEMPERATURES ARE BASED  
ON TRANSITION CRITERIA  
( $Re_\theta/M_i = 200$  ).

ABORT:  
 $V_i = 18,200$  FT/SEC  
 $\gamma_i = 4.3^\circ$



# M2-F1 RESEARCH VEHICLE

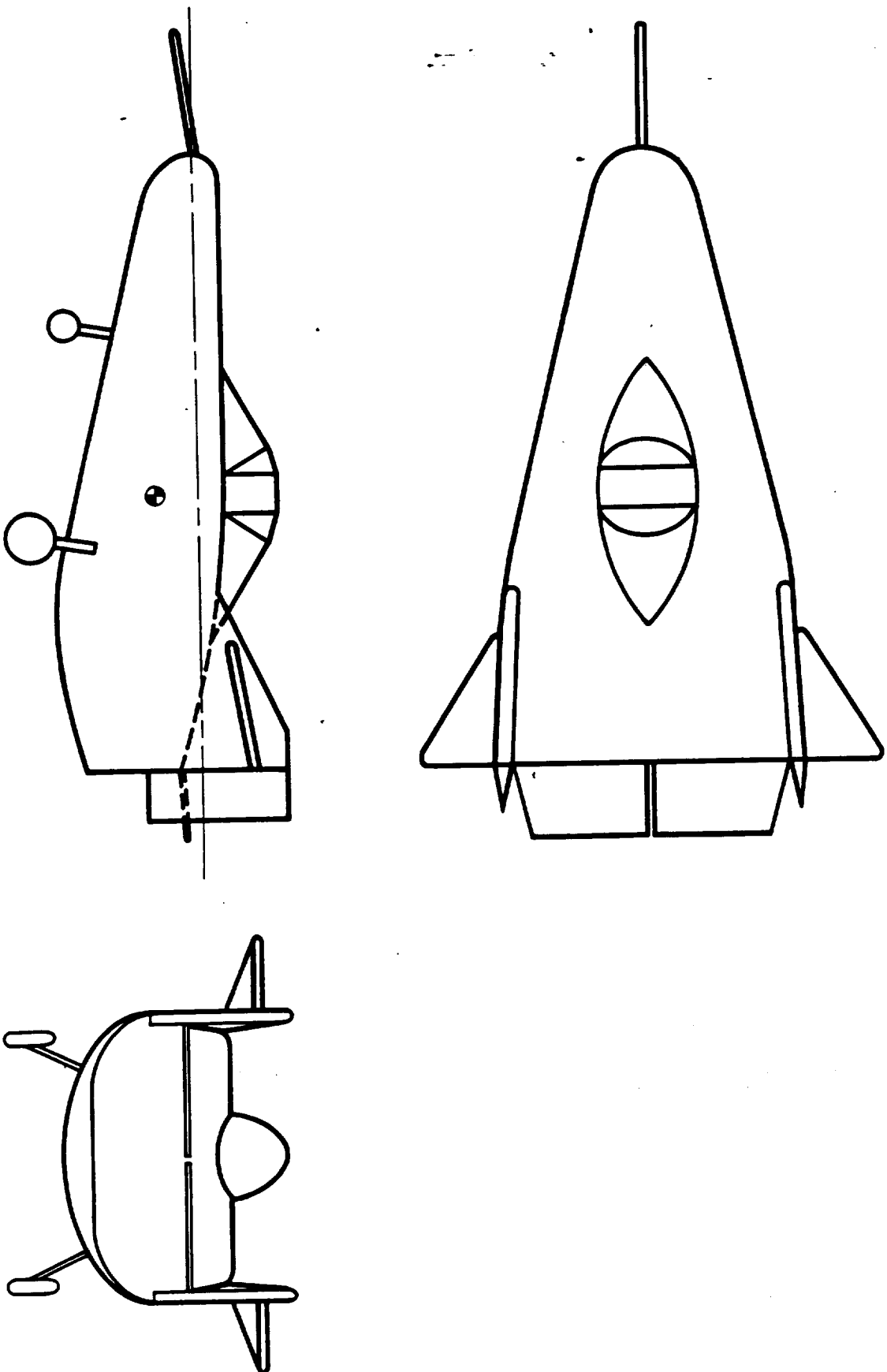
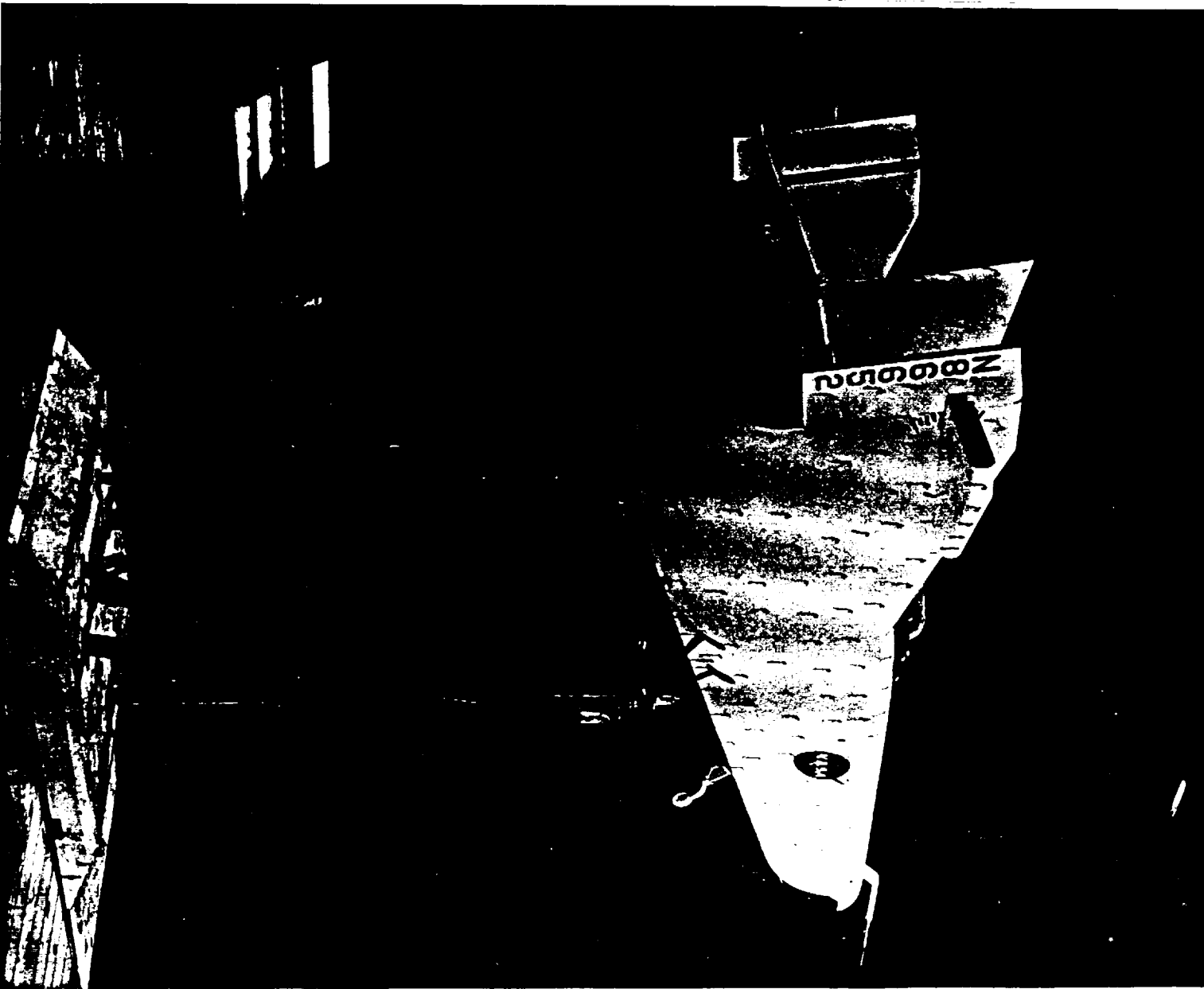


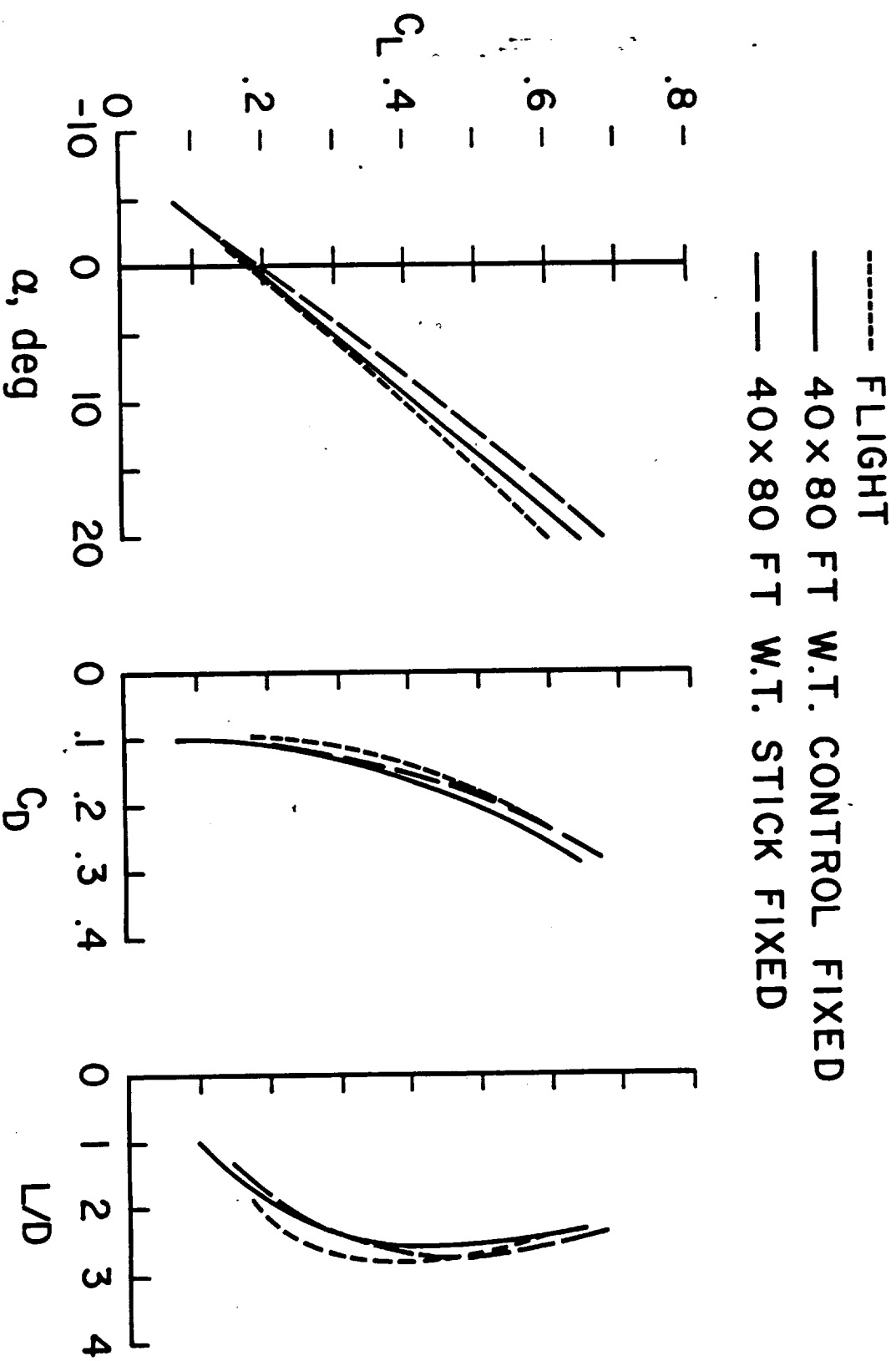
Figure 8

NASA RV65-16279  
11-22-65

NASA RV65-16261  
11-22-65

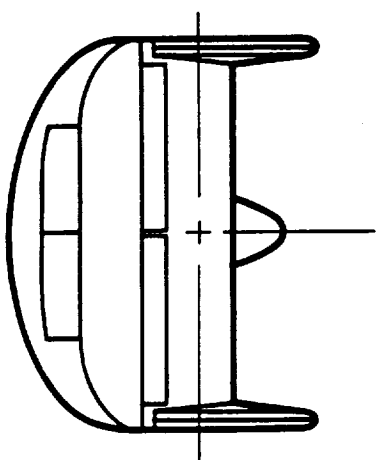
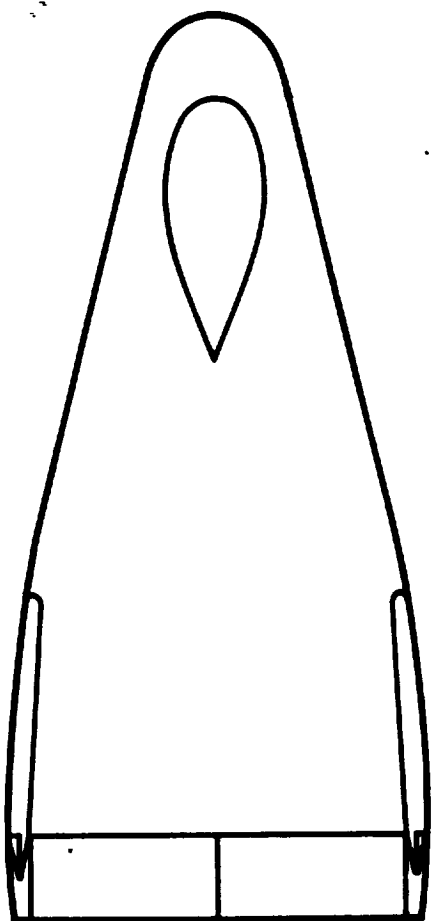


# M2-F1 LOW SPEED TRIMMED LIFT-DRAG CHARACTERISTICS





# M2-F2 CONFIGURATION



~~CONFIDENTIAL~~

# COMPARISON OF LOW SPEED L/D FOR M2-F1 AND M2-F2

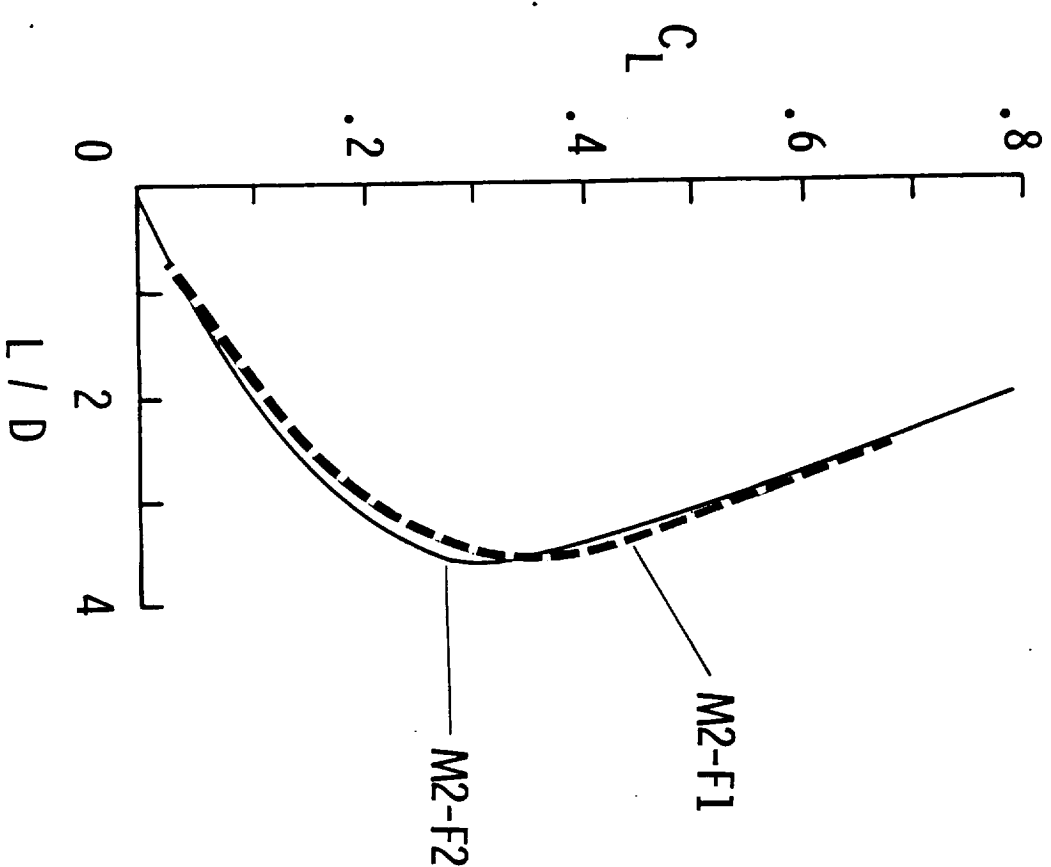
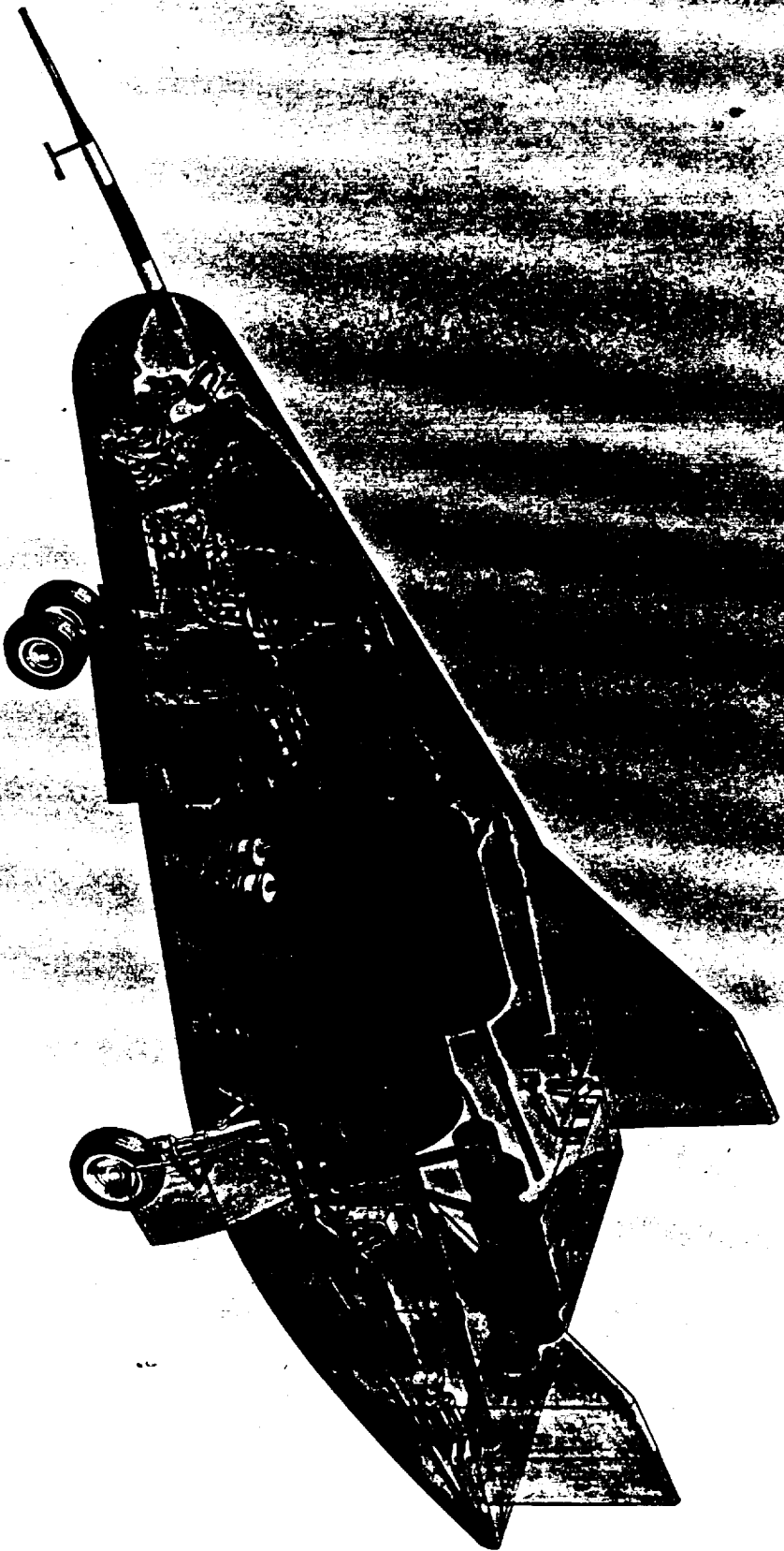


Figure 17

~~CONFIDENTIAL~~

# M-2/XLR-11 VEHICLE



NASA RV65-16270  
11-22-65

NORTHROP

# LOW SPEED CHARACTERISTICS

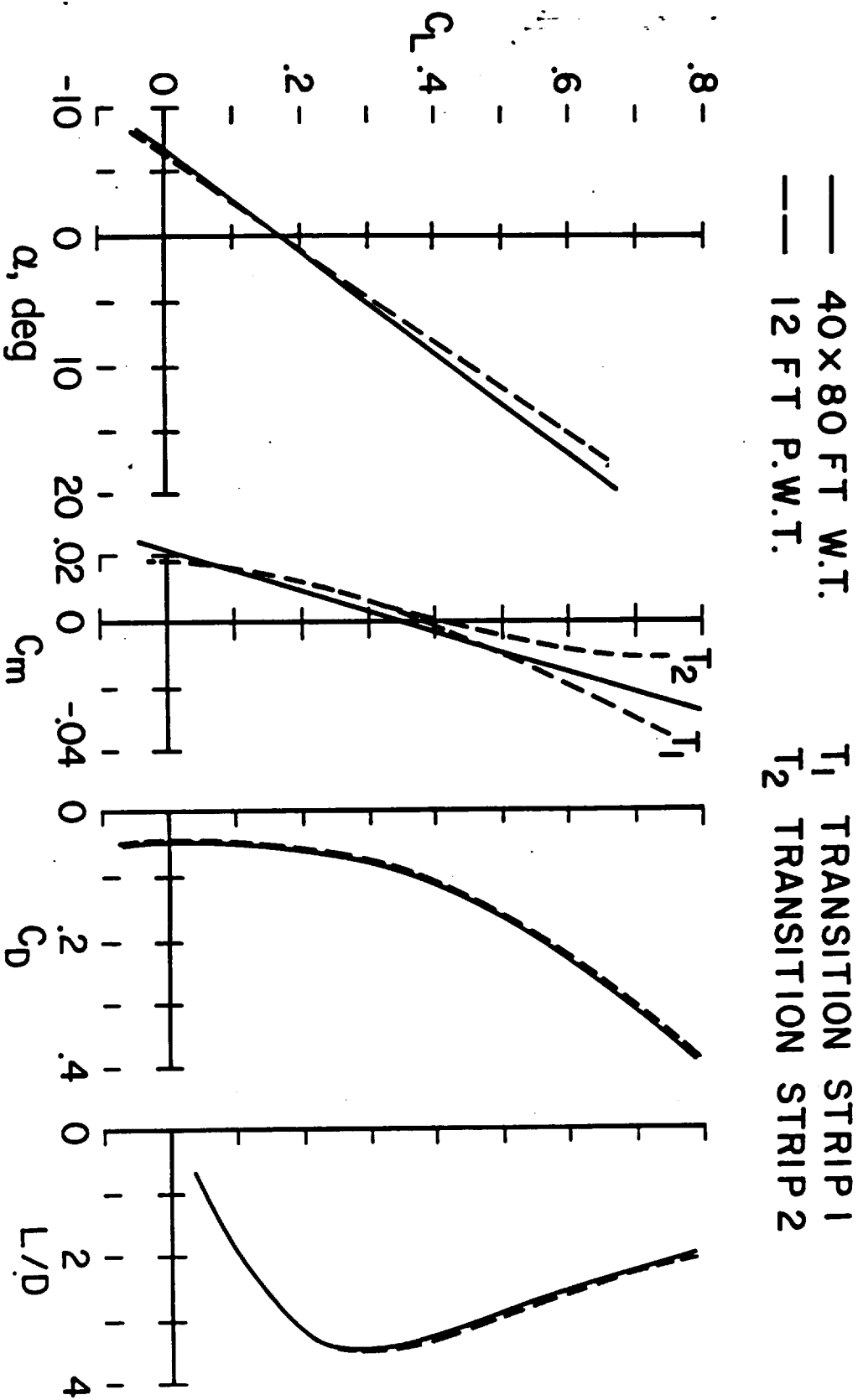


Figure 14

# M2-F2 TRANSONIC PITCH-UP?

$\delta f_u = -20^\circ$

$\delta f_l = 35^\circ$

$M = 0.8$

0.95

1.0

STRAKES

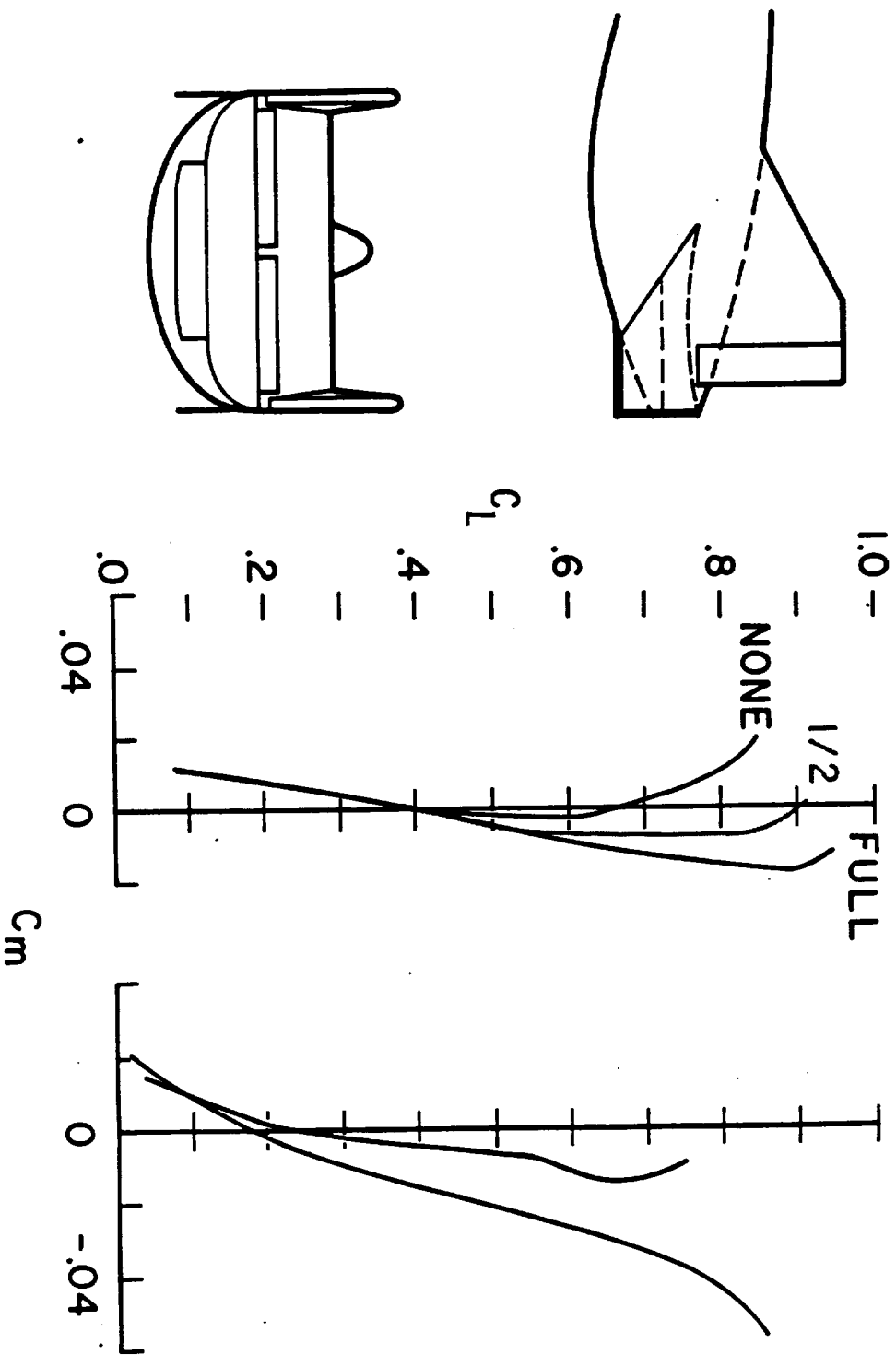
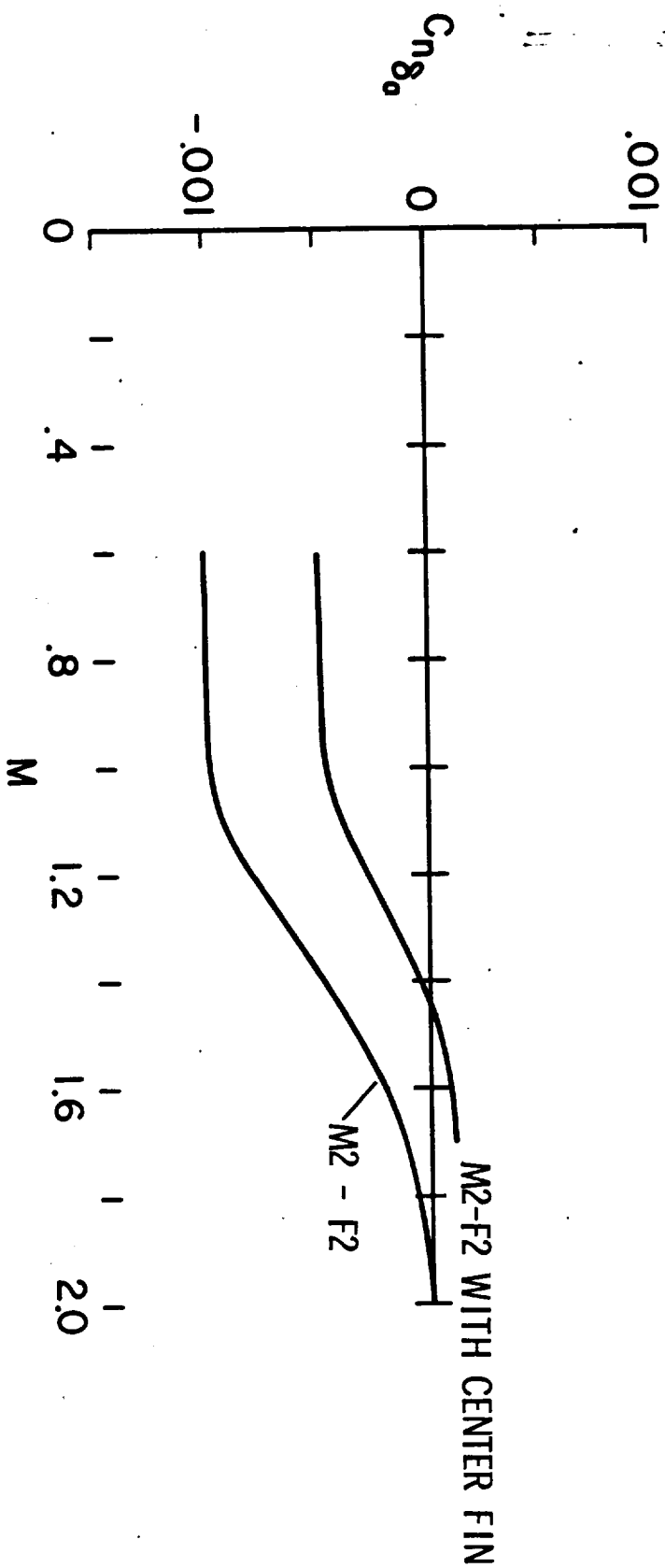
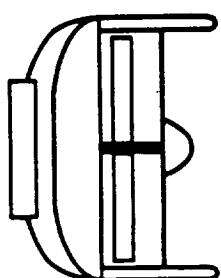
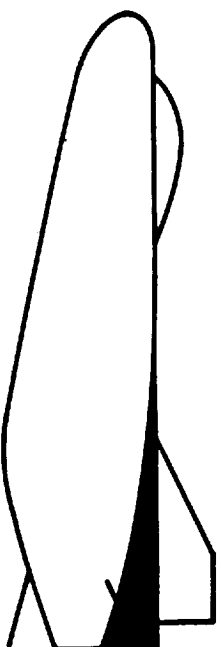


Figure 15

# M2-F2 CONTROL CROSS COUPLING



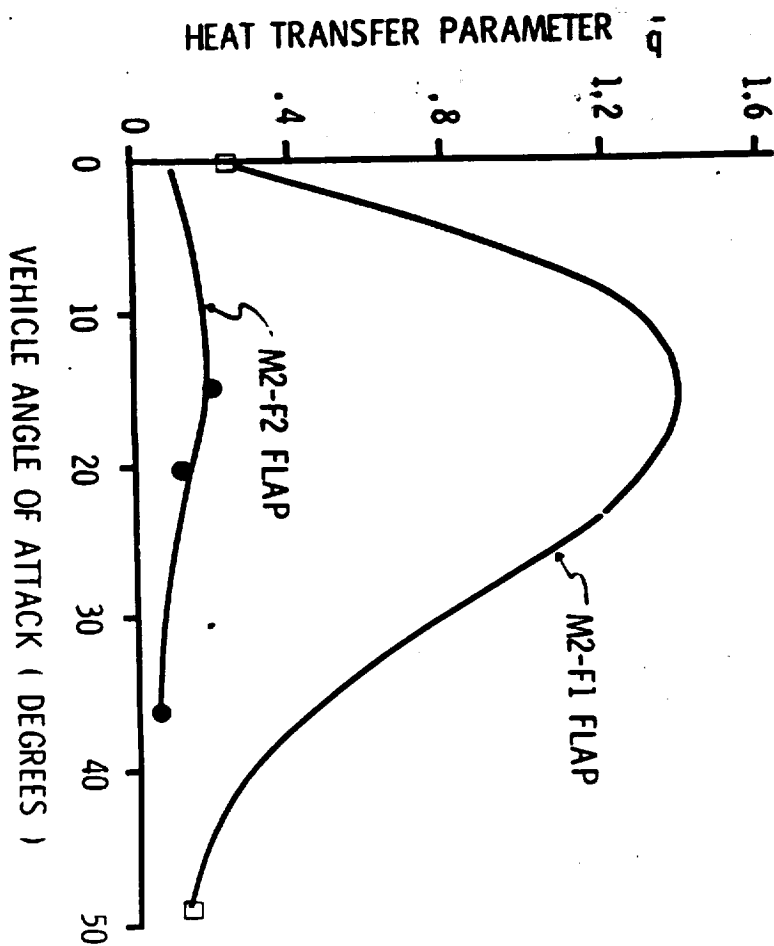
# M2-F1 AND M2-F2 PITCH CONTROL HEATING COMPARISON



M2-F1



M2-F2



# SOME OF THE HL-10 FIN ARRANGEMENTS STUDIED

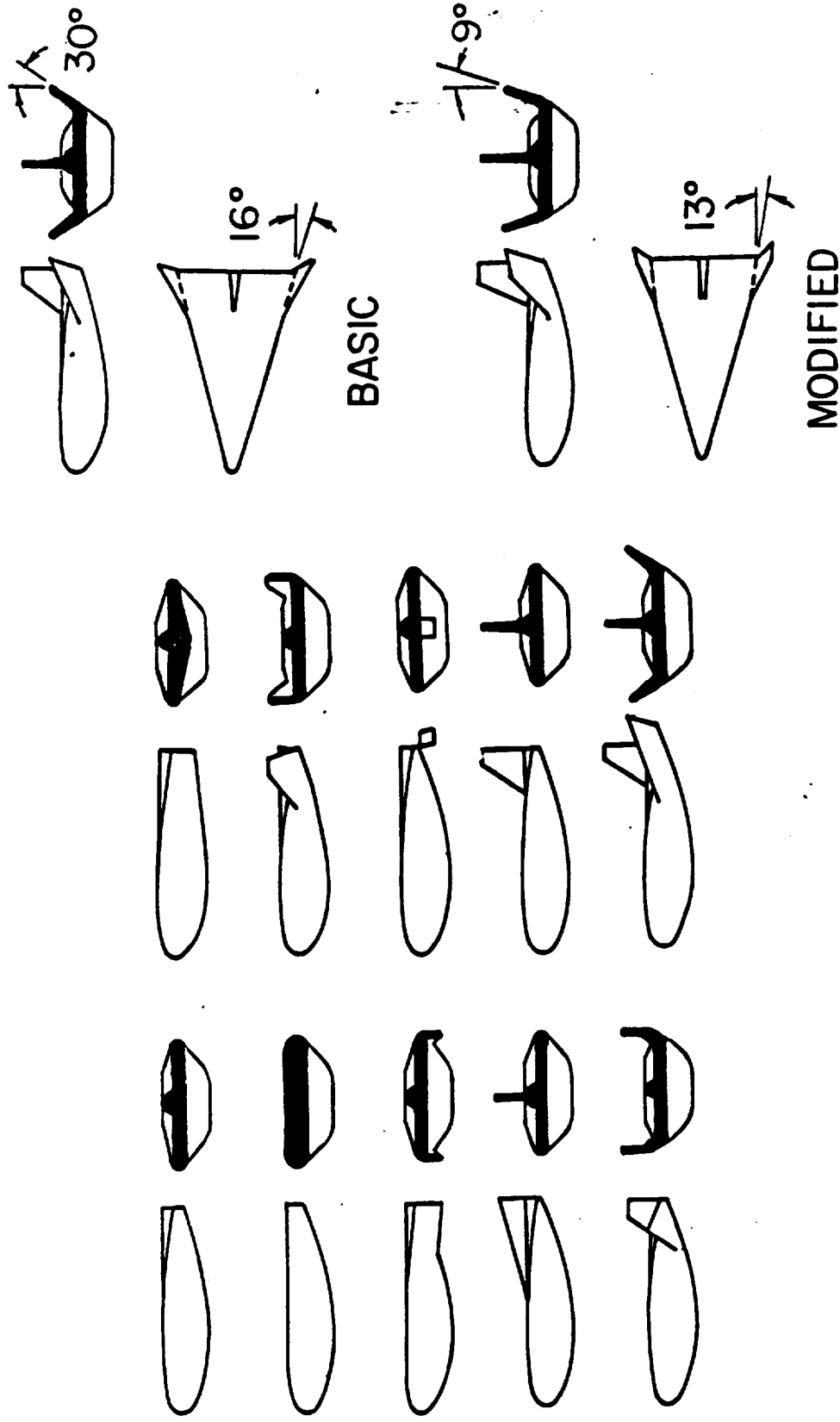


Figure 18



# HL-10 TRANSONIC LONGITUDINAL STABILITY

$M \approx 0.8; \delta e = 0^\circ$

- WITHOUT TRANSONIC FIXES
- WITH TRANSONIC FIXES

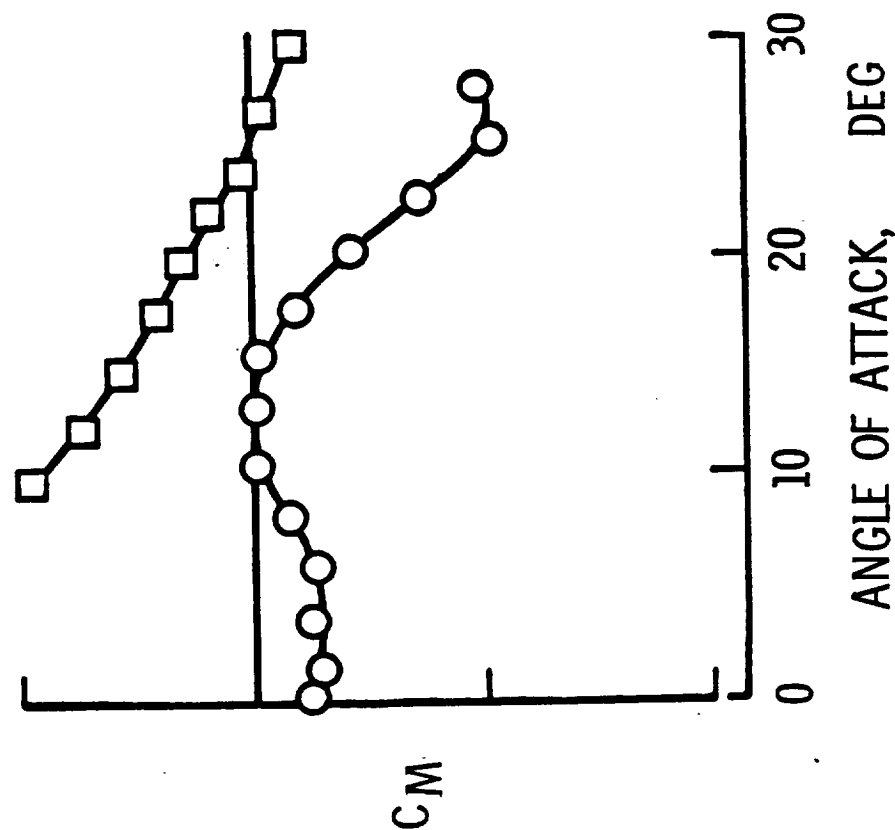


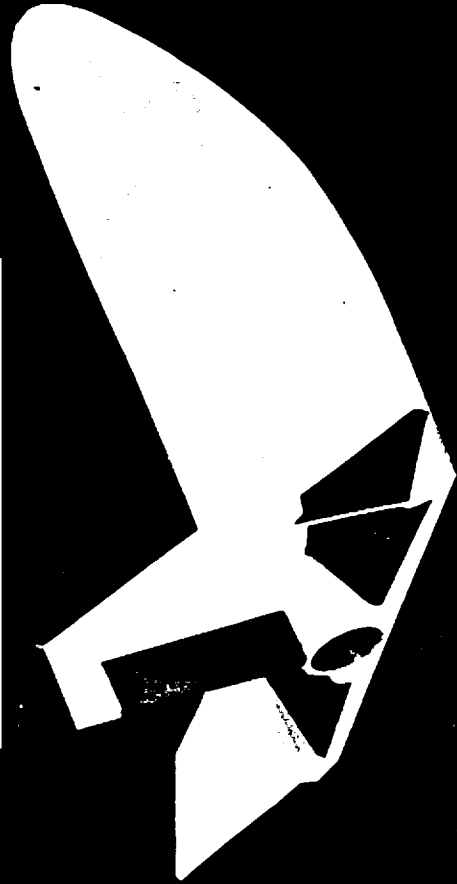
Figure 19

# HL - 10 VEHICLE WITH MODIFICATIONS



WITHOUT FIXES

WITH SUBSONIC FIXES



WITH TRANSONIC FIXES



NASA RV65-16260  
11-22-65

Figure 20

# HL-10 IN LRC FULL SCALE WIND TUNNEL



Figure 21

# M2-F2 RESEARCH VEHICLE IN AMES 40x80 FT. WIND TUNNEL

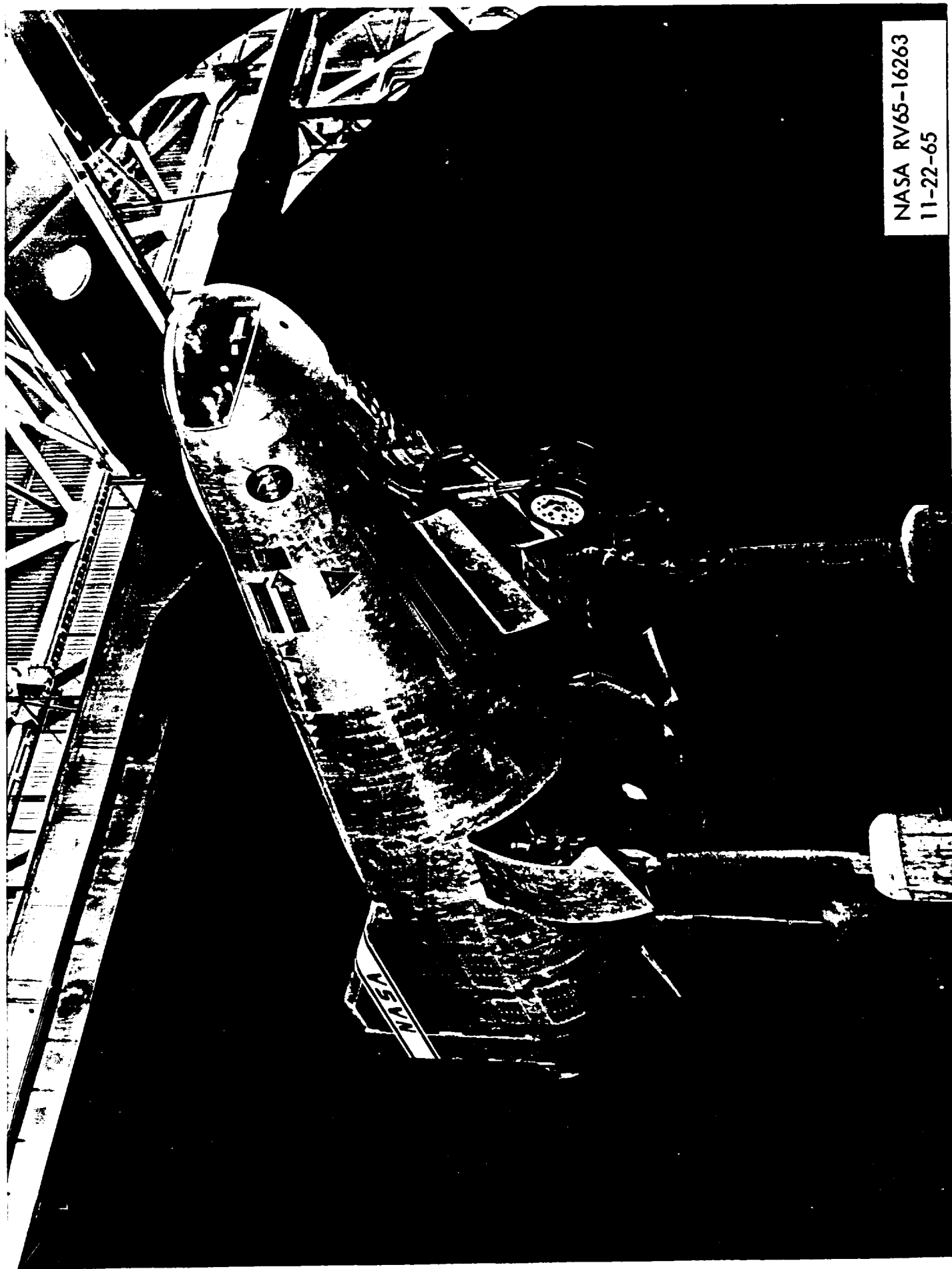


Figure 22

# M2-F2 STABILITY CHARACTERISTICS

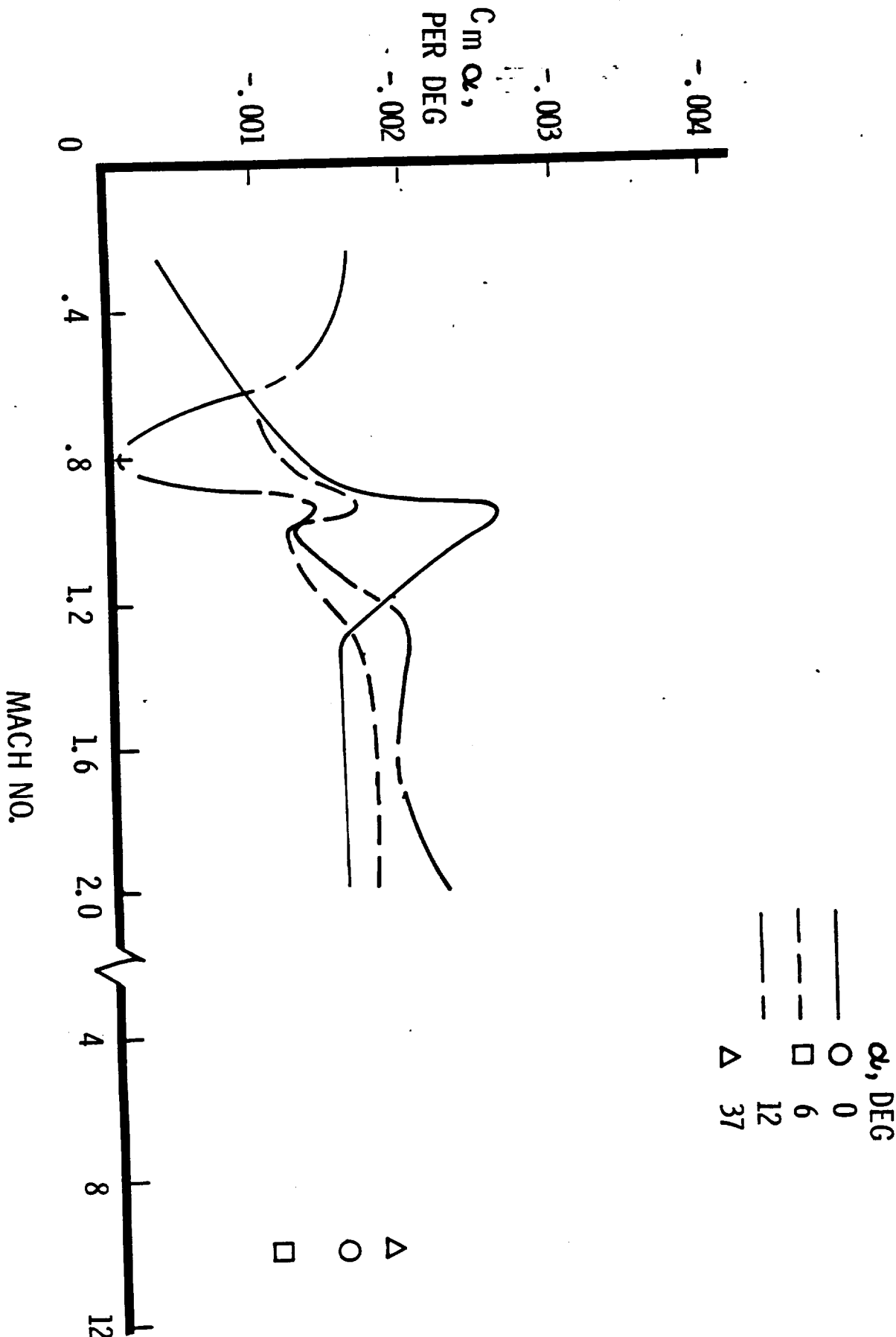
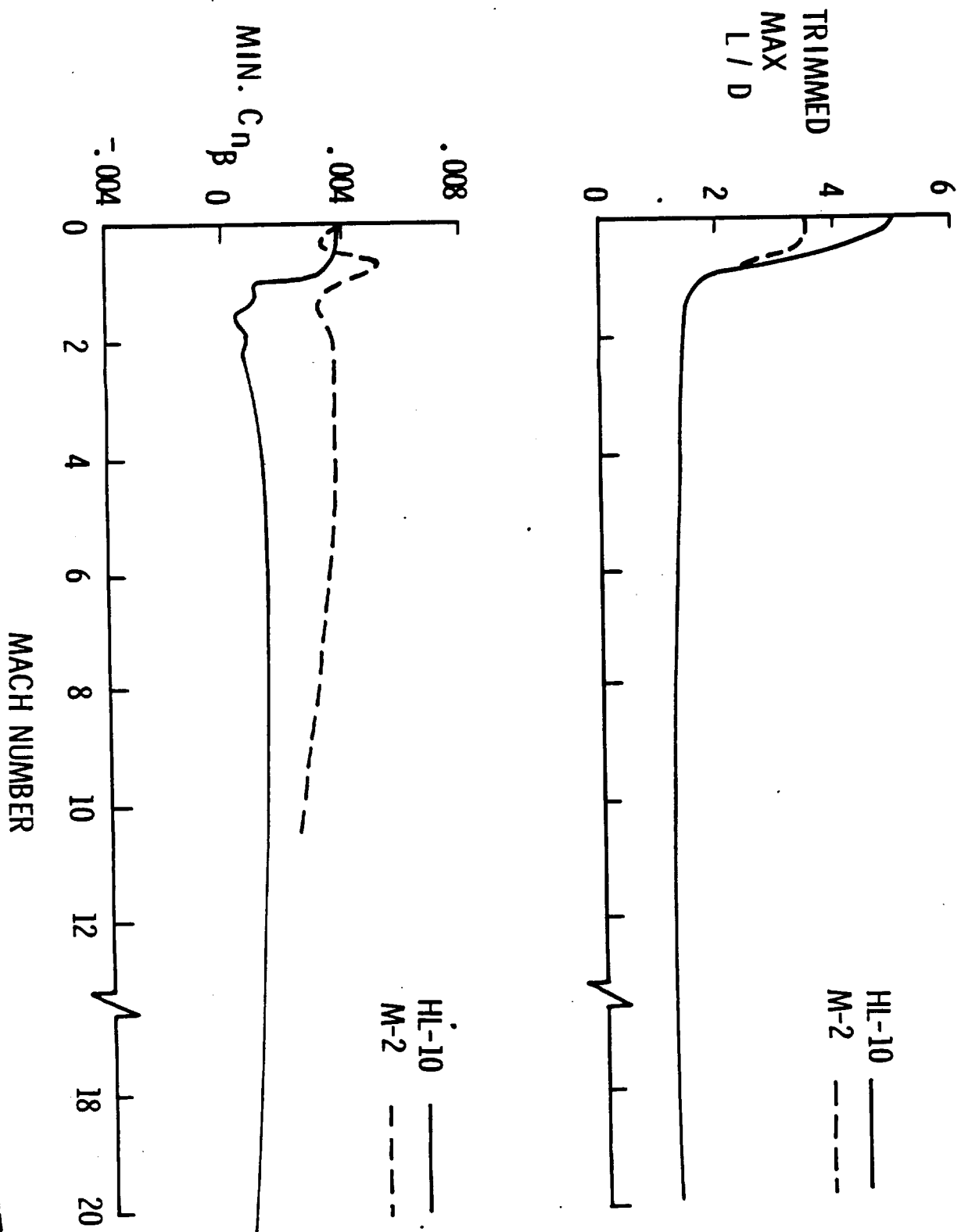
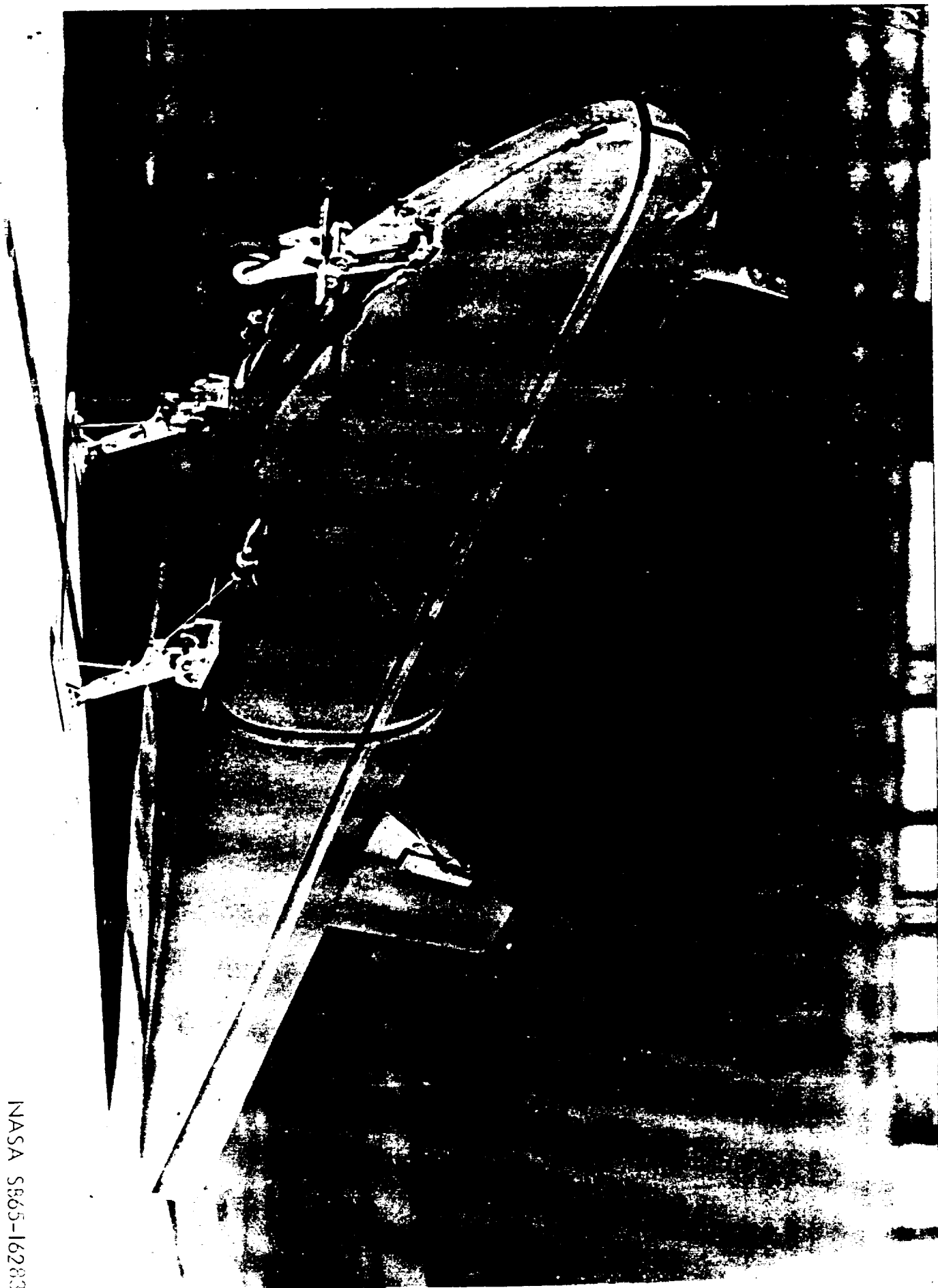


Figure 23

# M2-F2 AND HL-10 CHARACTERISTICS



# HL-10 GROUND LANDING STUDIES



NASA S865-16283  
11-22-65

# HL-10 NEAR VERTICAL WATER LANDINGS

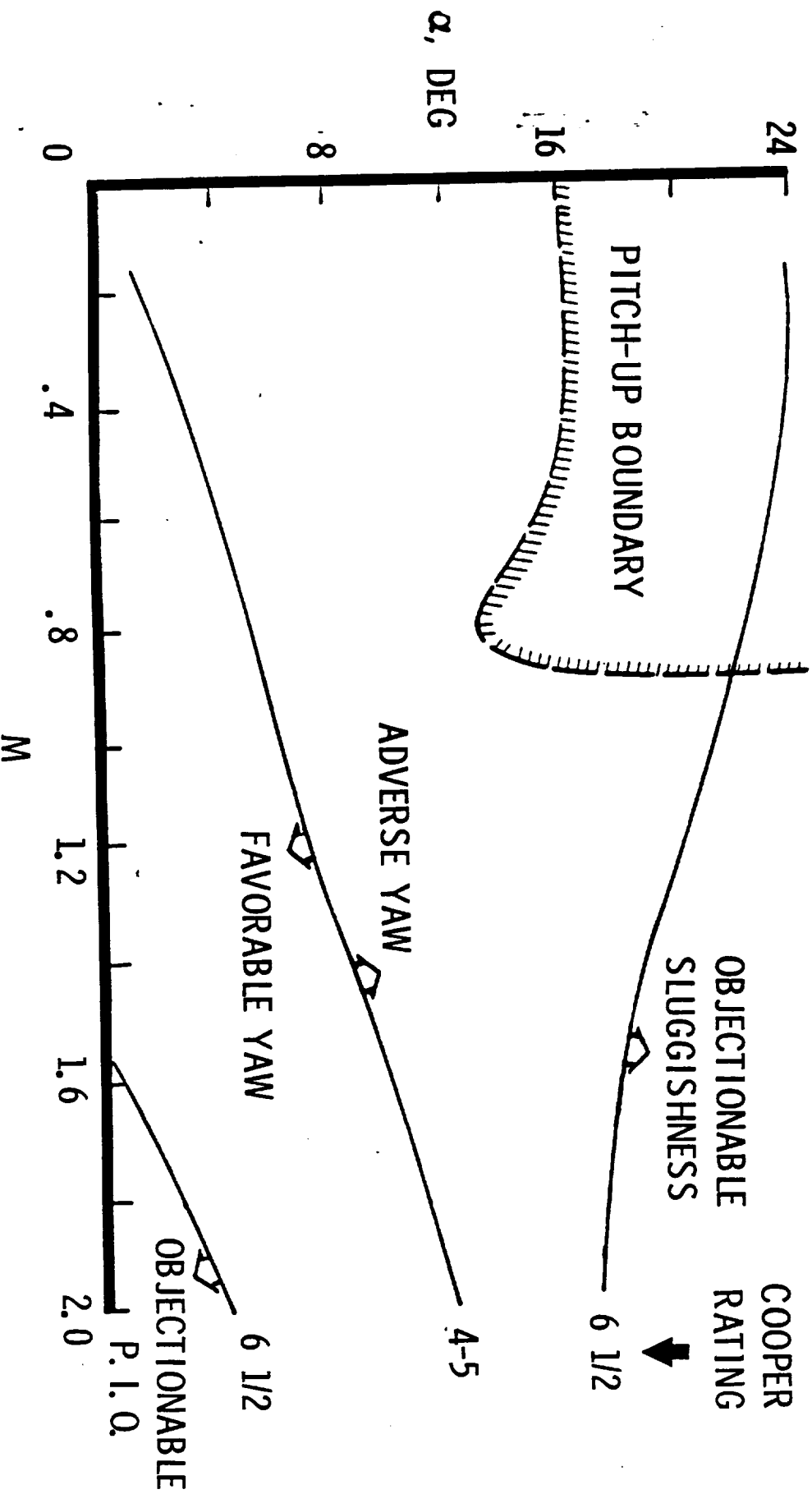


NASA RV65-16272



# M2-F2 ROLL CONTROL CHARACTERISTICS

WITH RUDDER INTERCONNECT  
DAMPERS OFF,  $q = 100$  PSF



# VARIABLE GEOMETRY SPACECRAFT MODEL

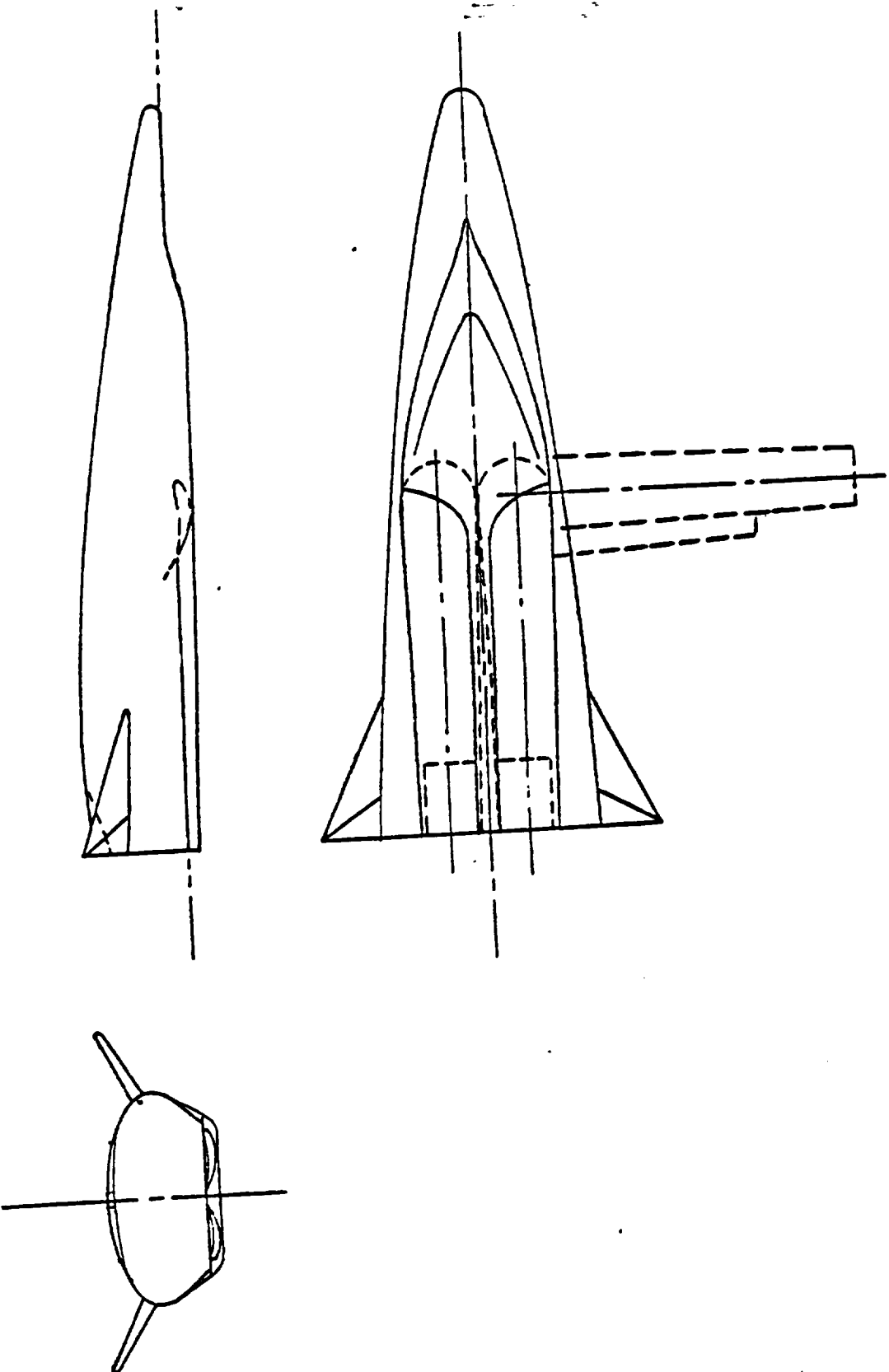


Figure 28

# VARIABLE GEOMETRY SPACECRAFT SUPERSONIC-HYPERSONIC CHARACTERISTICS

$$\Lambda_c = 90^\circ$$

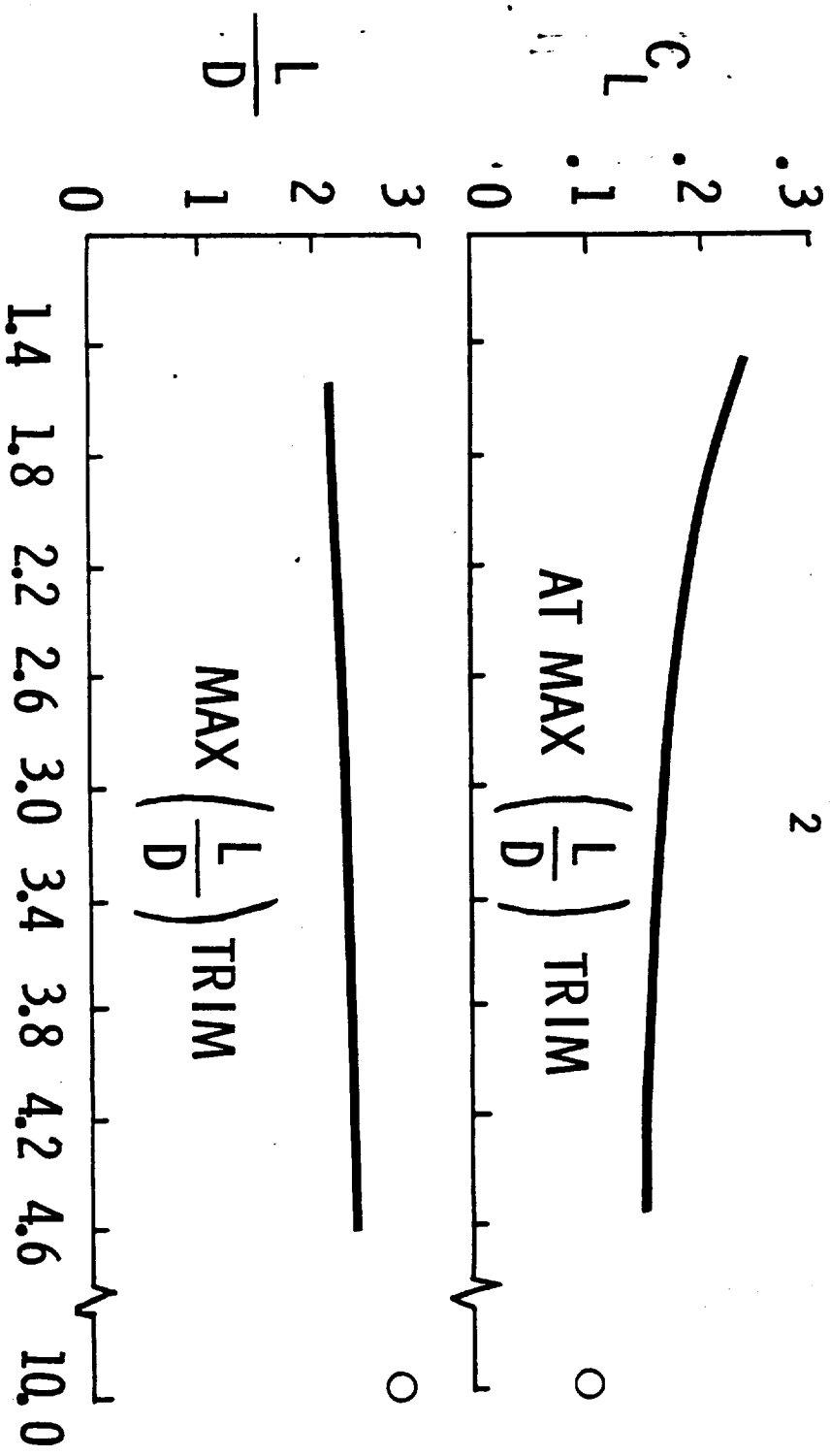


Figure 30

**M**

NASA RV65-16264  
11-22-65

# VARIABLE GEOMETRY SPACECRAFT LANDING

## CHARACTERISTICS - $M=0.3, \Delta C^2 = 0^\circ, R/FT=12 \times 10^6$

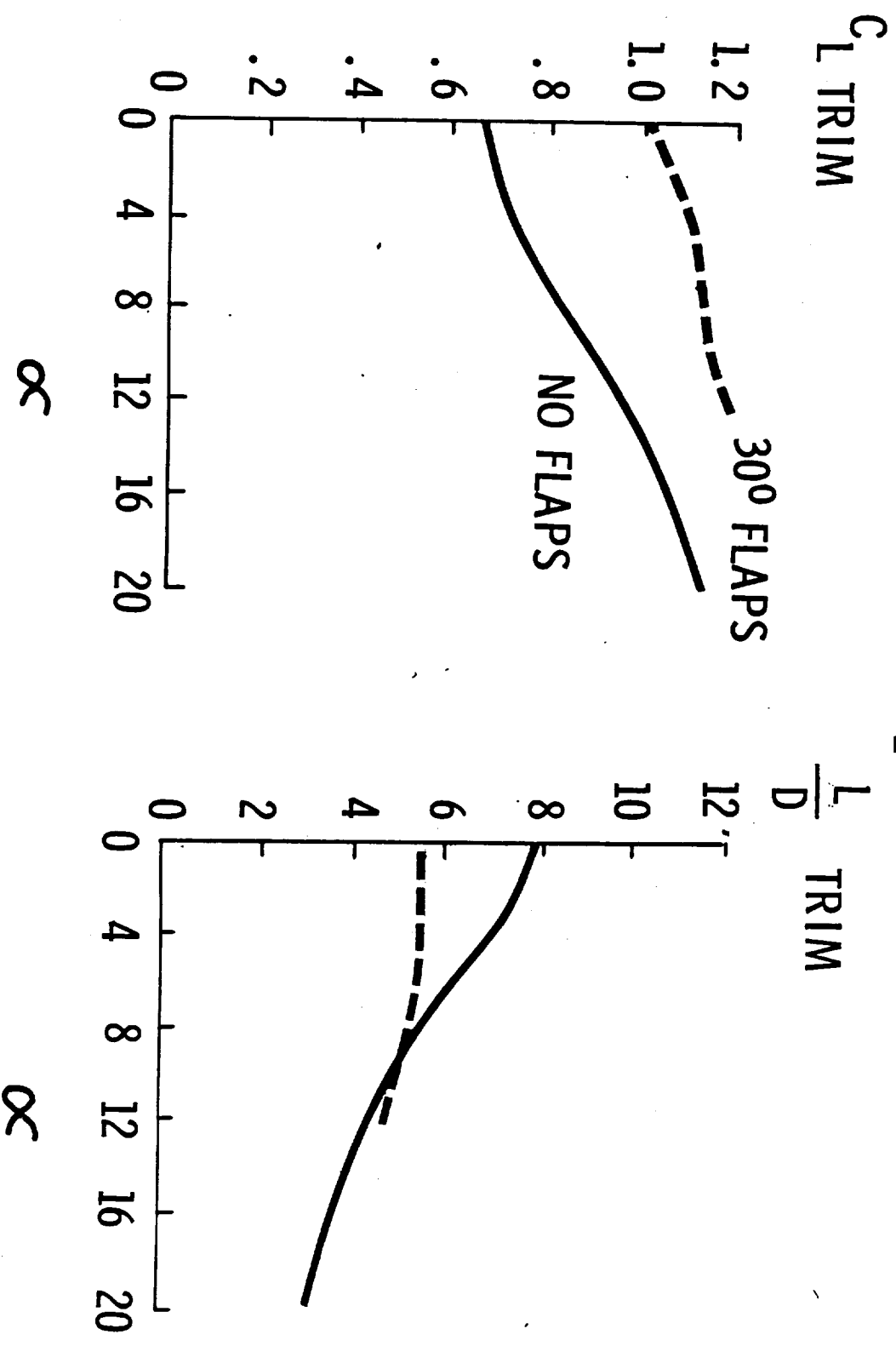
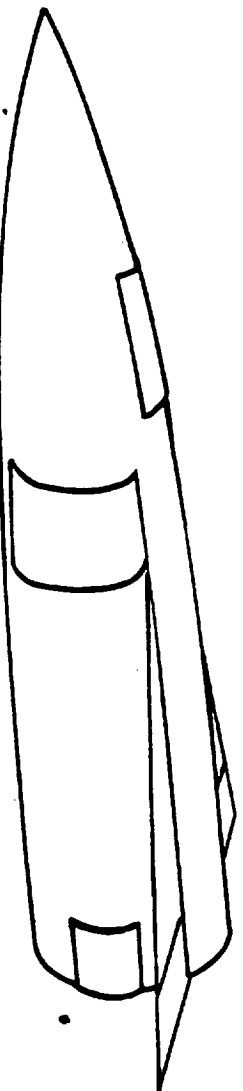


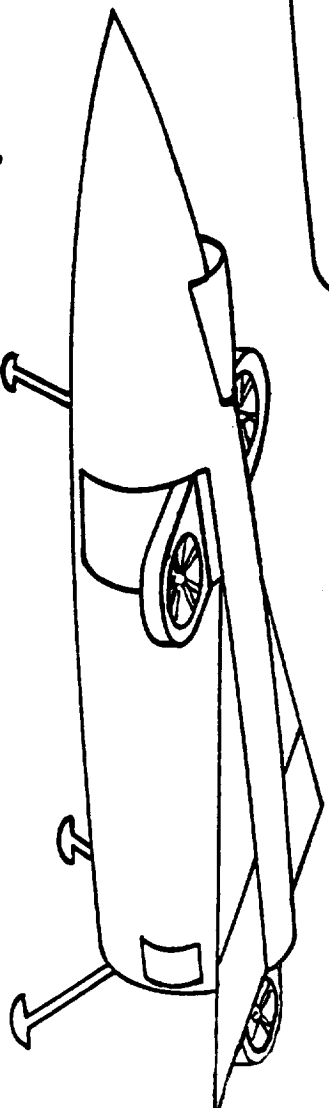
Figure 29

# VERTICAL LANDING CONCEPTS

## ILLUSTRATIVE LIFT-FAN APPLICATIONS



HIGH L/D



MODERATE L/D

